Republic of Iraq
Ministry of Higher Education
and Scientific Research
University of Babylon
College of Engineering
Civil Engineering Department

EVALUATION OF THE BEHAVIOR OF TWO-WAY R.C. SLABS WITH OPENINGS STRENGTHENED WITH CFRP

A Thesis

Submitted to the College of Engineering of the University of Babylon in Partial Fulfillment of the Requirements for the Degree of Master of Science in Civil Engineering
(Structures)

BY

Hussein Talab Nhabih Al-Wetaifi

B.Sc. in Civil Engineering 2007
Supervised by

Prof. Dr. Nameer A. Alwash

August 2009 **Shabbyne 1430**

جمهورية العراق
وزارة التعليم العالي والبحث العلمي
جامعة بابل
كلية الهندسة
قسم الهندسة المدنية

تقييم التصرف للسقوف الخرسانية المسلحة ذات الاتجاهين الحاوية على فتحات والمقواة بواسطة ألياف الكاربون البوليمرية

رسالة
مقدمة إلى كلية الهندسة في جامعة بابل
كجزء من متطلبات نيل درجة ماجستير في علوم الهندسة المدنية
(إنشاءات)

من قبل

حسين طلب نهابة الوطيفي

بكالوريوس هندسة مدنية 2007

أشراف

الأستاذ الدكتور نمير عبدالامير علوّش

آب 2009م

شعبان 1430هـ

بسم الله الرحمن الرحيم

قالوا سبحانك لا علم لنا إلا ما علمتنا إنك أنت العليم الحكيم

صدق الله العلي العظيم

سورة البقرة (الآية ٣٢)

LIST OF CONTENTS

LIST OF FIGURES

LIST OF TABLES

NOTATION

Most commonly used symbols are listed below, these and others are defined where they appear in the research.

ABBREVIATIONS:-

ABBREVIATIONS	Description
CFRP	Carbon fiber reinforced polymer.
FRP	Fiber reinforced polymer.
GFRP	Glass fiber reinforced polymer.
AFRP	Aramid fiber reinforced polymer.
HM	High modulus of elasticity.
HS	High strength.
N.A	Not applicable.
NSM	Near surface mounted.
EB	Externally bonded.
ANSYS	ANalysis SYStem.
ASTM	American society for testing and materials.
RC	Reinforced concrete.
ACI	American concrete institute.
EBR	Externally bonded reinforcement.
GUI	Graphical user interface.
PREP	Pre-processor.
POSTI	Post-processor.
ShrCf-Op	Shear transfer coefficient for the open cracks.
ShrCf-Cl	Shear transfer coefficient for the close cracks.

SYMBOLS:-

SYMBOLS	Description
$f'c$	Nominal concrete compressive strength (cylinder test).
$f\,y$	Yield strength of steel reinforcement.
St	Temperature scale factor.
Sf	Stress scale factor.
ρp	Densities of protytep.
fsp	Splitting tensile strength.
n	Number of layers of FRP.
βt	Shear transfer coefficient.
SL	Length scale factor.
As	Area of steel.
fu	Ultimate strength of steel reinforcement.
w/c	Water/cement.
d	Diameter of cylinder.
Ef	Modulus of elasticity for FRP.
tf	Thickness of layer for FRP.
Km	Coefficient of limits the strain in the FRP.
Ec	Modulus of elasity of concrete.
σh	Hydrostatic stress.
ft	Tensile strength.
w	Vertical deflection.
q	Uniformly distributed load.
D	Flexural rigidity of plate.
$S\varepsilon$	Strain scale factor.
ε_{fu}	The rupture strain of the FRP.
γ	Poisson's ratio.
L	A typical dimension of the structure.
p	Any applied pressure on the structure.
P	Any applied force on the structure.
ρ	The density of the material of the structure.
g	The gravitational acceleration.
t	The temperature of the structure.

REFERENCES

Abbasi, M.S.A., Baluch, M.H., Azad, A.K. and Abdel-Rahman, H.H.,(2008), "Nonlinear Finite Element Modeling of Failure Modes in Reinforced Concrete Slabs", Journal of Computers and Structures, Vol. 42, No. 5, pp. 815-823.

Abdual –Wahid , B.F.,(1989), " Yield – Line Analysis of Reinforced Concrete Slab –Beam Panels Under Combined Loading ", M.Sc. Thesis Presented to The University of Baghdad ,April.

Abdullah, S.M., (2006), "Nonlinear Analysis of Reinforced Concrete Slabs Using Assumed Strain Elements", M.Sc. Thesis, Mosul University, December, 119 PPS.

Achintha, P.M., Burgoyne C.J. (2006),"A Fracture-Mechanics Model for Debonding of External Fiber Reinforced Polymer Plates on Reinforced Concrete Beams", The Tenth East-Pacific Conference on Structural Engineering and Construction, Bangkok, Thailand.

ACI Committee 440 (2002), "Guide for the Design and Construction of Externally Bonded FRP Systems for Strengthening Concrete Structures", American Concrete Institute, Detroit.

Alkhrdaji , T. and Nanni, A.(2001), "Surface Bonded FRP Reinforcement for strengthening / Repair of structural Reinforced concrete",proc.ICRI-NRCC work shop , Baltimore , MD,OCT,30,19P.P.

Al-Mahaidi, R. (2003), "Use of FRP Composites for Strengthening of Concrete Buildings and Bridges. "Monash University, Melbourne, Australia.

Almusallam T. H. , (2005), "Flexural Behavior of R.C slabs strengthened with FRP polymers, "Final Report, King saud university, Kingdom of Saudi Arabia.

Al –Shadidi ,R.M.,(1985), " Analysis of R.C Square Slabs Subjected to Combined Loading Using Yield Line Theory ", M.Sc. Thesis Presented to The University of Baghdad ,April.

American Concrete Institute, ACI Committee 318, (2005), "Building Code Requirements for Structural Concrete (ACI 318-05) and Commentary (ACI 318R-05)", American Concrete Institute, Farmington Hills, MI.

American Concrete Institute, Committee 440 (2002), ACI 440.2R-02, "Guide for the Design and Construction of Externally Bonded FRP Systems for Strengthening Concrete Structures", 45 pp.

Annex, J., (1998), "Strengthening with carbon fiber: Rehabcon strategy for maintenance and rehabilitation in concrete structures", Innovation and SME Programmer, pp.63.

ANSYS, (1998), "ANSYS user's manual revision 9" ANSYS, Inc., Canonsburg, Pennsylvania.

Anthony, J. (2004), "Flexural behavior of reinforced and prestressed concrete beams using finite element analysis" MSc thesis, Department of Civil and Environmental Engineering, Marquette University, May.

An, W., Saadatmanesh, H. and Ehsani, Mr.,(1993), "RC beams strengthened with FRP plates .II .Analysis and parametric study", Journal of Structural Engineering, ASCE, Vol.117, No. (11), pp.3434-3455.

Arduini, M., and Nanni, A., (1997), *"*Behavior of Precracked RC Beams Strengthened with Carbon FRP Sheets", ASCE Journal of Composites for Construction, Vol. 1, No. 2, pp. 63-70.

Arduini, M., Tomaso, A. and Nanni. A., (1997), "Brittle failure in FRP plate and sheet bonded beams", ACI, Structural Journal, 94(4), pp.363-370.

Arnesen, A., Soreson, S.I. and Bergam,(1998),"Nonlinear analysis of reinforced concrete", Computer and Structural Journal, Vol.12, pp.271 579.

ASTM Designation C39-01, (2001), "Stander specification for testing method for compressive strength of cylindrical concrete specimens", Annual Book of ASTM Standards, American Society for Testing and Material, Philadelphia, Pennsylvania, section4, Vol. 4.02,pp 20-24.

ASTM Designation C150-02, (2002), "Standard specification for Portland cement", Annual Book of ASTM Standards, American Society for Testing and Material, Philadelphia, Pennsylvania, section4, Vol. 4.02, pp 89-93.

ASTM Designation C39-01,(2001), "Stander specification for testing method for compressive strength of cylindrical concrete specimens", Annual Book of ASTM Standards, American Society for Testing and Material, Philadelphia, Pennsylvania, section4, Vol. 4.02,pp 20-24.

ASTM Designation C78-02,(2002), "Standard specification for testing method for flexural strength of concrete (using simple beam with third-point loading)", Annual Book of ASTM Standards, American Society for Testing and Material, Philadelphia, Pennsylvania, section4, Vol. 4.02, pp 32-34.

ASTM Designation C 496-96,(1996), "Standard specification for Splitting tensile strength of cylindrical concrete specimens", Annual Book of ASTM Standards, American Society for Testing and Material, Philadelphia, Pennsylvania, section4, Vol. 4.02, 1-4pp.

Bathe, K.J., Walczak, J. and Mistry, N. (1989), "Nonlinear Analysis of Concrete Structures", Journal of Computers and Structures, Vol.32, No. 3/4, pp. 563-590.

Borges, J.Ferry, Arga, E.and Lima, J.(1959), "crack and deformation similitude in reinforced concrete". RILEM symposium, Madrid.

Brosens ,K.(1999), "Strengthening of Concrete Structures with Externally Bonded Reinforcement-Design philosophy and practical applications" ,K.U. Leuven, Belgium.

Buyukozturk, O., and Yu, T., (2006), "Understanding and Assessment of Debonding Failures in FRP-Concrete Systems", Seventh International

Congress on Advances in Civil Engineering, Yildiz Technical University, Istanbul, Turkey.

Buyukozturk, O., Gunes, O., and Karaca, E.(2004), “Progress on Understanding Debonding Problems in Reinforced Concrete and Steel Members Strengthened using FRP Composites”, Construction and Building Materials , Vol. 18, pp. 9-19.

Carolin, A., (2003), "Carbon Fiber Reinforced Polymers for Strengthening of Structural Elements", Ph.D. Thesis, university of Lulea, Sweden, pp.194.

Casadei P. , Nanni A. and Ibell T. (2006), " Experimental results of Two-way slabs with openings strengthened with CFRP laminates ", Accepted to sixth International symposium on Fiber Reinforced polymer Reinforcement of Reinforced Concrete structures, Singapore.

Charlton, T.M. (1954), "Model Analysis of Structures", E. and F.N.spon, London.

Chen, W.F., (1982), “Plasticity in reinforced concrete”, Third Edition, Mc Graw-Hill Company, New York. U.S.A.

Dyana, LS., (1990), “Theoretical manual”, Technical Report, Livermore Software, Technology Corporation, pp.498.

Figueiras, J.A., (1985), “Practical Approach for Modeling the Nonlinear Response of Reinforced Concrete Shells”, in Computational modeling of reinforced concrete structures, edited by E. Hinton and R. Owen, Pineridge Press, Swansea.

Fumagalli, E. (1958), "suitable materials for static and dynamic tests on model concrete dams. C. and C.A. Library Translation No.72.

Fu-Ming Lin and Hsuan-The Hu, (2004), "strengthening of square Reinforced concrete plates with FRP", National cheng Kung University.

Gere, I.M. and Timoshenko, S.P., (1997), “Mechanics of material”, PWS Publishing Company, Boston, Massachusetts.

Gemert, D. (2000), "Strengthening of Concrete Structures with Externally Bonded Reinforcement-Design philosophy and practical applications" ,K.U. Leuven ,Belgium.

Hand, F.R., Pecknold, D.V. and Schnobrich, W.C., (1973), "Nonlinear Layered Analysis of Reinforced Concrete Plates and Shells", Journal of the Structural Division, ASCE, Vol. 99, No. ST7, July ,pp. 1491-1505.

Hidayat, A.,(1994), "Influence of High Temperature on the Behavior of Reinforced Concrete Slabs", M.Sc. Thesis, University of Technology,.128pp.

Hemmaty, Y., (1998), "Modeling of the shear force transferred between cracks in reinforced and fiber reinforced concrete structures" Proceedings of the ANSYS Conference, Vol. 1, Pittsburgh, Pennsylvania, August.

Isabel Burkart,(2002), "Concrete and Concrete Structures: Numerical Modeling and Applications", Elsevier Science Publishers Ltd., London, England.

Johansson, H., Blanksvard, T. and Carolin, A., (2007), "Glulam Members Strengthened by Carbon Fiber Reinforcement." Materials and Structures, Vol.40, No. 1, pp 47-56.

Johnson, R.P. (1962), "Strength test on scaled-down concretes suitable for models ", with a note on mix design: Magazine of concrete Research,14,47.

Kachlakev Damian and Thomas Miller, (2001),"Finite element modeling of reinforced concrete structures strengthened with FRP laminates", Technical Report, Oregon Department of Transportation, May, pp.99.

Kachlakev, D.I. and David, D.Jr. (1992),"Testing of full-size reinforced concrete beams strengthened with FRP composites: Experimental results and design methods verification", Final Report, Oregon, June, pp.36.

Limam Oualid , Foret Gilles , Ehrlacher Alain, (2007),"R.C Two-way slabs strengthened with CFRP strips : experimental study and a limit analysis approach"

Link, R.A. and Elwi, A.E., (1995),"Composite Concrete-Steel Plate Walls Analysis and Behavior", Journal of Structural Engineering, Vol. 121, No. 2, February.

Lorenzis, L., Miller, B., and Nanni, A.,(2001)," Bond of Fiber-Reinforced Polymer Laminates to Concrete ", ACI material journal, V.98,No.3, pp.256-264.

Lundqvist, J., (2007),"Numerical analysis of Concrete Element with Carbon Fiber Reinforced Polymers", PhD Thesis. Lulea University of Technology, Lulea, Sweden.

Maurizio, G., Kypros, p., and Peter, w., (2002), "Shear performance of FRP reinforced concrete beams", Journal of Reinforced Plastics and Composites, 22, 1389, Jrp.sagepub.com.

Meier, U., and Kaiser, H., (1991),"Strengthening of Structures with CFRP Laminates'", Proc. Advanced Composite Materials in Civil Engineering Structures, Mats. Div., pp 224–232.

Mohammed, Dhiyaa H., (2007)," Behavior of Reinforced Concrete Beams Strengthened by CFRP in Flexure ", PhD Thesis, University of Technology , Iraq.

Muhsen ,H.N.,(1993),"Three-dimensional nonlinear finite element analysis of axially loaded concrete-filled steel tube short columns", Master Thesis, University of Technology, Iraq.

Mukhopadhyaya, P., and Swamy, N., (2001)," Interface Shear Stress: A New Design Criterion for Plate Debonding." Journal of Composites for Construction , Vol.5,No.1, pp. 35-43.

Nanni , A. and Iball,T.(2003),"Experimental results of Two-way slabs with openings strengthened with CFRP laminates " , Accepted to sixth International symposium on Fiber Reinforced polymer Reinforcement of Reinforced Concrete structures, Singapore.

Ngo, D. and Scordelis, A.C., (1967), "Finite Element Analysis of Reinforced Concrete Beams", ACI J., Proc., Vol. 64, No. 3, March., pp.152-163.

Nilson, Arther H.,(1997),"Design of concrete structures" McGraw-Hill, New York.

Nordin, H., (2003),"Flexural Strengthening of Concrete Structures with Prestressed Near Surface Mounted CFRP Rods", Licentiate Thesis. Lulea University of Technology, Lulea, Sweden.

Oloffsson et al., (1994),"Using finite element in mechanical design", McGraw-Hill Book CO., International, London, England,.

Preece ,B.W. and Davies, J.D. (1964),"Models for structural concrete",1 st Edition,CR Books Ltd.

Raphael,J.M.(1961),"structural models evaluate behaviour of concrete dams, Journal of the American Concrete Institute,32,1111.

Ross, C.A., Jerome, D.M., Tedesco, J.W., and Hughes, M.L.,(1999), "Strengthening of Reinforced Concrete Beams with Externally Bonded Composite Laminates", ACI Structural Journal, Vol. 96, No.2, pp:212-220

Rusimowski,p.(2005),"Two-way concrete slabs with openings, Experiments, Finite Element Analyses and Design "master's thesis 2005:Lulea university of Technology.

Saadatmanesh, H., and Ehsani, M., (1991), "R.C. Beams Strengthened with GFRP Plates I: Experimental Study.", Journal of Structural Engineering, Vol.117, No.11, pp.3417–3433.

Santhakumar, R., and Chandrasekaran, E., (2004),"Analysis of retrofitted reinforced concrete shear beams using carbon fiber composites", Electronic Journal of Structural Engineering. eJSE 4.

Seliem H. M., Sumner E. A., & Seracino R. (2008),"Field testing of R.C. slabs with openings strengthened with CFRP ",constructed Facilites labortary, North Carolina state university,Raleigh, Nc.USA.

Shahawy, M. A. and Beitelman, T.E., (2003), "Structural applications of advances composite material in bridge construction and repair", Proc., ASCE Struct. Congr. XIII, ASCE Reston.

Shin, Y., and Lee, C.,(2003), "Flexural Behavior of Reinforced Concrete Beams Strengthened with Carbon Fiber-Reinforced Polymer Laminates at Different Levels of Sustaining Load", ACI Structural Journal, Vol. 100, No. 2, pp. 231-239.

Sika (2005), "SikaCarboDur Plates-Pultruded Carbon Fiber Plates for Structural Strengthening System", Technical Data Sheet, Edition 2, (web site: www.sika.co.id).

Sika (2005), "Sikadur 30-Adhesive for Bonding Reinforcement ",Technical Data Sheet, Edition 2, (web site: www.sika.co.id).

Sika (2005), "Sikadur 330-Two Part Epoxy Impregnation Resin", Technical Data Sheet, Edition 2, (web site: www.sika.co.id).

Sika (2005), "SikaWrap230C-Woven carbon fiber fabric for Structural Strengthening", Technical Data Sheet, Edition 2, (web site: www.sika.co.id).

Strang, G. and Fix, G.J., (1973), "An Analysis of the Finite Element Method", Preptice-Hall,.

Tan k.h. and Zhao . H. (2004), "Strengthening of openings in one-way Reinforced Concrete slabs using carbon fiber reinforced polymer systems"; journal of composites for construction.

Tan, K.,Y.,(2002), " Evaluation of Externally Bonded CFRP Systems for the Strengthening of RC Slabs" MSc. Thesis, University of Missouri-Rolla.

Timoshenko, S.& Woinowsky-Krieger, S.(1959), "Theory of plates and shells". Second edition, NewYork, McGraw.

Toong,K.(2002), "Improving crack behavior of one-way slabs with carbon fibre plates", school of civil and structural engineering :hanyang Technological University.

Traintafillou, T.C. and Pleverise, N.,(1991),“Flexural behavior of concrete structures strengthened with epoxy-bonded fiber-reinforced plastics***”***, Poc. Int. Seminar on Plate Bonding Technique, University of Sheffield, U.K.,.

Triantafillou, T.,(1998),"Strengthening of Masonry Structures Using Epoxy-Bonded FRP Laminates", Journal of Composite for Construction, V.2,No.2,pp. 96-104.

U. Ebead, H. Marzouk, and L. M. Lye (2002),"Strengthening of Two-way slabs using FRP materials :A simplified Analysis Based on Response Surface Methodology ",Faculty of Engineering and Applied Science , Memorial university of New found land.

Veljkovic ,(1993,1994,1996), "FEAP: A finite element analysis program user manual: Version 9", Dept. of Civ. and Envir. Engig. University of California, Berkeley, Calif.,<http:// www.ce.berkeley.edu/~rlt/feap/>.

Willam, K. J., and Warnke, E. D., (1975) ,"Constitutive Model for the Triaxial Behavior of Concrete", Proceedings, International Association for Bridge and Structural Engineering, Vol. 19, ISMES, Bergamo, Italy, 174 pp.

Winter, G.,(2004),"Design of Concrete Structures", Thirteen Edition,Vol.278,

Yasuhiro, C.O and Chen, W.F., (1987), “Hypo elastic-perfect plastic model for concrete materials”, Journal of Engineering Mechanics, ASCE, Vol.113, No.12, December, pp.1840-1858.

Zienkiewicz, O.C. (1962), "The use of slab analogy in the determination of thermal stresses" , Int. Journal of Mech. Sciences, 4, 285.

Zienkiewicz, O.C, (1977), "The Finite Element Method", Mc Graw-Hill, third edition,.

Zienkiewicz, O.C., (1989), "The Finite Element Method", Vol.1, Basic formulation and linear problems, McGraw-Hill, Fourth Edition.

الخلاصـــة

ذات الاتجاهين مع وبدون فتحات و المقواة بألياف الكاربون البوليمرية وذلك من خلال تقديم دراسة مختبريه وتحليلية.

يتضمن العمل ألمختبري أعداد وفحص ثلاثين سقف خرساني مسلح, هذه السقوف أعدت بواسطة تطبيق مبدأ النمذجه العملية, نماذج السقوف ر□تبت بالمجموعات (A,B,C,D), حيث مجموعة النماذج (A) هي سقوف بدون فتحات, بينما مجموعة النماذج (B) تمتلك فتحات في منطقة تقاطع شريحتين طرفيتين, مجموعة النماذج (C) تمتلك فتحات في منطقة تقاطع شريحة وسطية مع شريحة طرفية وموقع الفتحة لمجموعة النماذج (D) في منطقة تقاطع شريحتين وسطيتين. ستة وعشرون منها مقواة باستخدام رقائق البوليمر المسلحة بألياف الكاربون, اثنان من السقوف المقواة حملت ب(40%) من الحمل الأقصى ثم أزال التحميل وتم تقويتها برقائق البوليمر المسلحة بألياف الكاربون لغرض دراسة الفرق بين تصليح وتقوية السقوف الخرسانية, تتضمن متغيرات الفحص موقع الفتحة وشكل التقوية, و مما تجدر الإشارة إلية أن كل السقوف قد تم فحصها تحت ظروف الإسناد البسيط.

أظهرت النتائج المختبرية زيادة مهمة في التحمل الأقصى يمكن أن تصل إلى 42% في السقوف المقواة لمجموعة (A) بالمقارنة مع نماذج السيطرة, حيث التقوية باستخدام رقائق البوليمر المسلحة بألياف الكاربون بالاتجاه الموازي لحديد التسليح والعمودي على اتجاه الشقوق المتوقعة كما في النموذج (A-5) هي أفضل حالة. كذلك, الزيادة في التحمل الأقصى يمكن أن يصل إلى 41% في السقوف المقواة لمجموعة (D) بالمقارنة مع نماذج السيطرة, حيث أفضل حالة هي نموذج (D-5) الذي يمتلك تقوية بالاتجاه الموازي لحافات الفتحة والعمودي على اتجاه الشقوق المتوقعة. بينما أظهرت النتائج المختبرية للسقوف المقواة لمجموعتي (B,C) نقصان مهم في التحمل الأقصى تراوحت بين 2.5% إلى 25% بالمقارنة مع نماذج السيطرة, ذلك بسبب فشل القص المفاجئ في هذه النماذج. إضافة إلى ذلك فان وجود رقائق البوليمر المسلحة بألياف الكاربون في الوجه المعرض للشد سوف يحول تصرف المنشأ من المطاوع إلى القصيف.

المواصفات التصميمية لمعهد الخرسانة الامريكي تعطي حدود للانفعال في رقائق البوليمر المسلحة عن طريق استخدام معامل ربط لمنع حدوث الفشل بالربط لرقائق البوليمر المسلحة ولقد تبين أن هذا الحد غير ملائم للتحريات ألحاليه.

العمل التحليلي قدم أنموذجاً لاخطياً ثلاثي الأبعاد للعناصر المحددة ملائماً لتحليل السقوف الخرسانية المسلحة ذات الاتجاهين مع وبدون فتحات و المقواة انحنائيا بألياف الكاربون البولميرية تحت تأثير أحمال تزايدية باستخدام برامج الحاسوب (ANSYS). بشكل عام تم الحصول على توافق بين النتائج المستحصلة من طريقة العناصر المحددة والنتائج المختبرية المتوفرة بنسبة اختلاف تراوحه بين (2%-8%) بالاعتماد على الهطول.

ABSTRACT

This research is devoted to investigate the behavior and performance of R.C. two-way slabs with and without openings and strengthened with (CFRP) sheet, through introducing experimental and analytical study.

The experimental work consists of fabrication and testing of thirty reinforced concrete model slabs, these model slabs were fabricated by application the experimental modeling, the model slabs were arranged in serieses (A,B,C,D), where specimens series (A) are slabs without openings, while specimens series (B) have openings in the common intersection area of column strips. Specimens series (C) have openings in the common intersection area of column strip and middle strip and the location of the opening for specimens series (D) are in the common area of intersection of middle strips. Twenty- six of these slabs have been strengthened with (CFRP) sheet. Two strengthened slabs were loaded by (40%) from ultimate load then, they were unloaded and strengthened with (CFRP) sheet before reload them to study the difference between repairing and strengthening.

The experimental variables considered in the test program include the location of openings and the form of strengthening. All slabs were tested under simply supported condition.

The experimental results showed a significant increase in the ultimate load capacity may reach to 42 percent in strengthened slabs for series (A) as compared to the control slabs, where strengthening by CFRP strip was in parallel direction of reinforcing steel bars and perpendicular to the expected crack, as in specimen (A-5). Also, increase in ultimate load capacity may reach to 41 percent in strengthened slabs for series (D) as compared to the control slabs, where the best case is specimen (D-5) which has strengthening in direction parallel to opening edges and in a perpendicular direction on expected crack which started at opening corners. While the experimental results of strengthened slabs for clarify serieses (B and C) showed a significant decrease in ultimate load capacity ranging from 2.5 to 25 percent as compared to the control slabs, that because suddenly shear failure in these specimens. It was observed that the presence of CFRP sheet on the tension face will transfer the behavior of the slab from ductile to brittle.

The design specification of ACI Committee 440-02 gives a limitation on the strain of FRP sheet using a bond dependent coefficient in order to prevent debonding of FRP sheet and this limitation is shown to be inadequate with present investigation.

The analytical work presents a three-dimensional nonlinear finite element model suitable for the analysis of reinforced concrete two-way slabs with and without openings flexurally strengthened with CFRP sheet under monotonic load using the ANSYS (ANalysis SYStem) computer program. In general, a good agreement between the finite element solutions and experimental results has been obtained with difference about (2 %-8%) based on deflection.

ACKNOWLEDGEMENT

In the name of Allah, the most gracious, the most merciful

At first, thank to ***Allah*** *my* ***God*** *who helped and enabled me to complete this research, and say "from you and to you my lord".*

I wish to express my thanks to my supervisor ***Prof. Dr. Nameer A. Alwash*** *for his advice, guidance and encouragement throughout this work; I am really indebted to him.*

I would like to express my respect and thank to ***Dr. Fathil Al-Hilli*** *for his assistance and explanations which are concerned with the static analysis for* ***ANSYS*** *program.*

I do not know how can I reach my big respect and thank to ***Dr. Chen W.F., Dr. Preece B.W., Dr. Timoshenko S., Dr. Winter G.*** *and* ***Dr. Davies J. D****. because of their useful and beautiful books.*

Deepest thanks are also expressed to the Head and all staff of the Civil Engineering Department in the College of Engineering, University of Babylon for providing facilities throughout the duration of study.

Thanks also extended to the staff of the Structures Laboratory at Engineering College / Kufa University for their help in presenting the various facilities.

A special thank and gratitude to ***my mother*** *and* ***my wife*** *for their care, patience and encouragement throughout the research period.*

Also I wish to thank ***my brothers*** *especially* ***Taha*** *and* ***my sisters*** *for their encouragement during the research period.*

Finally, Thanks to all who participated in providing help and assistance to complete this work.

Hussein Talab Nhabih Al-Wetaifi
2009

To

My Family

With

Love and Respect

Hussein

APPENDIX A

EXPERIMENTAL DATA

Table (A-1) : Physical properties of the cement.

Physical properties	Test results	I.Q.S.5:1984 limits
Fineness ,Blaine,cm^2/gm	3300	≥2300
Setting time ,Vicat's method Initial hrs: min Final hrs : min	 1: 40 3: 20	 ≥ 00 : 45 ≤ 10 : 00
Compressive strength of 70.0 mm cube , MPa 3 days 7 days	 24 34	 ≥ 15 ≥23

Table (A-2) : Chemical composition of the cement.

Oxide	(%)	I.Q.S.5:1984 limits
CaO	63.5	………
SiO_2	20.97	……..
Fe_2O_3	3.67	………
Al_2O_3	5.5	………
MgO	0.7	≤ 5.0
SO_3	2.5	≤ 2.8
Free Lime	0.68	-
Compound composition	**(%)**	**I.Q.S.5:1984 limits**
C_3S	46.97	………..
C_2S	24.77	………..
C_3S	8.37	……….
C_4AF	11.15	……….
L.S.F	0.9	0.66-1.02

Table (A-3): Physical and chemical properties of the aggregate.

Sieve size (mm) and No. of sieve	Percent passing For scale (1/4)
9.5 (3/8in)	100
4.75(3/16in)	100
2.36(no.7)	60
1.18(no.14)	50
0.6(no.25)	40
0.3(no.52)	4
0.15(no.100)	0
0.075(no.200)	0
Properties	**Test results**
Sulphate content SO_3%	0.29
Fineness modulus	2.64
Specific gravity	2.55
Absorption	1.5

APPENDIX B

Ultimate Load of Slab (A-1)

(B-1) by yield line method :-

$$Ext.work = Int.work.$$

$$\sum w\delta = \sum M\theta$$

$$u\sum w\delta = w_u * l^2 * \frac{\delta}{3}$$

$$\theta_x = \theta_y = \frac{2\delta}{l}$$

$$\sum M\theta = m_x * l * \theta_x + m_y * l * \theta_y$$

$$= 8m\delta$$

$$w * l^2 * \frac{\delta}{3} = 8 * m * \delta \Rightarrow M_n = \frac{wl^2}{24}$$

$$M_u = \phi\rho b d^2 f_y (1 - 0.59\rho \frac{f_y}{f_c^{/}})$$

$$M_u = 0.9 * 0.0098 * 1000 * 23^2 * 525(1 - 0.59 * 0.0098 * \frac{525}{27.05})$$

$$M_u = 2.174 kN.m/m$$

$$2.174 = \frac{w_u l^2}{24}$$

$$w_u = 52.176 kN/m^2$$

$$w_u = \phi w_n$$

$$w_n = \frac{52.176}{0.9} = 57.97 kN/m^2 \approx 58 kN/m^2$$

(B-2) BY Method – 3:-

$$ds = 23mm$$
$$dl = 19mm$$
$$\omega = \rho \frac{f_y}{f'_c}$$
$$c^{+D} = 0.036$$
$$c^{+L} = 0.036$$
$$As^{+} = 18 * \frac{\pi}{4} * 4^2 = 226.19mm^2 / m$$
$$\rho = \frac{As}{bd} = \frac{226.19}{1000 * 23} = 0.0098$$
$$\omega = 0.0098 * \frac{525}{27.05} = 0.19$$
$$\omega_{MAX} = 0.325$$
$$\omega < \omega_{MAX}$$
$$R = 0.1687$$
$$R = \frac{M_u}{\phi bd^2 f'_c}$$
$$M_u = 0.9 * 23^2 * 1000 * 27.05 * 0.1687$$
$$M_u = 2.173kN.m$$
$$M_u = (c^{+D} * 1.2w_d + c^{+l} * 1.6w_l) * l^2$$
$$2.173 = (0.036 * 1.2w_d + 0.036 * 1.6 * w_l) * 1^2$$
$$2.173 = 0.036(1.2 * w_d + 1.6w_l)$$
$$w_u = \frac{2.173}{0.036} = 60.36kN / m^2$$
$$w_n = \frac{60.36}{0.9} = 67kN / m^2$$

APPENDIX C

Numerical Data

Table (C-1):Real constant for slab specimen.

Real Constant Set	Element type	Constant			
1 (Concrete)	Solid 65		Real constant for Rebar 1	Real constant for Rebar 2	Real constant for Rebar 3
		Material number	0	0	0
		Volume Ratio	0	0	0
		Orientation Angle	0	0	0
2 (main reinforcement)	Link 8	Cross-sectional area(mm^2)	12.56		
		Initial strain(mm/mm)	0		
3 (CFRP)	Shell 41	Shell thickness at node J TK(J)	0.131		
		node K TK(K)	0.131		
		node L TK(L)	0.131		
		node I TK(I)	0.131		
		Element x axis rotation theta	0		
		Elastic foundation stiffness	0		
		Added mass/unit area	0		

Table(C-2):Material models for the calibration model.

<table>
<tr><th>Material model number</th><th>Element type</th><th>Material properties</th></tr>
<tr><td>1</td><td>Solid 65</td><td>
<table>
<tr><th colspan="2">Linear isotropic</th></tr>
<tr><td>Ex</td><td>24600MPa</td></tr>
<tr><td>PRXY</td><td>0.15</td></tr>
</table>
<table>
<tr><th colspan="3">Multilinear isotropic</th></tr>
<tr><td></td><td>Strain</td><td>Stress</td></tr>
<tr><td>Point 1</td><td>0.000329878</td><td>8.115</td></tr>
<tr><td>Point 2</td><td>0.00055</td><td>12.815</td></tr>
<tr><td>Point 3</td><td>0.00080</td><td>17.515</td></tr>
<tr><td>Point 4</td><td>0.00114</td><td>22.215</td></tr>
<tr><td>Point 5</td><td>0.00220</td><td>27.05</td></tr>
</table>
<table>
<tr><th colspan="2">Concrete</th></tr>
<tr><td>ShrCf-Op</td><td>0.05</td></tr>
<tr><td>ShrCf-Cl</td><td>0.4</td></tr>
<tr><td>UnTensSt</td><td>2.64</td></tr>
<tr><td>UnCompSt</td><td>27.05</td></tr>
<tr><td>BiCompSt</td><td>0</td></tr>
<tr><td>HydroPrs</td><td>0</td></tr>
<tr><td>BiCompSt</td><td>0</td></tr>
<tr><td>UnTensSt</td><td>0</td></tr>
<tr><td>TenCrFac</td><td>0.6</td></tr>
</table>
</td></tr>
<tr><td>2</td><td>Link 8</td><td>
<table>
<tr><th colspan="2">Linear isotropic</th></tr>
<tr><td>Ex</td><td>200000MPa</td></tr>
<tr><td>PRXY</td><td>0.3</td></tr>
</table>
<table>
<tr><th colspan="2">Bilinear isotropic</th></tr>
<tr><td>Yield Stss</td><td>525 MPa</td></tr>
<tr><td>Tang Mod</td><td>10 GPa</td></tr>
</table>
</td></tr>
</table>

<table>
<tr>
<td>3</td>
<td>Shell 41</td>
<td>
<table>
<tr><th colspan="2">Linear orthotropic</th></tr>
<tr><td>Ex</td><td>238000 MPa</td></tr>
<tr><td>Ey</td><td>1</td></tr>
<tr><td>Ez</td><td>1</td></tr>
<tr><td>PRXY</td><td>0</td></tr>
<tr><td>PRYZ</td><td>0</td></tr>
<tr><td>PRXZ</td><td>0</td></tr>
<tr><td>Gxy</td><td>1</td></tr>
<tr><td>Gyz</td><td>1</td></tr>
<tr><td>Gxz</td><td>1</td></tr>
</table>
</td>
</tr>
</table>

Table(C-3):Material models of repair slabs.

Material model number	Element type	Material properties
1	Solid 65	see nested tables below

Linear isotropic	
Ex	**21402MPa**
PRXY	**0.15**

Multilinear isotropic		
	Strain	**Stress**
Point 1	**0**	**0**
Point 2	**0.00048**	**10**
Point 3	**0.00070**	**15**
Point 4	**0.00104**	**20**
Point 5	**0.00252**	**24**

Concrete	
ShrCf-Op	**0.05**
ShrCf-Cl	**0.4**
UnTensSt	**2.64**
UnCompSt	**24**
BiCompSt	**0**
HydroPrs	**0**
BiCompSt	**0**
UnTensSt	**0**
TenCrFac	**0.6**

Table(C-4):Commands used to control nonlinear analysis.

Analysis option	Small displacement static
Calculate prestress effects	No
Time end of load step	0
Automatic time stepping	Off
Number of substeps	100
Max No of substeps	-
Min No of substeps	-
Write items to results file	All solution items
Frequency	Write every substep

Table(C-5):Commands used to control output.

Equation solvers	Program chosen solver
Number of restart files	1
Frequency	Write every substep

Table(C-5):Nonlinear algorithm and convergence criteria parameters.

Line search	On
DOF solution predictor	Prog chosen
Maximum number of iteration	100
Cutback control	**Cutback according to predicted number of iter.**
Equiv plastic strain	0.15
Explicit creep ratio	0.1
Implicit creep ratio	0
Incremental displacement	10000000
Points per cycle	13
Set convergence criteria	
Label	U
Ref.value	Calculated
Tolerance	0.01
Norm	Infinite norm
Min.Ref	Not applicable

Table (C-6): Advanced nonlinear control setting used.

Program behavior upon nonconvergence	Terminate but not exit
Nodal DOF Sol'n	0
Cumulative iter	0
Elapsed time	0
CPU time	0

APPENDIX D

Derivation of Levy's Equation

$$q(x,y) = q_{mn}\sin\frac{m\pi x}{a}\sin\frac{n\pi y}{b}$$

$$\int_0^a\int_0^b q\sin\frac{m\pi x}{a}\sin\frac{n\pi y}{b}\,dydx = \int_0^a\int_0^b q_{mn}\sin^2\frac{m\pi x}{a}\sin^2\frac{n\pi y}{b}\,dydx$$

$$q_{mn} = \frac{16q}{mn\pi^2} \Rightarrow m.and.n.odd$$

$$q_{mn} = 0 \Rightarrow m.and.n.even$$

$$q_{mn} = \frac{-8q}{mn\pi^2} \Rightarrow if.m.odd.and.n.even$$

$$q_{mn} = \frac{8q}{mn\pi^2} \Rightarrow if.m.even.and.n.odd$$

$$\nabla^4 w(x,y) = \frac{q(x,y)}{D}$$

$$w(x,y) = c_{mn}\sin\frac{m\pi x}{a}\sin\frac{n\pi y}{b} \Rightarrow c_{mn} = \frac{q_{mn}}{D\pi^4\left(\frac{m^2}{a^2}+\frac{n^2}{b^2}\right)^2}$$

$$a = b$$

$$at.centerX = \frac{a}{2}, y = \frac{b}{2}$$

$$w(x,y) = \frac{\frac{16q}{mn\pi^2}}{D\pi^4\left(\frac{m^2}{a^2}+\frac{n^2}{a^2}\right)^2}\sin\frac{m\pi}{2}\sin\frac{n\pi}{2} \Rightarrow w(x,y) = \frac{16qa^4}{D\pi^6 mn(m^2+n^2)^2}\sin\frac{m\pi x}{a}\sin\frac{n\pi y}{b}$$

$$w)center = \frac{16qa^4}{D\pi^6}\sum_{m=1,,3,5,\ldots}^{\infty}\sum_{n=1,3,5,\ldots}^{\infty}\frac{\sin\frac{m\pi}{2}\sin\frac{n\pi}{2}}{mn(m^2+n^2)^2}$$

$$w)center = 0.00406\frac{qa^4}{D}$$

CERTIFICATE

I certify that the thesis titled "***Evaluation of the Behavior of Two-Way R.C. Slabs with Openings Strengthened with CFRP*** ", was prepared by "***Hussein Talab Nhabih Al-Wetaifi*** **",** under my supervision at Babylon University in fulfillment of the partial requirements for the degree of Master of Science in Civil Engineering (Structural Engineering).

Signature:

Name**: Prof. Dr. Nameer A. Alwash**

Date: / / 2009

CERTIFICATE OF THE EXAMINING COMMITTEE

We certify as an Examining Committee that we have read this thesis entitled " ***Evaluation of the Behavior of Two-Way R.C. Slabs with Openings Strengthened with CFRP*** ", and examined the student "***Hussein Talab Nhabih Al-Wetaifi*** " in its content and what related to it, and found it meets the standard of thesis for the degree of Master of Science in Civil Engineering (Structural Engineering).

Signature:
Name: **Ass.Prof. Dr. Mustafa B. Dawood**
(Member)
Date: / / 2009

Signature:
Name: **Ass.Prof. Dr. Raad K. Shukur**
(Member)
Date: / / 2009

Signature:
Name: **Prof. Dr. Nameer A. Alwash**
(Supervisor)
Date: / / 2009

Signature:
Name: **Prof. Dr. Ammar Y. Ali**
(Chairman)
Date: / / 2009

Approved by The Head of the Civil Engineering Department

Signature:
Name: **Prof. Dr. Ammar Y. Ali**
(The Head of the Civil Engineering Department)
Date: / / 2009

Approved by The Dean of the College of Engineering

Signature:
Name: **Prof. Dr. Salah Tawfeek Al-Bazzaz**
(The Dean of the College of Engineering)
Date: / / 2009

CHAPTER ONE

INTRODUCTION

1.1 Introduction

Slabs are one of the most important parts of the structural constructions. They are the members in which the thickness is small compared with the other dimensions and they sustain loads normal to their planes. Concrete slabs are widely used as floors not only in industrial and residential buildings but also as decks in bridges. Slabs may be supported on two opposite only, as shown in figure (1.1a), in which case the structural action of the slab is essentially one-way, the loads being carried by the slab in the direction perpendicular to supporting beams. There may be beams on all four sides as shown in figure (1.1b). On the other hand, one-way slab action may be obtained using intermediate beams, as shown in figure (1.1c). **(Winter, 2004)**.

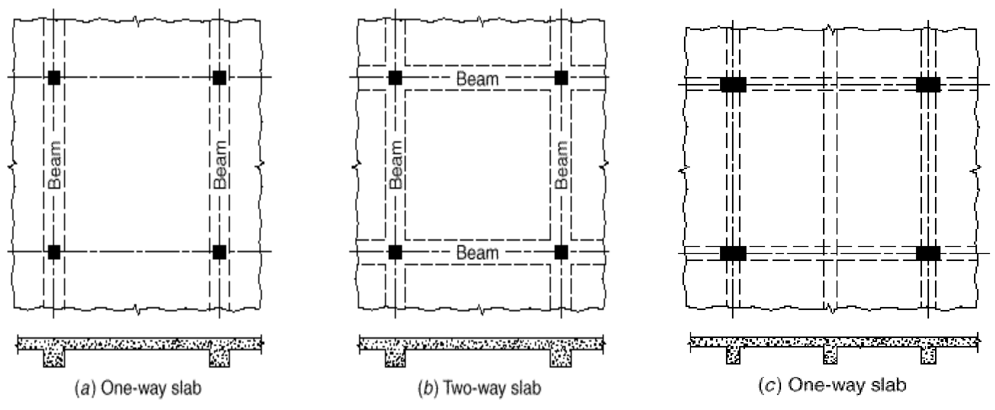

Figure (1-1): Several cases of one-way slab and two-way slab.

Figure (1-2): Several cases of strengthening of two-way R.C. slabs by CFRP with and without openings.

Openings in slabs are usually required for plumbing, fire protection pipes, heat and ventilation ducts and air conditioning. Large openings that could amount to the elimination of a large area within a slab, the locations and sizes of the required openings are usually predetermined in the early stages of design and accommodated accordingly.

It is well known that concrete is a building material with high compressive strength and poor tensile strength. A concrete slab without any form of reinforcement will crack and fail when subjected to a relatively small load **(Nordin, 2003)**.

The failure occurs suddenly in most cases, and in a brittle manner. The most common way to reinforce a concrete structure is to use steel reinforcing bars that are placed in the structure before the concrete is cast. Since a concrete structure usually has a very long life, it is not unusual for the demands on the structure to change with time. The structure may have to carry larger loads at a later date, or fulfil new standards.

In extreme cases, a structure will have to be repaired due to an accident. A further reason can be that errors have been made during the design or construction phase resulting in need for strengthening the structure before usage. If any of these situations should arise, it needs to be determined whether it is more economic to strengthen the existing structure or to replace it. In comparison to constructing a new structure, strengthening an existing one is often more complicated, since the conditions are already set **(Nordin, 2003).**

Strengthening or repairing deteriorating infrastructure, such as bridges and building, has become a major challenge to construction activity all over the world **(Mukhopadhyaya et al., 2001).**

There are many different ways to repair or upgrading a concrete structure. There is often a possibility to use an additional cast on technique to change the physical appearance of the structure and in that way giving it some different properties in strength and stiffness. However, this also means that the structure needs more space which is not always possible **(Nordin, 2003)**.

In the last decades, the development of strong epoxy adhesives has led to the plate bonding strengthening technique. This upgrading technique may be defined as one in which plates of relatively small thickness is bonded with an epoxy adhesive to, in most cases, a concrete structure to improve its structural behavior and strength. One advantage with this technique is that there are no large physical changes of the structure, another is that very high strengthening effects can be achieved.

1.2 Fiber Reinforced Polymer FRP

The term composite often refers to a material composed of two or more distinct parts working together often one of the parts is harder and stronger, while the other is more of a force transferring material. FRP is an abbreviation of fiber reinforced polymers and is a composite of fibers and adhesive. The materials FRP holds many advantages over other materials in civil engineering. It has very high stiffness-to-weight ratio and high strength-to-weight ratio. The material exhibit excellent fatigue properties, non-magnetic properties, corrosion resistance, and is generally resistant to chemicals. The thermal are controllable and both material and geometrical can tailored for the application. Fiber Reinforced Polymer, FRP, is a composite material consisting of fibers and a polymer matrix.

1.2.1 Fiber materials

Several materials are available for the fibers, e.g. glass, aramid, carbon. Almost 95 percent of all applications for strengthening purposes in civil engineering are by carbon fibers **(Nordin, 2003).** Figure (1.3) demonstrate some typical responses of uniaxially loaded fiber materials and steel. HM and HS are abbreviations of high modulus of elasticity and high strength, respectively. Fibers have a linear elastic behavior until failure which is brittle. Table (1.1) compares the material properties of carbon fiber, concrete and steel.

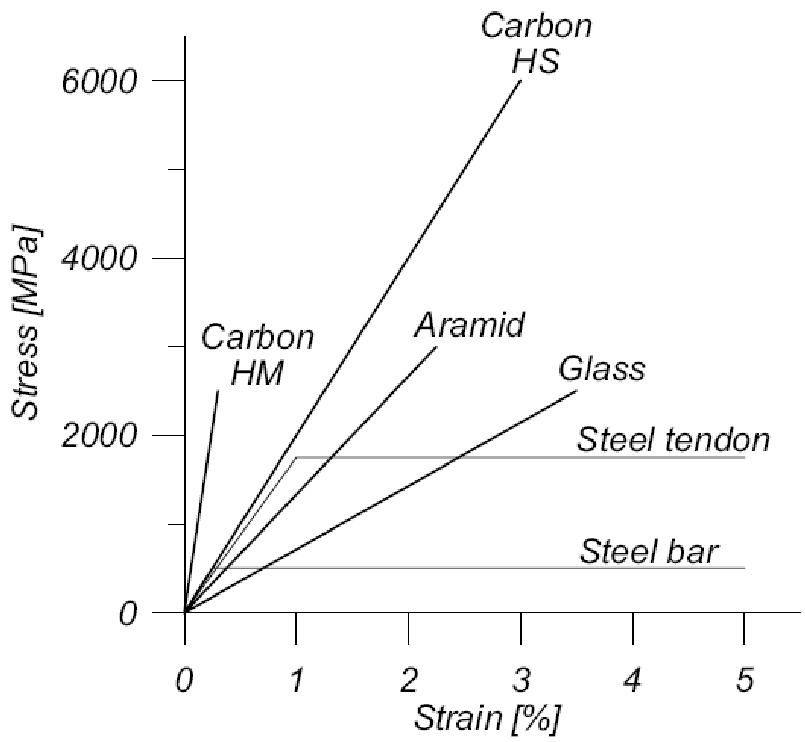

Figure (1-3) : Stress-strain relation ship of fibers and steel **(Carolin, 2003)**.

Table(1.1): Mechanical properties of common strengthening material **(ACI committee 440, 2002).**

Material	Modulus of elasticity GPa	Compressive strength MPa	Tensile strength MPa	Density (Kg/m3)
Concrete	20-40	5-60	1-3	2400
Steel	200-210	240-690	240-690	7800
CFRP	200-800	N.A*	2100-6000	1750-1950

*Not applicable plain fiber buckle

The fibers are what make the FRP strong and there are three things that control the mechanical properties of the FRP **(Nordin, 2003)**:-

- Constituent materials :-

As mentioned earlier there is a wide array of different materials to use. What is important to remember is that the choice of fiber materials determines, together with choice of polymer, what kind of quality, properties and behavior the FRP finally will obtain.

- Fiber amount :-

Regarding the amount of fiber used in the FRP it is easy to say that the more fiber used the better properties will be achieved. This is some what true but with too high fiber content there will be manufacturing problems. If the fibers are tightly packed the matrix will have problems enclosing the fibers which might deteriorate the FRP.

- Fiber Orientation :-

The FRP will be stiffer and stronger in the fiber direction. For example, a rod with all the fibers as very strong in its fiber direction but in perpendicular direction the FRP has not good properties. A typical FRP product for the construction industry has there for a anisotropic behavior compared to steel which is isotropic.

1.2.2 Matrix

The matrix, i.e. the polymer in the composite, is used to bind the fibers together, transfer the force between the fibers and to protect the fibers from external mechanical and environmental damage. The shear forces created between the fibers are limited to the properties of the matrix. The matrix is also the limited factor when applying forces perpendicular to the fibers.

It is important that the matrix has the capability to take a higher strains than the fibers. If not, there will be cracks in the matrix before the fibers fail and fibers will be unprotected. Common matrix materials in civil engineering application are polyester, vinyl ester, and epoxy. Though, epoxy is generally favored **(Lundqvist, 2007)**. The properties of matrix materials are shown in table (1.2).

Table(1.2): Material properties of matrix materials **(Lundqvist, 2007**).

Material	Modulus of elasticity (GPa)	Tensile strength (MPa)	Ultimate tensile strain (%)	Density (Kg/m3)
Polyester	2.1-4.1	20-100	1.0-6.5	1000-1450
Vinyl ester	3.2	80-90	4.0-5.0	------
Epoxy	2.5-4.1	55-130	1.5-9.0	1100-1300

1.3 FRP Strengthening of R.C Members

Fiber Reinforced Polymer (FRP) materials are composite materials consisting of high strength fibers in the shape of polymer matrix. Fibers are selected based on the strength, stiffness, and durability required for specific applications; like wise the resins are selected based on environmental to which the FRP will be exposed to and the method by which the FRP is manufactured. The use of FRP bonded to deteriorated,deficient,and damaged reinforced concrete structures has gained popularity in Europe, Japan, and North America. High–strength FRPs offer great potential for light weight, cost-effective retrofitting of concrete infrastructure through external bonding to concrete members to increase their stiffness and load carrying capacity **(Buyukozturk et al., 2006)**. However, these materials are still almost unknown to engineers in the civil engineering industry **(Nordin, 2003)**, although the knowledge seems to be increasing.

Strengthening with FRP composite can be applied to various types of structural members including slabs,beams,columns and walls. Depending on the member types, the objective of strengthening may be one or a combination of several of the following **(Buyukozturk, 2004)**:-

(1) to increase flexural, axial or shear load capacities.

(2) to increase stiffness to reduce deflections under service and design load.

(3) to increase the remaining fatigue life.

(4) and to increase durability against environmental effects.

1.4 FRP In Infrastructures Rehabilitation

Rehabilitation is a generic term for three concepts; repair, strengthening , and retrofit. Repair is defined as restoring a degraded or damaged structure member to its original capacity. Strengthening is used to increase the capacity of a structural member beyond its designed performance level. The term retrofit is reserved for the seismic upgrade of a structure. FRP material can be utilized for all three applications. The benefits of using FRP in strengthening operations includes simplicity of handling, cutting and installation, small change in strengthened structural member's dimensions. Strengthening with FRP is a rehabilitation method not just reserved for concrete structures. Successful applications have been done for steel **(Carolin, 2003)**, timber **(Johansson et al., 2007)**, and masonry **(Triantafillou, 1998)**. Another field of application for FRP is prestressing of bars and plates, e.g. **(Nordin, 2003)**.

1.5 Objective and Scope of Study

The objectives of the present work are :-

- Investigating the structural responses of CFRP strengthened R.C. slabs under static loading.
- Investigating the effect of location of openings on two-way R.C. slabs and investigate the effect of strengthening it by using CFRP.
- The experimental modeling on two-way slabs and strengthening by CFRP.
- Finite element analysis using **ANSYS** program and comparing the results with those obtained experimentally.

1.6 Layout of Thesis

This thesis is arranged into eight chapters. Chapter one introduces the problem within hand and its importance and applications in structural engineering.

Chapter two reviews literature relevant to the topics of this research including experimental studies and theoretical studies (Finite Element Method).

Chapter three, deals with the description of the experimental modeling, types of models (Indirect models and Direct models), laws of structural similitude and similitude requirements, stress scale factor, length scale factor, strain scale factor, concrete models and uses of concrete models. The next chapter, chapter four deals with the description of the experimental program carried out at the structural laboratory of the civil Engineering Department of Babylon University. The slabs specimen details, materials properties, instullation procedures and test setup for the experiment are presented.

Chapter five presents a discussion regarding the use of CFRP strengthening and the results obtained from the tests presented in chapter four. Chapter six deals with the description of the finite element modeling by **ANSYS** program. The nonlinear solution techniques, element types and material properties are presented.

Analysis results obtained from finite element solution are discussed by using **ANSYS** program and compared with the experimental results in chapter seven.

Finally, chapter eight gives the conclusions of this work, together with suggestions for further work.

CHAPTER TWO

LITERATURE REVIEW

2.1 Introduction

Fiber Reinforced Polymer (FRP) composites as a strengthening material in the construction industry has been in use for almost twenty five years now, with the first applications in Japan and Switzerland. The first commercial use of the material in itself occurred in the mid fifty's. The number of strengthening projects utilizing FRP around the world is increasing as the method becomes more accepted and design guidelines are developed. During the last two and half decades of the previous century, the use of FRP composites in reinforced concrete members has emerged as one of the most promising technologies to address the rehabilitation of infrastructures. There is a wide range of applications for FRP reinforcement that covers new construction as well as the rehabilitation of existing structures. The aim of this chapter is to present a review for the available information concerning the behavior of reinforced concrete slabs with and without openings strengthening by FRP laminates and use of nonlinear finite element analysis for the assessment of strengthening with FRP laminate.

2.2 Experimental Studies

To overcome some of the shortcomings that are associated with steel plate bonding, it was proposed in the mid-1980s that fiber reinforced polymer (FRP) plates could prove advantageous over steel plates in strengthening applications **(Meier et al., 1991)**. Unlike steel, FRPs are unaffected by electrochemical deterioration and can resist the corrosive effects of acids, alkalis, salts and similar aggressive materials under a wide range of temperatures **(Al-Mahaidi, 2003)**. The high material cost of FRP might be a deterrent to its use, but upon a closer look, FRP can be quite competitive. The FRP plates are much thinner than its steel counterpart, which allow lap joints to be made between different elements. The reduced eccentricity of the plate also reduces the tendency for peeling failure. Many published test data showed that flexural strengthening with FRP plates behaves very similarly to steel plates. Besides the classical failure modes, such as steel fracture, concrete crushing or shear failure, bond failures could occur in the interface between the externally bonded FRP plates and the concrete substrate **(Tan, 2002)**. In recent years, many researchers have focused on the flexural performance of the RC slabs strengthened with FRP composites through experimental investigations. During the period from **1980** through **1997**, there were at least 32 documented bridge projects (20 with vehicular traffic) using concrete with FRP reinforcement **(Annex, 1998)**. Of these, six bridges were constructed in Europe (primarily in Germany), seven in North America, and 19 in Japan. Prestressed applications predominated, including 11 bridges constructed with pretensioned FRP-reinforced concrete girders and 10 with post tensioned girders. Five bridges utilized FRP for prestressed slabs, and 11 had FRP rebar in the deck slab or beams. Several bridges utilized more than one type of FRP reinforcement. In general, carbon FRP was used for prestressed reinforcement, although there were also glass and aramid FRP applications.

Non-prestressed reinforcement was typically glass FRP, although carbon FRP was also used.

(Brosens, 1999) repaired the roof slab of the swimming pool of Kalmthout, Belgium, that was constructed in 1974. The roof structure was built up with prestressed concrete beams, on top of which the roof is made using prefabricated reinforced concrete plates covered with cast-in-situ concrete. Tests carried out in the laboratory indicated that chloride ingress and carbonation, combined with an insufficient concrete cover, only about 6 mm on the reinforcement bars, induced steel corrosion. Since the deterioration caused an unacceptable reduction of safety, a thorough repair and strengthening of the roof slab was absolutely necessary. Because of the high amount of chlorides and the high humidity in the swimming pool atmosphere, a real danger of corrosion of externally bonded steel plates existed. The existing steel rebars were removed from the concrete slab. So the rebars could not corrode any further and the deterioration process of the concrete was stopped. The reinforcement of the concrete slab was taken over by the CFRP reinforcement, glued on the concrete surface. The concrete surface was leveled again using epoxy mortar. Figure (2-1). Finally, the repairs were hidden from view by a completely new false ceiling.

Figure (2-1): Concrete damage on roof slab of a swimming pool and end result of CFRP strengthening.

In year **(2000**, **Gemert)** repaired the roof slab of a former school building in Leuven, Belgium, that was transformed into a city library with a considerable increase of load as a consequence. The floor slabs had to be strengthened to increase the bearing capacity from 3 kN/m^2 to 6 kN/m^2. An extensive material investigation was done to determine the material properties and the condition of the construction. Six concrete cores (Ø113 mm) were drilled to determine the concrete compressive strength, resulting in a characteristic value of 22.1 N/mm^2. The concrete tensile strength at the surface was measured by a pull-off test, giving 2.96 N/mm^2. The location and the dimensions of the internal steel reinforcement were found using electro-magnetic waves. The longitudinal reinforcement in the ribs consists of two rebars Ø16 mm. No internal steel stirrups were found. An experimental program revealed that externally bonded CFRP sheets at one side of a beam as shear reinforcement are almost as effective as CFRP sheets bonded at both sides of a beam. For that reason, two layers of CFRP sheets were applied at only one side of the ribs in order to increase the shear capacity of the floor slab. Figure (2-2) gives a view of the repair works and the final result (the alternative).

Figure (2-2): Hybrid strengthening of a ribbed floor slab and application of the CFRP sheets.

Within the next year, **(Alkhrdaji et al., 2001)** investigated the use of FRP strengthening techniques of externally bonded FRP laminates and near surfaces mounted (NSM) FRP rod, prior to demolition, a full-scale bridge was strengthened using the two techniques. Test results indicated that both techniques are effective in increasing the flexural capacity and failure modes of the bridge decks and bridge piers. The bridge was built 1932 and consisted of three simple supported decks made of 460 mm thickness solid reinforced concrete slabs with original roadway width of 7.6m and each simple supported deck spanned 7.9m. The same deck using near surface mounted FRP rods and number of (NSM) reinforcement used was determined to 20 rods spaced at 375 mm and NSM reinforcement considered of CFRP rods with surface roughened by sand blasting to improve bond properties.

(Toong, 2002) presented the behavior of reinforced concrete one-way spanning slabs strengthened by carbon fiber reinforced plastic (CFRP) plates to increase the flexural capacity with particular emphasis on the cracking behavior at working load levels. A total of nine slab specimens were cast to investigate three parameters: steel ratio, pre-loading, and length of CFRP plate. Six specimens were utilized to study the effects of pre-loading before the CFRP plates were attached. The final specimen had a full length CFRP plate to compare with the efficacy of taking the plates beyond the supports. Details of the specimens and failure load are tabulated in table (2-1). Preload of 60% and 80% of the ultimate capacity of the member was applied. All the CFRP strengthened specimens exhibited large increase in load carrying capacity ranging from 60% to 140% with no significant difference in the load carrying capacity for slabs with and without preload. CFRP strengthened members which were preloaded and precracked resulted in wider cracks compared to the members which were not preloaded. Significant improvement in the crack behavior can be achieved with the addition of CFRP plates at the crack widths.

Table (2-1): Specimen details and failure loads **(Toong, 2002)**.

Specimen Symbol	Area of Steel (mm^2)	(Width*Thickness) of CFRP Plates(mm*mm)	Preload (kN)	Ultimate Load (kN)
S6	113	-	-	12.94
S6-50-0	113	50*1.2	0.0	29.79
S6-50-1	113	50*1.2	7.8	30.84
S6-50-2	113	50*1.2	10.4	29.87
S8	201	-	-	20.85
S8-50-0	201	50*1.2	0.0	35.82
S8-50-1	201	50*1.2	12.5	41.13
S8-50-2	201	50*1.2	16.7	34.21
S8-50-0F	201	50*1.2	0.0	32.87

In the same year **(Ebead et al., 2002)** tested six two-way slabs specimens to evaluate the effectiveness of using fiber reinforced plastics as strengthening materials for two way slabs against flexural loads. The tested specimens were square with side length equal to 1900 mm and 150mm thickness. Six (6) specimens were tested and two specimens were used as control (unstrengthened) specimens. The test specimens were simply supported along the four edges with corners free to lift and were axially loaded through the column stub. A parametric study is also carried out to study the impact of the strengthening material type, strengthening material area ratio, span of the slab, reinforcement ratio, and thickness of the slabs. Strengthening specimens using CFRP strips showed an average gain in the ultimate load carrying capacity of about 40% over that of the control un-strengthened specimen. In addition, strengthening specimens using GFRP laminates showed an average gain in the ultimate load carrying capacity of about 31% over that of the control un-strengthened specimen.

A testing program including three slabs was carried out by **(Nanni et al., 2003)** to investigate the behavior of two-way RC flat slabs with a centered square opening. The slabs were tested to failure, consisting of a control specimen with no opening, one specimen with an opening and no strengthening, and one with an opening and three CFRP plies applied to the tension face along each side of the opening. These results revealed that externally bonded CFRP laminates significantly increased both the overall stiffness and flexural capacity of the slabs with an opening. It is shown that such positive-moment strengthening of cutout slabs is entirely viable using CFRP laminates. CFRP anchoring can further increase the performance of the strengthening scheme adopted. Table (2-2) summarizes the overall dimensions of the three two-way RC slabs that were constructed for this experimental program.

Table (2-2): Specimen details **(Nanni et al., 2003)**.

Specimen Symbol	**Dimensions of square slab (m)**	**Thickness of slab (cm)**	**Cut out dimensions (m)**	**Steel ratio in each direction %**	**Steel reinforcement lost in the cut out in each direction %**
SQ1	3.66*3.66	14.0	-	0.419	-
SQ2	3.66*3.66	14.0	1.22*1.22	0.419	33
SQ3	3.66*3.66	14.0	1.22*1.22	0.419	33

The slabs were tested under simply supported conditions and subject to four symmetrical concentrated loads. A 227 ton capacity hydraulic jack, activated by a manual pump, was used to load each specimen. The test results for SQ1-SQ3 shown in table (2-3).

Table (2-3): Test results for SQ1-SQ3 **(Nanni et al., 2003).**

Specimen Symbol	Failure load kN	Load capacity %	Load at first yield of steel reinforcement kN	Max . FRP elongation as % of ultimate
SQ1	489	100	124	-
SQ2	336	69	102	-
SQ3	676	138	147	50%

(Tan et al., 2004) tested six prototype one-way RC slabs with openings at middle span were strengthened with externally bonded carbon fiber-reinforced polymer (CFRP) systems and subjected to concentrated line loads. The following conclusions are drawn:

1. CFRP systems provided an effective method to enhance the load-carrying capacity and stiffness of RC slabs with an opening. All strengthened slabs exhibited a higher load carrying capacity than that of unstrengthened slab.
2. CFRP sheets appear to provide a more effective strengthening system than CFRP strips because of premature debonding failure due to the higher stiffness of the latter.
3. The opening width has a significant effect on the load-carrying capacity of the slabs, compared to the opening length.

In the next year, **(Almusallam, 2005**) tested six reinforced one way solid slabs. The RC one way slabs considered in the study were divided in to three groups. These are:

a) Group SC slabs: they consist of two RC-one way slab which represents the control group without GFRP bars or sheet strengthening.

b) Group SGB slabs: they consist of two RC-one way slab strengthened with five GFRP bars (bar diameter =12.7 mm) at the bottom tension face of the steel bars @ 250 mm c/c, and spacing between bars are 30 cm. They placed in slab using near surface mounted bars method (NSM).

c) Group SGS slabs: they consist of two RC-one way slab strengthened with five GFRP sheets. The dimensions 1080 mm x 210 mm (Length x width) and thickness 0.35 mm. From the test results the following conclusions were drawn:

1) Strengthening of the RC slabs with GFRP bars and sheets increase service, yield, and ultimate strength.

2) The gain in service, ultimate loads obtained in all RC slabs strengthened with GFRP bars is higher than that of control slab by 89.99% and 79.1% respectively.

3) The gain in service, ultimate loads obtained in all RC slabs strengthening with GFRP sheets is higher than that of control slab by 48.95% and 80.1% respectively.

4) Strengthening of RC slabs with GFRP bars show better bonding system than the slabs strengthened and GFRP sheets.

5) Strengthened of RC slabs with GFRP bars and GFRP sheets increase the stiffness of all tested slabs.

(Casadei et al., 2006) presented the results of an experimental program that investigated the behavior of RC one-way continuous flat slabs with openings in both the positive and negative moment regions, strengthened with externally-bonded CFRP laminates following two different schemes of strengthening. The significance of this work is that instead of testing specimens manufactured in the laboratory, the authors had the possibility of using as a research test bed, an old parking garage scheduled for demolition. Experimental results revealed that externally-bonded CFRP sheets can significantly increase the flexural capacity of the system for those specimens containing an opening in the positive moment region. For specimens with an opening in the negative moment region and strengthened using top-surface CFRP laminates, shear failure occurred at a lower load capacity than the original unstrengthened specimen. This has considerable implications for the design of such negative-moment strengthening schemes, and reasons for this behavior are discussed. A total of six one-way square slab specimens were available to be tested within the deck of the garage. The slabs tested with an opening at mid span experienced flexural failure. Table (2-4) reports the test results.

Table (2-4): Test results for S1-S3 **(Casadei et al., 2006)**.

Specimen Symbol	Failure Load (kN)	Max FRP Elongation as % of Ultimate	Load capacity%	Failure mode
S1	307	N/A	100	Flexure (crush)
S2	400	20.6%	130	Flexure (debonding)
S3	337	17.6%	110	Flexure (debonding)

The slabs tested with an opening near to the support line all experienced shear failure in the concrete near the support, with no positive contribution from the FRP. Table (2-5) shows the test results.

Table (2-5): Test results for S4-S6**(Casadei et al., 2006)**.

Specimen Symbol	Failure Load (kN)	Max FRP Elongation as % of Ultimate	Load capacity%	Failure mode
S4	231	N/A	100	Shear
S5	182	19.8%	79	Shear
S6	214	20.6%	92	Shear

(Limam et al., 2007) tested two 7 cm*130 cm*170 cm R.C. two-way slabs with carbon fiber reinforced plastic (CFRP) strips bonded to the tensile face. Results of the experimental study indicate that externally bonded CFRP plates can efficiently used to strengthen two-way R.C. slabs. Results were compared to those of a solid slab without opening and a slab with an unstrengthened opening. The CFRP system proved to be effective in enhancing the load-carrying capacity and stiffness of RC slabs with an opening, provided that premature failure due to CFRP debonding is excluded.

(Seliem et al., 2008) tested five R.C. slabs specimen to use of Carbon Fiber Reinforced Polymers (CFRP) strengthening alternatives to restore the flexural capacity of the R.C. slab after having large openings cut out in the positive moment region. The uniqueness of this study is that the tests were performed on an existing multi-storey RC structure that was scheduled for demolition. Testing a real structure allowed incorporating factors and boundary conditions that typically cannot be simulated in the laboratory. Five tests on five different slabs were conducted to evaluate the ability of the CFRP strengthening alternatives to restore the flexural capacity of the slab after introducing the openings. Three different strengthening techniques were investigated to determine the most effective system for strengthening. The three different strengthening techniques are the use of externally bonded (EB) CFRP laminates, EB CFRP laminates with CFRP anchors, and Near Surface Mounted (NSM) CFRP strips. Test results showed that the three strengthening techniques enhanced the load-carrying capacities of the slabs with openings with the NSM technique more effective than the EB technique. Use of CFRP anchors with EB laminates prevented complete detachment, and hence enabled the slab to restore its full flexural capacity. The slabs were subjected to cyclic loading, involving cycles of loading and unloading as shown in figure (2-3) also this figure show the cross- sectional elevation of the test setup, which is based on the loading protocol of ACI 437R-03 (2003).

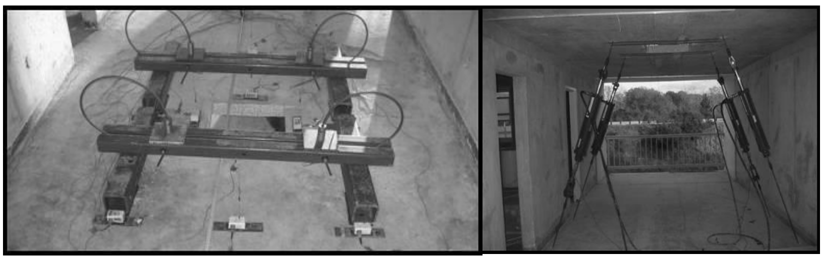

Figure (2-3): Involving cycles of loading and unloading and cross-sectional elevation of the test setup**(Seliem et al., 2008)**.

2.3 Theoretical Studies (Finite Element Method)

The application of the finite element method to the analysis of concrete structures has been growing rapidly since **(Ngo et al., 1967)** first introduced it. Constant strain triangular elements are used to model the concrete and steel and special linkage elements are used to simulate the bond between concrete and steel.

Researches were being carried out simultaneously both at the basic level of material characterization and for the application of the finite element method for analyzing complex structural members with different types of elements. Nonlinear relation between stress and strain of concrete in compression, cracking of concrete in tension, yielding of the reinforcement and the nonlinear relation between steel and concrete are all taken into account.

(Hand et al., 1973) were the first that used the layered finite element model for determining the load-deflection history up to failure of reinforced concrete plates and shells with the incremental-variable elasticity technique. Each layer might have different material properties, but these properties were assumed to be constant over the layer thickness.

The finite element method was used for the nonlinear analysis of reinforced concrete plates and shells by **(Figueiras et al., 1985)**. Both an elastic-perfectly plastic and strain hardening plasticity approach were used to model the compressive behavior of the concrete. Material and geometric nonlinearities were considered in the analysis. Degenerated quadratic thick shell elements using layered discretization through the thickness were used.

(Dyana, 1990, 1991) used plane beam elements to model one-way composite slabs. Special ten-degree of freedom beam elements that can take into account nonlinear slip behavior between the steel deck and concrete slab was used. For this purpose, a special finite element code was developed. By using **ABAQUS**, a commercial general-purpose finite element code, two-node plane **Timoshenko** beam elements were used by **(An 1993)** for one-way slab systems. Two series of beam elements were generated, one for the concrete slab and the other for the steel deck. Shear bond interaction was modeled by using series of spring elements and additional set of equations to the stiffness equations to prescribe imposed relations among the degree of freedoms of the spring, concrete beam and steel deck beam nodes. Three dimensional brick elements were used for a two-way composite slab system. Some difficulties concerning numerical convergence was reported in the 3D model **(An, 1993)**. The problem was thought to be due to mesh sensitivity in relation to the tension-stiffening model of the concrete material. Because of this problem, the concrete material model was replaced by two different plasticity models, each of which was representing the tension and compression parts of the concrete separately.

Other 3D models using brick elements were proposed by **(Veljkovic, 1993, 1994, 1996)**. In their study, **ADINA** was used. It was reported that some trials for concrete tension stiffening functions were needed in some cases before a stable numerical result can be obtained.

(Arduini et al., 1997) used finite element method to simulate the behavior and failure mechanisms of RC slabs strengthened with FRP plates. The FRP plates were modelled with two dimensional plate elements. However the crack patterns were not predicted in that study.

An important numerical study was reported by **(Arnesen et al., 1998)** on the assessment of different cross-sectional configurations for pultruded FRP bridge deck panels. The authors used commercial finite element package **ABAQUS** to compare the behavior of seven shapes most used in research and application, hexagonal (honeycomb), triangular, rectangular, square, thick-top square, enhanced triangular, and enhanced channel were analyzed. The analysis was based on equal cross-sectional area for all seven shapes to reach the optimum cost-performance one since the area of the cross section was the main parameter governing the cost of the bridge deck. The overall depth of the shapes was also kept constant. The authors assumed orthotropic properties for the material and used 3-D block and shell elements for the static and buckling analyses, respectively. It was concluded that the enhanced triangular configuration was the optimum section amongst the seven evaluated. It provided the highest global stiffness and significant improvements in local stiffness and buckling strength.

(Ross et al., 1999) used **ADINA** to analyze their tested slabs. The slabs were 2000 mm square and 150mm thickness and had a clear span of 1900mm using four points bending. Two dimensional, eight-node plane stress elements were used to represent the concrete, while the reinforcing steel and FRP plates were modeled by three-node truss elements. A hypo-elastic constitutive relationship was used for the concrete based on uniaxial stress-strain relationship that accounts for biaxial and triaxial conditions. An elastic-plastic response was assumed for the steel and the CFRP was modeled as linear elastic until failure. The results of the FE analyses were compared to the experimental results and good agreement for the global behavior observed. However, the predicted failure mode was not achieved due to the delamination of the FRP plate. It was concluded that the single most important factor affecting the slab behavior was the bond strength between the concrete and FRP. The use of an anchorage system was suggested to prevent debonding and to utilize the full capacity of the plate.

(Kachlakev et al., 2001) described a linear and nonlinear finite element models for a reinforced concrete deck bridge that had been strengthened with fiber reinforced polymer composites. **ANSYS** and **SAP2000** modeling software were used; however, most the development effort used **ANSYS**. In their study, Perfect bond between materials was assumed. An eight-node solid brick element was used to model the concrete and link element was used to model the steel reinforcement. Two nodes were required for this element. A layered solid brick element was used to model the FPR composites. The model results agreed well with measurements from full-size laboratory deck bridges. Guidelines for developing finite element models for reinforced concrete deck bridges were discussed.

(Burkart, **2002)** described square concrete slabs reinforced with steel and different types of FRP. They were exposed to thermal gradients and mechanical loads. For verification of the experimental results, the experiments were modelled and analysed utilizing the finite-element program **ADINA**. Because of the symmetry of the slab and the load cases, modeling of one quarter of the slab was sufficient, large differences between the calculated and experimental results but in general the development of the results with increasing thermal or mechanical loads was similar. Better correspondence might be achieved by optimizing the finite-element grid.

(Shahawy et al., 2003) made deck panels of E-glass stitched fabric wrapped around foam blocks. The deck was designed using finite element analysis and stresses in the composite materials were limited to only 20% of their ultimate strength, deflection was also limited to Span/800. This extremely conservative design was due to the lack of data and experience on composite bridge decks. Composite action between the FRP deck and the steel girders was deliberately eliminated during design.

(Fu-Ming et al., 2004) presented a reasonable numerical model for reinforced concrete structures strengthened by FRP. Proper constitutive models were introduced to simulate the nonlinear behaviors of reinforced concrete and FRP. The finite element program **ABAQUS** was used to perform the nonlinear failure analysis of the discussed problems. The validity of proposed material models was verified with experimental data and some strengthening schemes were discussed in detail for engineering applications. It has been shown that the use of fiber reinforced plastics can significantly increase the stiffness as well as the ultimate strengths of reinforced concrete slabs. In addition, the nonlinearity of FRP in-plane shear stress-strain relation does not influence the behavior of such composite slabs, because of the small failure shear strain of the composite plates. By considering the proper constitutive models, the authors present a rational numerical model to analyze the reinforced concrete structures strengthened by FRP. In verification, the behavior of both RC slab and retrofitted slab were predicted accurately against the experimental data. If longitudinal directions of the FRP coincide with the yielding lines of RC slabs, the ultimate load of the slab may not increase too much. The best strengthening scheme can be achieved if the longitudinal directions of the FRP and the directions of the maximum bending stress were in parallel.

(Rusinowski, 2005) introduced thesis deals with the problem of opening in two-way concrete slabs. The aim of this thesis was to carry out finite element analysis of tested R.C. slabs with a nonlinear concrete model satisfying complex support conditions. Four types of slabs have been analyzed with help of the program **ABAQUS**. Despite difficulties met in the design of proper boundary conditions, the obtained results were found satisfactory in comparison with the experiments. In the thesis, questions were outlined for further research on finite element modeling of strengthening with carbon fiber reinforcement. Discussion of results lead to general conclusion that using extra reinforcement only in openings corners is not sufficient method of strengthening, where are similar application of CFRP strips in strengthening of cut-offs gives better results thought. This can be explained by the fact that carbon fiber reinforcement is distributed directly on concrete surface in tension which delays cracking furthermore, very important in this case are material properties of carbon fibers. This type of material, in contrast to steel, keeps its elastic properties until failure. Convergence difficulties, possibly caused by snap back behavior, cause limitations in further modeling of the post-failure behavior. The damaged plasticity model is less sensitive to the variable supporting conditions than alternative smeared cracking model and was the only one used in FEM calculations.

(Abbasi et al., 2008) modeled RC slabs strengthened with CFRP plates and sheets using **ANSYS** computer program (version 9.0, 2004) under Microsoft Windows XP (service pack 1, 2002) based on a smeared cracking approach. Perfect bond was assumed between CFRP sheets and concrete interface. This method, however, neglects the premature debonding failure of slabs; with the assumption slip does not take place at the CFRP plate/concrete interface.

In the present study, experimental modeling and theoretical (finite element) investigation are carried out on simply supported square R.C. slabs strengthened with CFRP strips with and without openings. Different CFRP strips arrangements are tested experimentally as well as by finite element method. Also, different possible locations of openings are examined.

CHAPTER FOUR

EXPERIMENTAL WORK

4.1 Introduction

The main objective of the present study is to investigate the behavior of two-way reinforced concrete slabs with and without opening strengthened with externally bonded carbon fiber reinforced polymers (CFRP) sheets. Thirty one specimens were performed for the purpose of investigating the response of strengthened two-way R.C. slabs with and without opening under uniform distributed static loading. One specimen was aborted due to problems with casting operations, resulting in a total of thirty successful tests.

First, program of the work, which describes the experimental variables considered in the present work. Details of the tested specimens and strengthening schemes are described. Next, properties of the constituent materials used in manufacturing the specimens are tabulated. Finally, the experimental setup and instrumentation part of the test program will be explained.

4.2 Program Of The Work

During this research, the study of the behavior of slabs was based on thirty reduced scale reinforced concrete slab specimens casted in laboratory of Civil Engineering Department of Babylon University. The chosen dimensions of all slab specimens were (1050*1050*30mm) (length*width*thickness) according to experimental modeling i.e. (according to length scale factor). All slab specimens had compressive strengths equal to (27.05MPa) and steel ratio equal to (0.00983). The specimens were casted and cured for 28 days. Then at age of 28 days they were strengthening by (CFRP). The slab specimens were arranged in four series. Eight slab specimens without opening existing in series (A), eight slab specimens are put in series (B). These specimens consisted of square opening in the common area intersecting column strips i.e. (at distance 150 mm from a corner edge of specimen). The size of square opening in all modeling slab specimens is (60*60mm), (in prototype equal to (240 *240 mm)). Series (C) consisted of seven specimens with location of opening in these specimens in the common area between a column strip and a middle strip i.e. (at distance 150*400 mm from a corner edge of specimen). Series (D) consisted of seven specimens with location of opening in these specimens is in the common area intersecting two middle strips i.e. (at distance 400*400 mm from a corner edge of specimen). In all slab specimens, reinforced steel bars were spread in two directions at distance equal to twice thickness of slab (i.e. maximum spacing) and make the concrete cover equal to (15mm) in each side of specimen. The cover in bottom surface of slab is equal to (5mm), the steel bars in location of opening were cut in two directions and added on edges of opening to make cover equal to (15mm).

4.3 Details Of The Experimental Work

4-3-1 Moulds preparation

The slab specimens were cast in MDF wood moulds to give a slab specimen with clear dimensions of (1050*1050*30mm). Each one of these MDF wood moulds consisted of a MDF wood plate of (1050*1050*20mm) enclosed by four MDF wood plate. Two plates (50*1090*20mm) were fixed with the MDF wood plate by nails and other plates (50*1050*20mm) were fixed with the MDF wood plate by spikes the contact between four plates satisfied by four locks in corner of mould as shown in figure (4-1). These moulds were cleaned and their internal surface were greased to prevent adhesion with concrete after hardening.

Figure (4-1) : Details of the MDF wood moulds of slab specimens.

4-3-2 Reinforced Concrete Slab Specimens And Strengthening Schemes

Thirty slab specimens of (1050*1050*30mm) were casted. These slab specimens were divided into four series A, B, C and D with target compressive strength (27.05MPa) and with steel ratio of (0.00983). The reinforcement bars were cut to the desired length, then they were uniformly spaced and placed in two directions according to the limited distances of (60mm) i.e. (maximum distances (twice thickness of slab)) to obtain the desired steel ratio of (0.00983). After greasing the moulds of the slab specimens, reinforcement meshes were held carefully in their position inside these moulds. In order to get a constant clear cover, small pieces of steel of (5mm) diameter were placed under the reinforcement. The slab specimens were assumed to be simple supported on the four edges. The clear span after supporting was (950mm). Figure (4-2) shows the details of reinforcement.

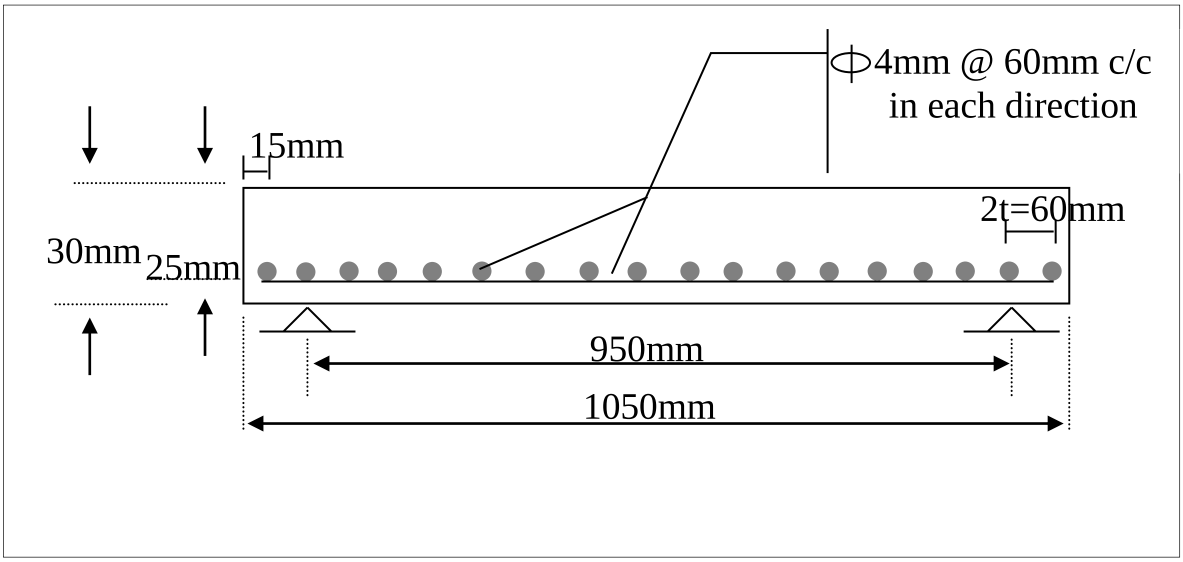

Figure (4-2): Details of reinforcement of the slab specimens.

After 28 days from curing of specimens in water, the CFRP strip were applied on tension face of slab specimens. The strip of CFRP sheet had width equal to 30mm applied in each direction and/or parallel to direction of crack or perpendicular to direction of crack or compound the two types of strengthening. More details of strengthening schemes are given in section 4-3-3.

4-3-3 Specimens Description

In this work, twenty four CFRP strengthened RC slabs, four control slabs without strengthening and two repair slabs were tested. All slabs were designed for flexural failure in order to study the flexural behavior of the strengthened slabs. The parameters considered in this study are technique of strengthening of R.C. two-way slabs by CFRP sheet, location of opening in slabs and methods of strengthening by CFRP sheet and acquaintance the difference between strengthening and repair. The first concrete slab specimen in each series (A,B,C,D) was kept without strengthening and was considered as a control slab for comparison and called to these specimen (A-1,B-1,C-1,D-1). A-1 specimen without opening, A-2 specimen strengthening by CFRP strip in parallel direction of crack, A-3 specimen strengthening by CFRP strip in parallel direction of expected crack and parallel direction of reinforce steel bars in each direction, A-4 specimen strengthening by CFRP strip in parallel direction of reinforced steel bars in each direction, A-5 strengthening by CFRP strip in parallel direction of reinforce steel bars and perpendicular direction of crack, A-6 specimen strengthening by CFRP strip in perpendicular direction of expected crack, A-7 specimen strengthening by CFRP strip parallel direction and perpendicular direction of expected crack, A-8 specimen is called repaired specimen i.e. the specimen loading by 40% from ultimate load and strengthening by CFRP strip by stronger pattern of strengthening. B-2 specimen strengthening by CFRP strip parallel direction of crack pattern started of opening corner, B-3 specimen strengthening in direction parallel of opening edges and in parallel direction of crack pattern started of opening corner. B-4 specimen strengthening by CFRP strip in parallel direction of opening edges, B-5 specimen strengthening in direction parallel of opening edges and perpendicular direction of crack which started of opening corner, B-6 specimen strengthening by CFRP strip perpendicular direction of crack which started of opening corner, B-7 specimen strengthening by CFRP strip perpendicular and parallel of direction crack which started of opening corner, B-8 specimen called repaired specimen i.e the specimen loading by 40% from ultimate load and strengthening by CFRP strip in stronger pattern of strengthening. Series(C) of specimen consisted of seven specimens and this series of specimen like of series (B) from side of strengthening pattern but the location of opening in a common area of intersection of column strip and middle strip. Also series (D) like of series (C) from side of strengthening pattern but the location of opening is in the common area of intersection of middle strip and middle strip, as shown in figure (4-3).

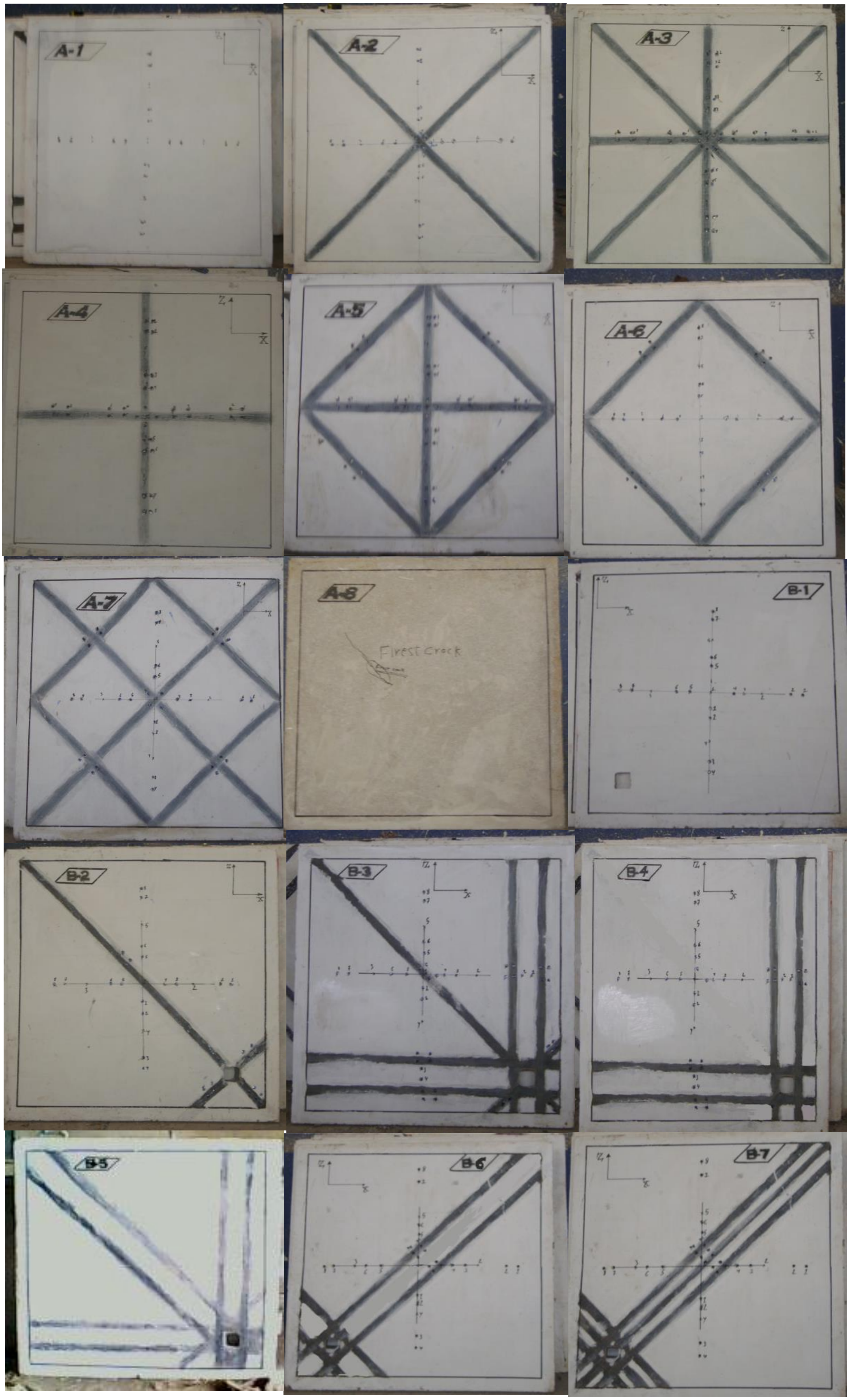

Figure (4-3): Slab specimens.

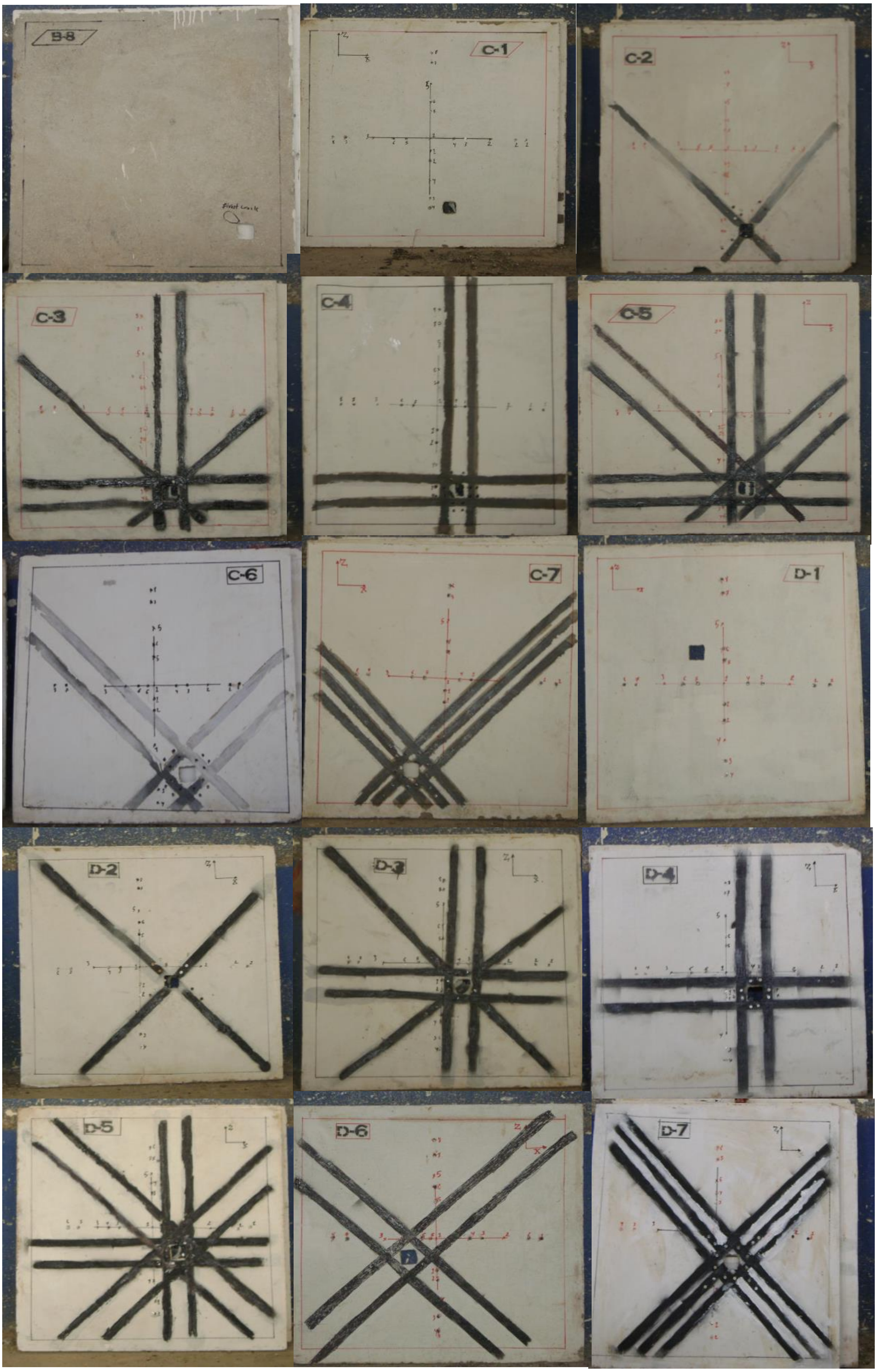

Figure (4-3): Continued.

4-3-4 Dimensions Of Opening

(60*60mm) opening in all specimens are chosen according to ACI-code 2005, 13.5 p.p 64 as shown in figure (4-4).

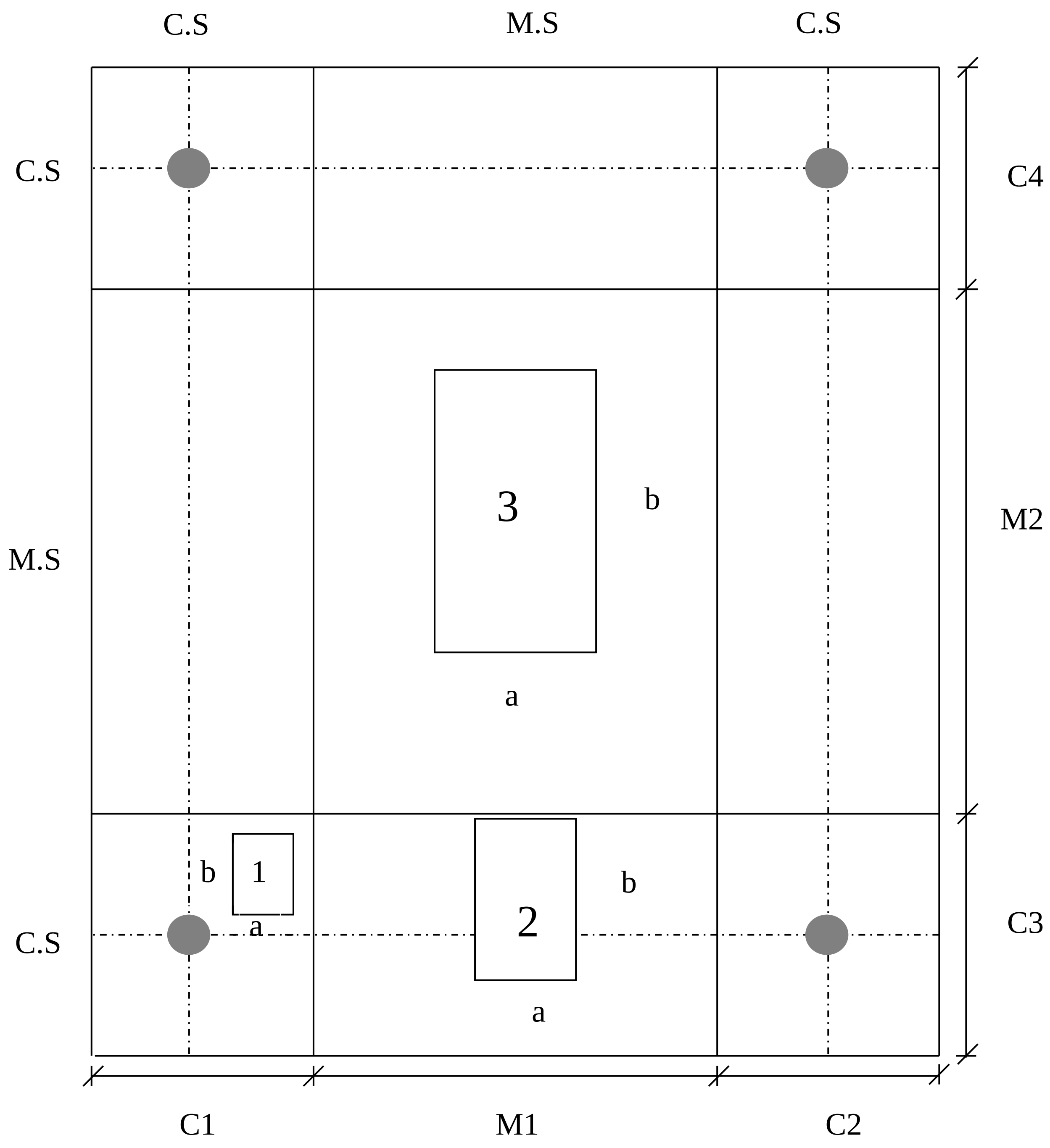

Figure (4-4): Location and the limiting dimensions of opening in two-way slab.(ACI-code, 2005).

Opening	limiting dimension
1	a ≤ 1/8 C1, b ≤ 1/8 C3
2	a ≤ 1/4 M1, b ≤ 1/4 C3
3	a ≤ M1, b ≤ M2

The dimensions of square opening is equal to 60*60mm according to the dimensions of opening (1) and these dimensions are fixed for all openings in the specimens to study the effect of changing the location of opening in two-way slabs.

4.4 Materials

4-4-1 Carbon Fiber Reinforced Polymer and Epoxy

Sika Corporation, Syria branch, provided the CFRP wrap used in this research. **SikaWrap Hex 230C** as shown in figure (4-5), which is a kind of woven composite fabric, was employed in this study. CFRP fabric is unidirectional and has a longitudinal tensile strength of (4300 MPa). The lateral strength of the fabrics is negligible. The fabric strips are elastic until break. The represented properties are given in Table (4-1).

The advantages of the CFRP are: very high tensile strength, outstanding fatigue resistance, non-corrosion, excellent alkali-resistance, low weight, low thickness, available in any length, economical to apply. The disadvantage is its relatively high material cost.

The epoxy resin (**Sikadur-330**) as shown in figure (4-5) used in this research was also provided by Sika corporation, Syria branch. The epoxy consists of two components; part **A** is in white, part **B** is in dark gray. The mix ratio of part **A** and part **B** is four to one by weight. The properties are also given in table (4-1). The advantages of this epoxy can be listed in the following: high mechanical strength, high creep resistance under permanent load, high temperature resistance, long open life, easy to mix and apply, solvent free. This epoxy can be applied to slightly damp concrete surfaces.

Also the epoxy exhibits non-sag in vertical and overhead applications, sets without tackiness, rapid curing even at low temperatures, and shrinkage free curing.

Table (4-1) :Properties of sika's CFRP system.

	Sika Wrap Hex-230C	Sikadur-330
Tensile Strength(MPa)	4300	30
Flexural E-Modulus(GPa)	238	3.8
Specific Gravity	1.5-1.9	1.25-1.45
Density	1.8(g/cc)	1.31(kg/l)
Elongation at break (%)	1.8	0.9
Thickness (mm)	0.131	-

Figure (4-5): Sikawrap hex 230C and sikadur-330.

Ordinary portland cement (type I) of Al-Tasloje mark produced in Iraq was used throughout this investigation. This cement complied the Iraqi specification No.5/1984. The cement was stored in a dry place to avoid the exposure to the atmosphere. The physical properties and chemical composition are presented in appendix A.

4-4-3 Water

Tap water was used throughout this work for both mixing and curing of concrete.

4-4-4 Aggregate

AL-Akhaidher aggregate was used in this investigation. According to aggregate/cement concrete modeling and (1/4) scale, the aggregate grading must be satisfied the grading curve in figure (3-1) in chapter three. Two tons from aggregate are sieved on six save with suitable selection of size aggregate and then remix to satisfied of grading curve in figure (3-1). The physical and chemical properties of the aggregate are listed in appendix A. Figure (4-6) show the aggregate group passing from specific sieve size in table (A-3).

Aggregate before bolted   Aggregate passing from sieve size 3/16 in

Aggregate passing from sieve No.7 Aggregate passing from sieve No.14

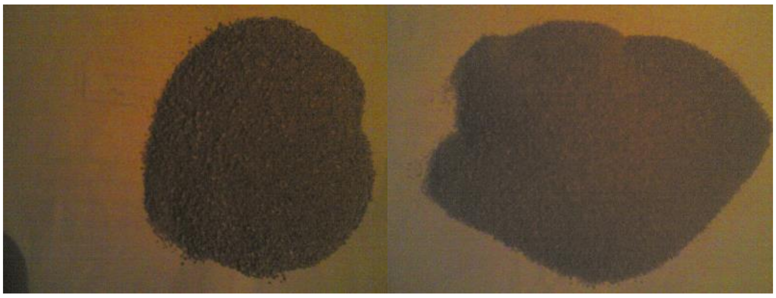

Aggregate passing from sieve No.25   Aggregate passing from sieve No.52

Figure(4-6): Aggregate group passing from specific different sieves size in table (A-3).

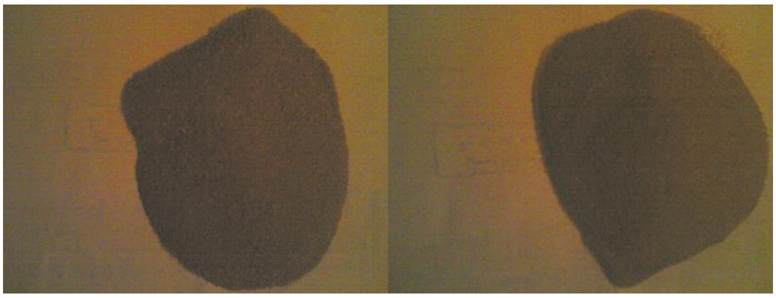

Aggregate passing from sieve No.100Aggregate passing from sieve No.200

Aggregate after selection of size and mixing.

Figure (4-6): Continued.

4-4-5 Steel Reinforcement

Deformed steel bars (4mm) in diameter were used as reinforcement to tested slab specimens. Three specimens of these bars were tested under tension. Configuration of tested steel specimen and machine test is given in figure (4-7).

Figure (4-7): Tested steel reinforcing bar specimens and machine test.

The bars are tested in the Material Laboratory of the Material Engineering Department at Babylon University.

Table (4-2): Show the test results for the used reinforcement bars.

Φ (mm)	Φ equivalent	Pattern	Weight (kg/m)	A_s (mm^2)	f_y (MPa)	f_u (MPa)	Elongation (%)
4	4.984	C*	0.10316	12.56	525	650	2

* Deformation pattern C consists of diagonal ribs inclined at an angle of 60 degrees with respect to the axis of the bar.

4-4-6 Mix Design And Proportion

The concrete modeling mixes were designed according to figure (3-4) in chapter three. The maximum size of modeling aggregate was (3/16in) equal to (4.75mm), the water/cement ratio was equal to 0.5, the cement/aggregate ratio was equal to 1:3.8, and the proportions of the modeling concrete mixes are summarized in table (4-3).

Table(4-3):Mix proportions of modeling concrete mixes.

Mix Proportions (kg/m^3)			
W/C	Water	Cement	Aggregate
0.5	226	453	1721

4.5 Concrete Casting And Curing

Thirty one slab specimens were cast and cured under laboratory conditions at the Civil Engineering Department of the University of Babylon. Also, twelve standard cylinders (38*76mm) were cast from the modeling mortar concrete see figure (4-8).

Figure (4-8):Standard cylinders (38*76 mm) and its steel mould.

The modeling mortar concrete casting and curing procedure is described below:

Slab specimens and cylinders were treated with oil before putting the reinforcement cage or casting control specimens. Before mixing, all the quantities were weighted and backed in a clean plastic container. Prior to starting rotation of the mixer with a capacity of $0.1m^3$, The interior surface of mixer was cleaned and moistened before placing the mix contents. Start the mixer, then add the aggregate, cement, and water with mixing running. Mix the concrete, after all ingredients are in the mixer, for 3 min. followed by a 3 min rest, followed by 2 min final mixing. To eliminate segregation, deposit machine-mixed concrete in the clean, damp mixing pan and remix by hand trowel until it appears to be uniform. Concrete was poured in the moulds in one layer, and the layer was compacted using a plunger mechanical vibrator (3000 vibration per minutes) having a metal rod with diameter of 50 mm for 5 seconds for each insertion (see figure(4-9)). The upper surface of concrete was smoothly finished after casting was completed using hand trowel. Slab specimens were removed from their forms and molds, within 24 hours and then burlap sacks were placed over the slabs and wetted down. Then, a plastic sheet was placed over the slabs. The burlap sacks were monitored and kept wet until the fully twenty-eight days had past. After the water curing and strengthening by CFRP sheet, the slab specimens were painted by white emulsion to ensure clear appearance of crack growth. One slab specimen was aborted due to problems with casting operation, resulting in a total of thirty successful slab specimen.

Figure (4-9): Casting and curing slab specimens.

4.6 Tests of Hardened Concrete

4-6-1 Compressive Strength Test

For the hardened mortar modeling concrete, the compressive strength test was carried out according to modeling of mortar concrete in chapter three, using a machine of (2000kN) maximum capacity as shown in figure (4-10). The load was applied and gradually increased at a constant rate. Cylinders were cast, demoulded and cured in a similar way as for slab specimens. Each compressive strength value was the average compressive strength of three cylinders at age of 3,7,28 days. The average compressive strength shown in table (4-4).

Table (4-4): The average compressive strength.

Age in days	Compressive strength (MPa)
3	10.52
7	18.13
28	27.05

The value of compressive strength is evaluated by equation (4-1).

$$f_c' = \frac{4P}{\pi * d^2} \text{..........}(4-1)$$

Where:-

$f_c' =$ compressive strength.

P=max applied load.

d=diameter of cylinder.

Figure (4-10): Compressive strength testing machine.

4-6-2 Splitting Tensile Strength Test

The splitting tensile strength was determined according to procedure outlined in **ASTM C-496** specification and it was compared with figure (3-3) in chapter three. The cylinders were cast, demoulded and cured in a similar way as for slabs specimens. Each splitting tensile strength value is the average for three specimens at age of 28 days. Apply the steel plate (0.75*6.25mm) (thickness*width) over the cylinder to provide the concentrated stress and the applied uniform load on the test surface of cylinder see figure(4-11).

The tensile strength is equal to (2.64MPa) obtained from the equation (4-2).

$$f_{sp} = \frac{2P}{\pi dl} \text{..................}(4-2)$$

Where:-

f_{sp} =splitting tensile strength.

P =max applied load.

d=diameter of cylinder equal to 38mm.

l=length of cylinder equal to 76 mm.

Steel plate
(0.75*6.25mm)
(thickness*width)

Figure (4-11) : Splitting tensile strength testing machine.

4.7 Installation Of CFRP Strengthening System

4-7-1 Member Surface Treatment

The most crucial part of any strengthening application is the bond between the FRP and the surface to which the FRP was bonded. Proper bond ensures that the force carried by the structural member is transferred effectively to the FRP **(Al-Mahaidi, 2003)**. Before the CFRP was applied to the soffit of the slabs, the surface of the concrete were grinded using an electrical hand grinder to expose the aggregate and to obtain a clean sound surface, free of all contaminants such as cement laitance, and dirt (see figures 4-12 and 4-13).

Figure (4-12): Concrete surface preparation by electrical grinder.

4-7-2 Bonding of Composite Materials to Members

The epoxy used is mixed by hand according to ratio of 4:1 by weight. The epoxy is applied uniformly to both carbon fiber and concrete substrate. The fabric wraps are compressed to the concrete substrate with an ordinary paint roller. The extra epoxy was squeezed out and removed at thickness equal to 1mm on concrete and 1mm on CFRP strip. The specimens were cured at room temperatures for at least 24 hours before testing. The whole procedure can be seen from figures (4-13) and (4-14). In order to investigate the effect of the wrapping configuration on the final load-deflection behavior of RC slabs, Two specimens were loaded by 40% from ultimate load and then repaired with CFRP strips.

Figure (4-13): Materials and mixing tools.

Figure (4-14): Installation of CFRP strengthening system.

4.8 Test Setup

After curing and strengthening by CFRP sheet, the slabs specimens were transported to the Structural Laboratory of Civil Engineering Department in Kufa University, this is to test them under static loading. All the slab specimens were tested in rigid steel frame with L-section, which was designed as a supporting system. Four 12mm in diameter plain bars were welded on the upper of the square steel base to obtain a simply supported condition for a square shape slab of clear dimension of 950mm. A box of dimensions of (1000×1000×100mm), made of steel plate of thickness 2mm and welded the 12mm diameter plain bars on it opened from upper and lower square areas and coated by a sheet of Nylon in the inner surfaces, was used to hold the sand to be placed over the slab as a part of the uniformly distributed load. The sand (100mm) furnishes a good media to distribute the load uniformly coming on the top surface of the sand by the loading base which transmit the load from the hydraulic machine to the layer of sand. Also, steel cube (65*65*65mm) (length*width*high) was put on the opening to prohibit the sand from fail from the opening.

A hydraulic machine with capacity of (2000kN) was used to measure the load applied by a hydraulic machine which transmitted the load to four points using a loading base which consisted of five steel members with I-section of (120×80mm) and length of 500 mm, two of these members were parallel and the other welded perpendicularly upon them. The parallel steel members were connected to four steel legs of (100mm) diameter by (60mm) height, these legs were connected by welding to four steel plates of (250×250×5mm), then, these plates were fixed over a steel plate of (750×750×5mm) by welding. This steel loading base transmitted the load to the 100 mm layer of sand used between the loading base and the slab specimen as shown in figure(4-15). This method of loading was adopted by **(Hidayat, 1994), (Al –Shadidi, 1985)** and **(Abdual –Wahid, 1989)** also.

Figure (4-15): Loading arrangement for uniform load test.

After the preparations were finished and the initial readings of the Demec discs were taken, the load was applied with a loading increment rate of about 5kN/m^2. The deflections were measured at all load stages using a dial gauge with a capacity of (13mm) and accuracy of (0.01mm) at mid span and four points in fourth span of the slab specimens. The dial gauge was fixed in such a way that it can contact the lower surface of the slab specimens. The deflection readings of dial gauge were taken at each 5 kN/m^2. Concrete strains were recorded at selected levels of loading. In addition to that, cracks were detected and drawn on the bottom face of the tested slab. Also the crack width was measured by crack meter.

4-8-1 Instrumentation

During testing, the main characteristics of the structural behavior of the specimens were detected at every stage of loading. At each test, the first cracking load and ultimate load were recorded.

The measurements, which were recorded during the tests, are the following: strain in concrete, strain in CFRP plates, deflection.

Deflection of the slab specimens was measured at mid-span and four points at quarter span of slab using dial gage with travel distance of 13 mm and accuracy of 0.01 mm. A mechanical strain gage having an accuracy of 0.002 mm was used to measure the concrete and CFRP strains. Sixteen pairs of demec discs were used for each tested slab specimen. Demec discs were calibrated using an accompanying special ruler. Arrangement and distribution of these demec discs are shown in figure (4-3).

4-8-2 Testing Procedure

Test started with the application of 2.5 kN/m^2 load to set and check dial gauge, then unloading to zero. At zero loading, initial reading of dial gauges and mechanical stain gauges were obtained. The load was applied in stages. At each load increment, observations of crack development on the concrete slabs were marked with a heavy felt pen and the mechanically measured demec strains reading were taken. The process of reading the gauges and crack observations took approximately five to ten minutes. Once this process was completed, loading was resumed to the next load step. The same procedure was followed. The load was continued until ultimate load (defined as the highest capacity beyond which loading dropped).

CHAPTER FIVE

EXPERIMENTAL RESULTS AND DISCUSSION

5.1 Introduction

The main objective of the current research work is to investigate the effect of CFRP sheets on the flexural behavior of strengthened RC slabs with and without openings. In this chapter, test results from the experimental program will be presented. Different variables were studied experimentally. These experimental variables mainly include, forms of strengthening by CFRP sheet to slab with and without openings and the location of the openings. In the current research program, thirty slab specimens were tested, twenty six slabs were strengthened with CFRP sheet, four slabs were tested without strengthening and two slabs were loaded by 40% of ultimate load and then, repaired by pattern of CFRP in order to study the difference between strengthening and repair. The unstrengthened specimens act as reference slabs for comparison the performance of CFRP strengthened slabs. All the reinforced concrete slabs had the same dimensions and cross-sectional area. Test results were analyzed based on cracking behavior, vertical midspan deflection, ductility, strain distribution of the reinforced concrete slab along two orthogonal directions in tension face, CFRP strain, and failure mode.

5.2 Cracking Behavior

Crack formation was monitored throughout testing to assess the behavior of the strengthened specimens in comparison with the behavior of unstrengthened control slabs. However, this study focused on the debonding behavior, the formation of cracks that led to debonding of the CFRP sheets is discussed in Section 5.6. Only the first cracking load and cracking patterns of all specimens are presented in the following subsections.

5.2.1 First Cracking Loads

In specimens series A and D, external strengthening of RC slab showed better enhancement in first cracking loads when compared with referenced control slabs (A-1,D-1) ,Table 5.1, slab specimen A-2,A-3,A-4,A-5,A-6,A-7,A-8 showed an increase in first cracking load of 0,25,25,50,8.3,25and 0 percent, respectively, when compared with the control slab specimen A-1. From these results, A-5 shows the best behavior. A-5 strengthening was by CFRP strip in a parallel direction of reinforcing steel bars and perpendicular direction on expected crack. While slab specimens D-2,D-3,D-4,D-5,D-6,D-7 showed an increase in first cracking load of 0,10,20,50,20 and 30 percent, respectively, when compared with the control slab specimen D-1. D-5 is best case, where D-5 has opening in the common area of intersection of middle strip and middle strip and strengthening was in the direction parallel to opening edges and perpendicular to the expected crack which started at opening corner. In specimens series B and C external, strengthening of RC slab showed dropping in first cracking loads when compared with reference control slabs (B-1,C-1), Table 5.1, slab specimen B-2,B-3,B-4,B-5,B-6,B-7,B-8 showed an decrease in first cracking load of 0,12.5,12.5,12.5,0,0and 0 percent, respectively, when compared with the control slab specimen B-1. The worst case from above results is B-5, where B-5 like of D-5 from view of strengthening pattern but the location of opening in the common area of intersection of column strip and column strips. While slab specimens C-2,C-3,C-4,C-5,C-6,C-7 showed an decrease in first cracking load of 0,11,11,11,0 and 0 percent, respectively, when compared with the control slab specimen C-1. From these results, C-5 shows the worst behavior. where C-5 has opening in the common area of intersection of middle strip and column strip and strengthening in direction parallel of opening edges and perpendicular direction of expected crack which started at opening corner. On the other hand slab specimens B-1,C-1,D-1 showed a decrease in first cracking load of 33,25,17 percent, respectively, when compared with the control slab specimen A-1. This is due to opening existence.

Table (5-1) : First cracking load for the tested slab.

specimen	First cracking load , kN/m^2	Increase in cracking load, %	specimen	First cracking load , kN/m^2	Increase in cracking load, %
A-1	12	N.A	B-8	8	0
A-2	12	0	C-1	9	N.A
A-3	15	25	C-2	9	0
A-4	15	25	C-3	8	-11
A-5	18	50	C-4	8	-11
A-6	13	8.3	C-5	8	-11
A-7	15	25	C-6	9	0
A-8	12	0	C-7	9	0
B-1	8	N.A	D-1	10	N.A
B-2	8	0	D-2	10	0
B-3	7	-12.5	D-3	11	10
B-4	7	-12.5	D-4	12	20
B-5	7	-12.5	D-5	15	50
B-6	8	0	D-6	12	20
B-7	8	0	D-7	13	30

5.2.2 Cracking Patterns

The cracking behavior of each series slab specimen is discussed in the following:

- Series (A) slab specimen :-

The control slab specimen A-1 behaved in expected fashion under flexural loading. The appearance of flexural cracks was first at 12 kN/m^2 within the mid span. At 20 kN/m^2, new flexural cracks formed and developed diagonally from the mid span of the specimen. The shear crack appeared at a load of 30 kN/m^2 along the support. In compression face the cracks appearance in corner of specimen at load 15 kN/m^2 due to holding down force. At 50 kN/m^2, the cracks did not grow for the reminder of the test but the flexural cracks in the mid span widened. Failure of the test specimen was by yielding of steel followed crushing of the concrete at the compression fiber, as shown in figure (5.1).

While in strengthened slab specimen A-2, the first cracking was observed at 12 kN/m^2. The crack pattern of this specimen has mainly the same behavior of crack propagation of A-1 due to the CFRP strips along the diagonal of slab. Failure of the test specimen was by yielding of steel followed crushing of the concrete at the compression fiber, debonding failure occurred at 55.5 kN/m^2 due to flexural crack. As shown in figure(5-1). For strengthened slab specimens A-3, the first cracking was observed at the load of 15 kN/m^2 with initial crack forming in the mid span of slab. As the load was increased new cracks formed along the diagonal of slab. In fact, cracks did not open widely during the post-cracking behavior of the slab, since the presence of the CFRP sheet delay the crack initiation and arrested their propagation. Also, distinct reduction in the number of cracks was observed (figure 5-1). The formation of flexure cracks that occurred as a result of the yielding of embedded steel reinforcement generated high stresses in the CFRP sheet across the cracks. Since the concrete could not maintain the interface shear stresses, cracks at the interface between the

CFRP and the concrete were formed. Peeling of the CFRP sheet from the concrete slab occurred at 76 kN/m^2. The CFRP sheet ripped adhesive and a thin layer of the concrete off from the slab soffit. Finally, debonding failure occurred at 76 kN/m^2. The crack pattern of strengthened slab specimens A-4 is similar to crack pattern of slab A-3. As shown in figure (5-1). The cracks of strengthened slab specimens A-5 is veiled in mid span of slab due to the CFRP sheet perpendicular to the yield line of slab as shown in figure (5-1). The crack pattern of strengthened slab specimens A-6 is rather similar to crack pattern of A-5 as shown in figure (5-1). For strengthened slab specimens A-7, the crack pattern of this slab is complex from crack patterns of A-2 to A-6 as shown in figure (5-1). The repaired slab specimens A-8, which loaded by (40%) of ultimate load and strengthening by pattern of strongest specimen i.e (A-5), the crack pattern of this slab is similar to crack pattern of A-5 as shown in figure (5-1).

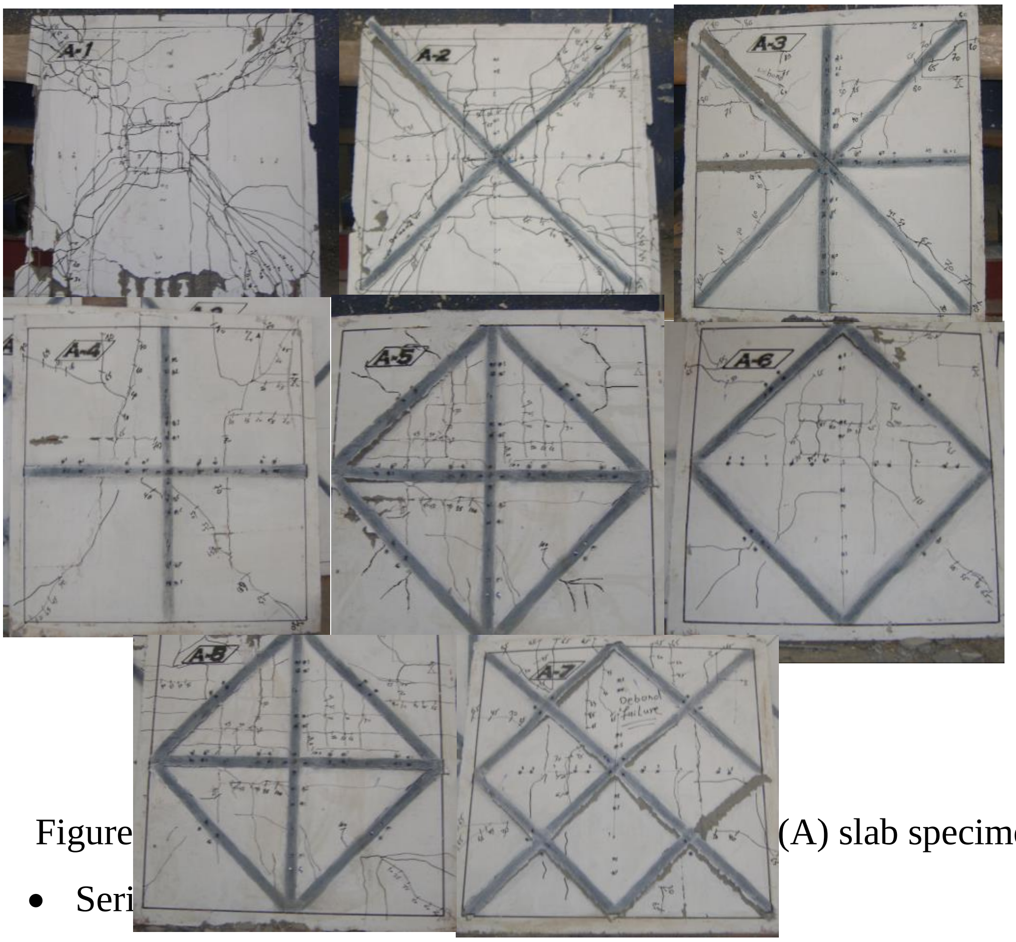

Figure (A) slab specimen.

- Seri

In control slab specimen B-1, the shear cracks appeared at the corners of opening at a load of approximately 8 kN/m^2 due to high stress concentration near the corners of openings. The flexural cracks appeared at the mid span at a load of approximately 12 kN/m^2. At 20 kN/m^2 flexural cracks were wide speared a long the diagonally of slab also the shear cracks in corner of opening wide speared diagonal on top face, in bottom face cracks developed circularly around the opening. Shear failure was sudden accour at load equal to 40 kN/m^2 as shown in figure (5-2).

For strengthened slab specimen B-2, the crack pattern of this slab is likely similar to crack pattern of specimen B-1, as shown in figure (5-2).

In strengthened slab specimen B-3, the first crack occurred at a lower load than of the unstrengthened slab specimen B-1, which was observed at an applied load of 7 kN/m^2. The flexural cracks appeared in the mid span at a load of 13 kN/m^2. At load 30 kN/m^2 flexure of cracks were wide speared a long the diagonal of slab also the shear cracks in corner of opening wide speared diagonally on top face, in bottom face cracks developed circularly around the opening. As shown in figure (5-2). The shear failure and debonding in CFRP near the opening were sudden occur in load equal to 31 kN/m^2. The cracks pattern of strengthened slabs specimens B-4 and B-5 is similar to crack pattern of B-3 as shown in figure (5-2).

For strengthened slab specimen B-6, the shear cracks appeared in the corners of opening at a load of approximately 8 kN/m^2 due to high stress concentration near the corners of openings. The flexural cracks appeared in the mid span at a load of approximately 10 kN/m^2. At 15 kN/m^2 flexural cracks propagated a long the diagonal of slab. Also the shear cracks at corner of the opening were wide speared diagonally on top face. In bottom face, cracks developed circularly around the opening. Shear failure and debonding in CFRP near the opening were suddenly accour at load level equal to 38 kN/m^2 as shown in figure (5-2). For strengthened slab specimen B-7, the crack pattern of this slab is similar to crack pattern of specimen B-

6, as shown in figure (5-2). While repaired slab specimen B-8, which was loaded by load (40%) from ultimate load and strengthening by pattern of strongest specimen i.e (specimen B-2), the crack pattern of this slab is similar to crack pattern of B-2 as shown in figure (5-2).

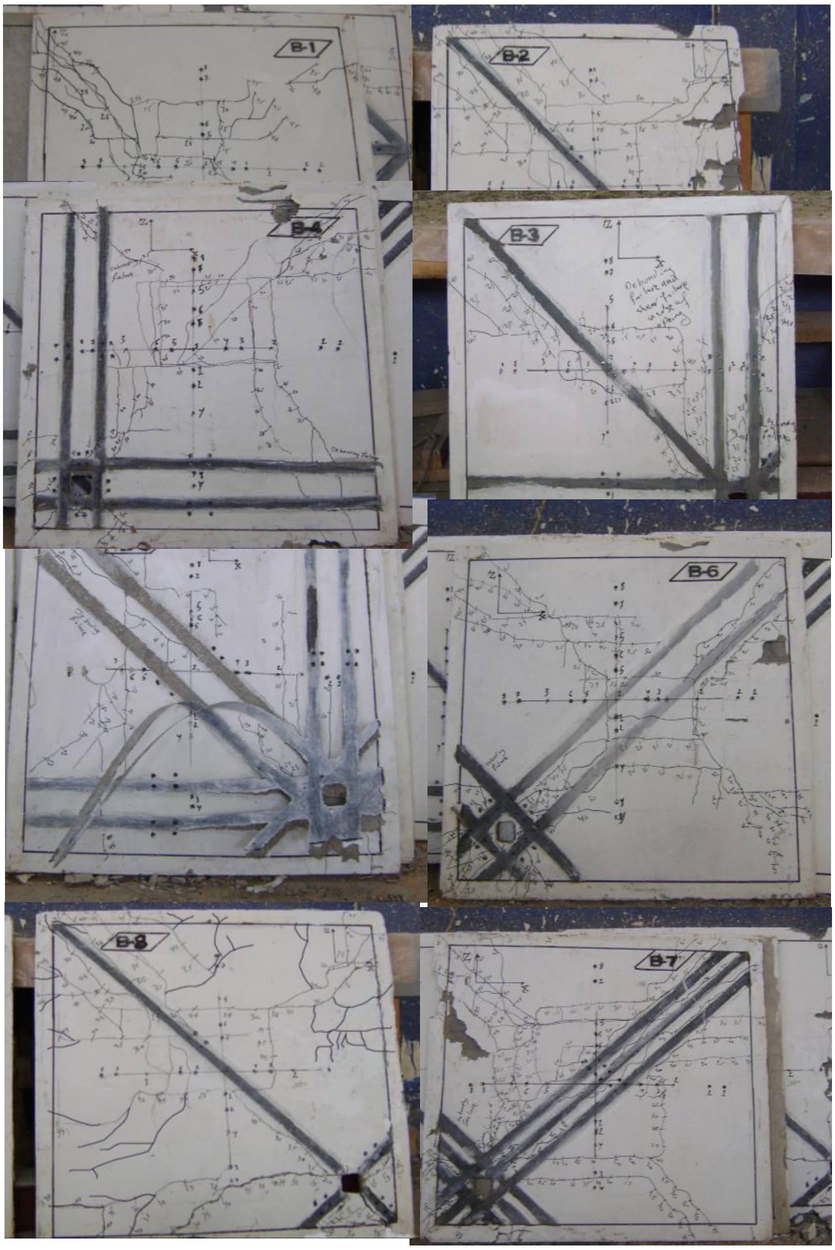

Figure (5.2): Crack pattern after failure for series (B) slab specimen.

- Series (C) slab specimen :-

In control slab specimen C-1, the shear cracks appeared in the corners of opening at a load of approximately 9 kN/m^2 due to high stress concentration near the corners of openings. The flexural cracks appeared at the mid span at a load of approximately 13 kN/m^2, at 30 kN/m^2 flexural cracks were propagate a long the diagonal of slab. Also the shear cracks in the corner of the opening wide speared in the diagonal direction on top face while in the bottom face cracks developed circularly around the opening as shown in figure(5-3). Shear failure was sudden accour in load equal to 46 kN/m^2. For strengthened slab specimen C-2, the crack pattern of this slab similar to crack pattern of specimen C-1, as shown in figure (5-3). In strengthened slab specimen C-3, the first crack occurred at a lower load than of the unstrengthened slab specimen C-1, which was observed at an applied load of 8 kN/m^2. The flexural cracks appeared in the mid span at a load of 14 kN/m^2, at load 35 kN/m^2 flexure of cracks were wide speared a long the diagonal of slab also the shear cracks in corner of opening wide speared diagonal on top face, in bottom face cracks developed circularly around the opening. As shown in figure (5-3). The shear failure and debonding in CFRP near the opening were sudden occur in load equal to 35.5 kN/m^2. The cracks pattern of strengthened slabs specimens C-4 and C-5 is similar to crack pattern of C-3 as shown in figure (5-3). For strengthened slab specimen C-6, the shear cracks appeared in the corners of opening at a load of approximately 9 kN/m^2 due to high stress concentration near the corners of openings . The flexural cracks appeared in the mid span at a load of approximately 13 kN/m^2, at 20 kN/m^2 flexural cracks were wide speared a long the diagonal of slab also the shear cracks in corner of opening wide speared diagonal on top face, in bottom face cracks developed circularly around the opening. Shear failure and debonding in CFRP near the opening were sudden accour in load equal to 43.5 kN/m^2 as shown in figure (5-3). For strengthened slab specimen C-7, the crack pattern of this slab similar to crack pattern of specimen C-6, as shown in figure (5-3).

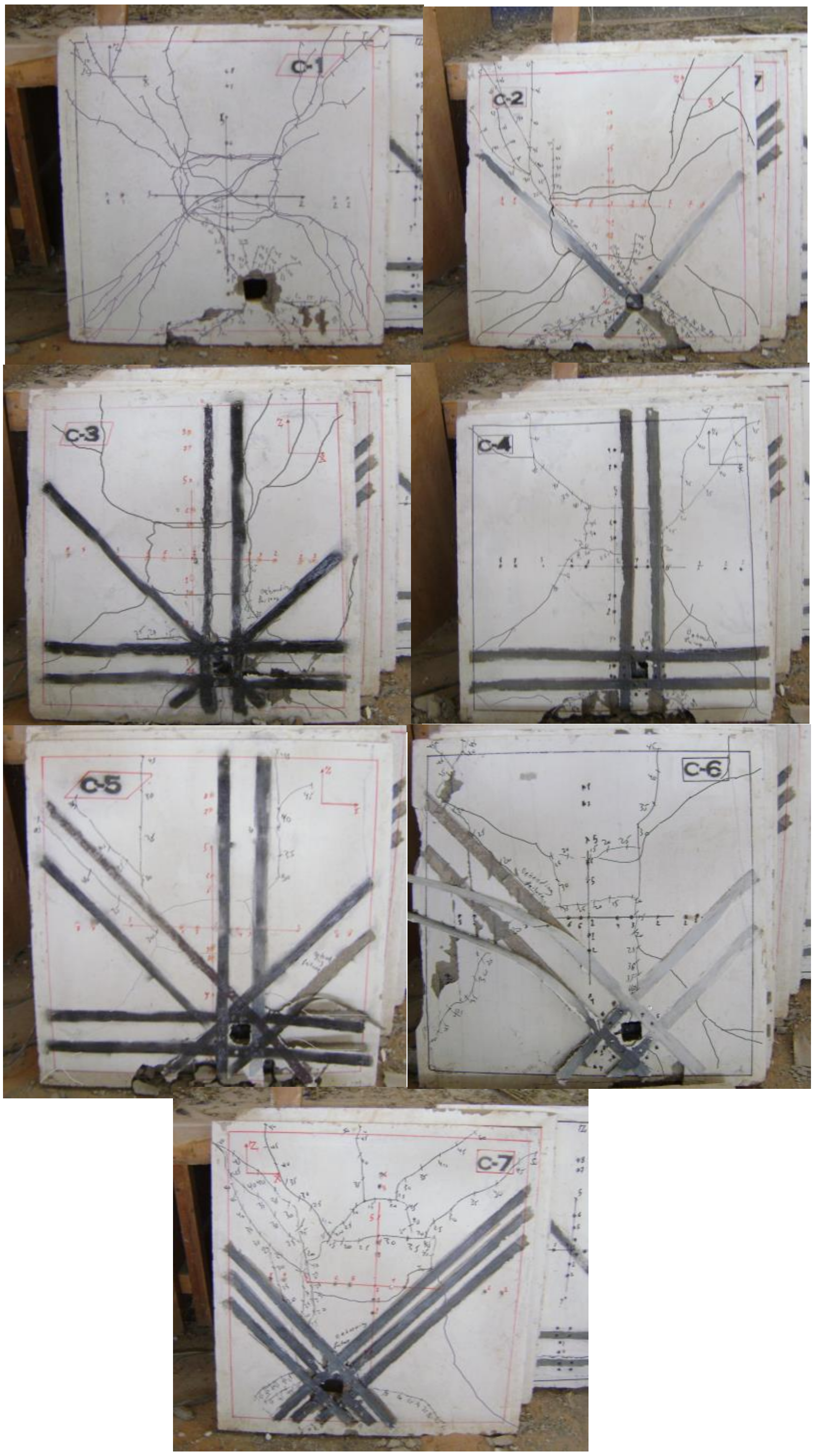

Figure (5.3): Crack pattern after failure for series (C) slab specimen.

- Series (D) slab specimen :-

The control slab specimen D-1 behaved in expected fashion under flexural loading. The appearance of flexural cracks was first at 10 kN/m^2

within the mid span. At 20 kN/m^2, new flexural cracks formed and developed diagonally from the mid span of the specimen. The shear crack appeared along the support side and the edge of opening. Failure of the test specimen was by yielding of steel followed crushing of the concrete at the compression fiber, as shown in figure (5.4).

While in strengthened slab specimen D-2, the first cracking was observed at 10 kN/m2. The behavior of crack to this specimen same behavior of crack to D-1 due to the CFRP strips along the diagonal of opening in slab. Failure of the test specimen was by yielding of steel followed crushing of the concrete at the compression fiber, debonding failure occurred at 49.5 kN/m^2 due to flexural crack. As shown in figure (5-4). For strengthened slab specimens D-3, the first crack occurred at a higher load than of the unstrengthened slab specimen D-1, which was observed at an applied load of 11 kN/m^2. Then developed diagonally from the corners of opening. The slab failed by yield of steel flowed crushing of the concrete on the top surface with extensive cracking on the bottom face and debonding accour at load of failure equal to 67 kN/m^2. The debonding was caused by flexural cracks developed diagonally from the corners of opening, as shown in figure (5-4). The crack pattern of strengthened slab specimens D-4 similar to crack pattern of slab D-3. As shown in figure (5-4). The cracks of strengthened slab specimens D-5 and D-6 is similar to crack pattern of D-7 as shown in figure (5-4).

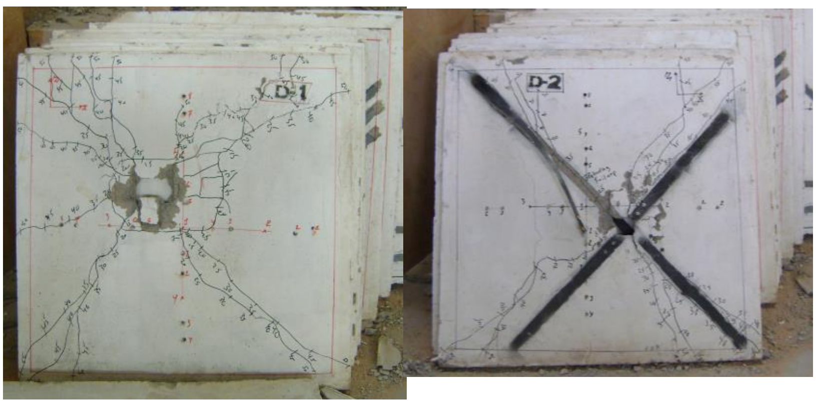

Figure (5.4): Crack pattern after failure for series (D) slab specimen.

5.2.3 Flexural Crack width

Cracking occurs when the concrete tensile stress in a member reaches the tensile strength. The presence of the CFRP sheet delays the crack initiation and arrested their propagation. Also, distinct reduction is observed in the number and width of cracks. For example, the crack width of the control slab A-1 was 0.4 mm at a load 35 kN/m^2 while the crack width of the slab A-5 was 0.23 mm at a load 35 kN/m^2. The relation between load and crack width for four series is shown in figures(5-5)-(5-8).

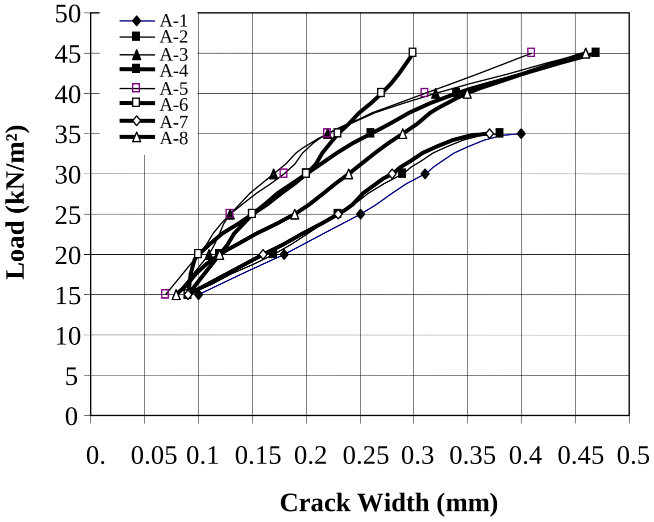

Figure (5-5) : Crack width for series A.

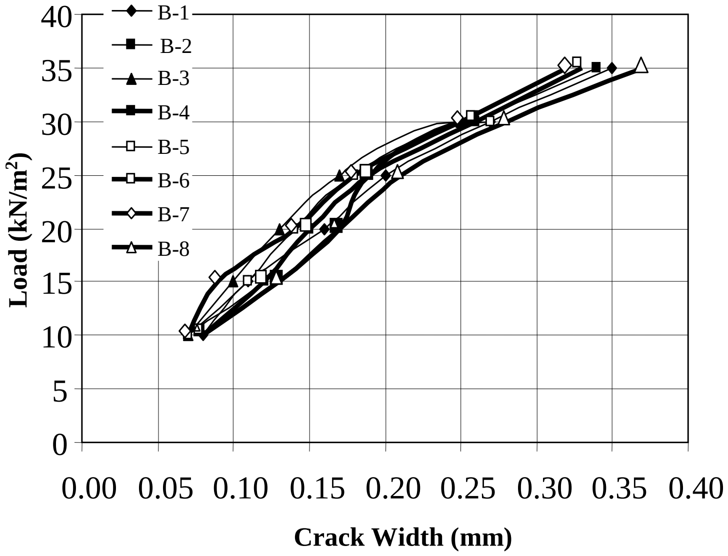

Figure (5-6): Crack width for series B.

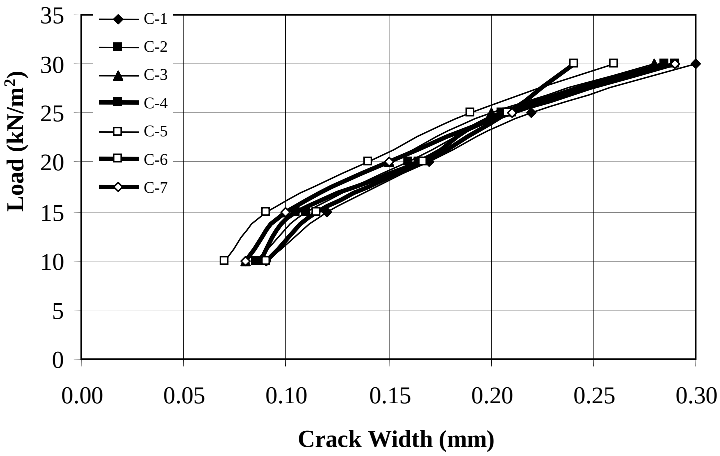

Figure (5-7): Crack width for series C.

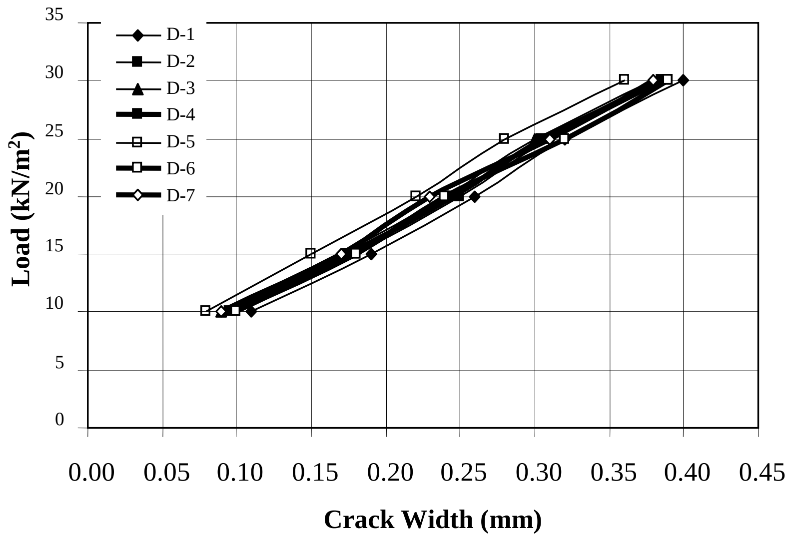

Figure (5-8): Crack width for series D.

5.3 Load–Deflection Curves

The structural behavior of tested slab specimens are represented here by their load versus midspan deflection shown in figures (5-9) to figure (5-13). To measure the deflection of slab, five dial gage were placed at mid span point and at quarter span points of slab for each specimen. Generally, it can be observed that the load versus midspan deflection response can be divided into three stages of behavior. The first stage was characterized by an approximately linear relationship between the load and the midspan deflection. During this stage of behavior, the section was uncracked and both the concrete and steel, in addition to the CFRP sheet , behave essentially elastic. The second stage represents the behavior beyond the initial cracking of the composite section where the stiffness of the slab was decreased as indicated by the reduced slope of the load versus midspan deflection curve. The end of this stage was distinguished when the main steel reinforcement start to exhibit inelastic behavior. The third stage was characterized by a clear decreasing slope of the curve, where the tension steel reinforcement reaches the strain ultimate stage. For the unstrengthened control specimens (A-1 and D-1), a large increase in deflection was noticed in the third stage, while the applied load changed little. The strengthened slab specimens in series (A,D) failed suddenly and exhibited no ductility. In addition, the specimens in series (B,C) failed suddenly and did not reach the third stage because these specimens failed in shear.

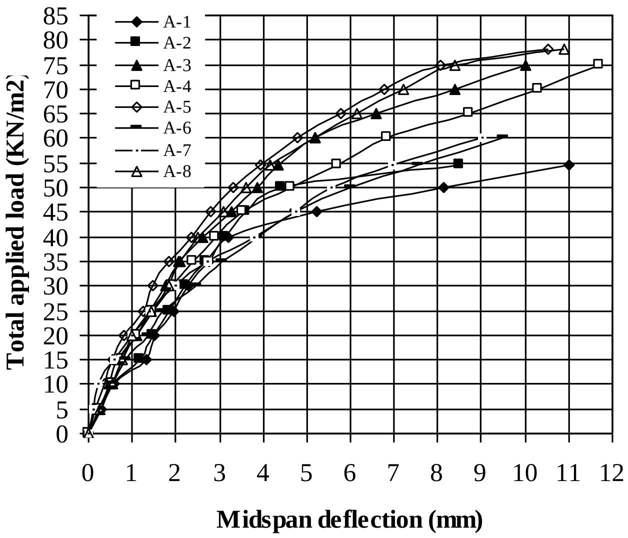

Figure (5-9): Load versus deflection for slab in series A.

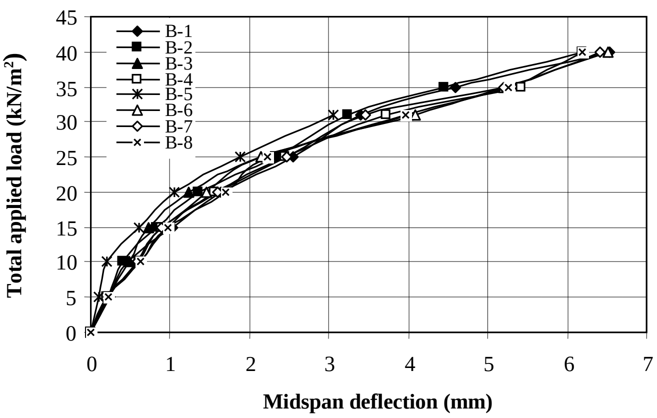

Figure (5-10) : Load versus deflection for slab in series B.

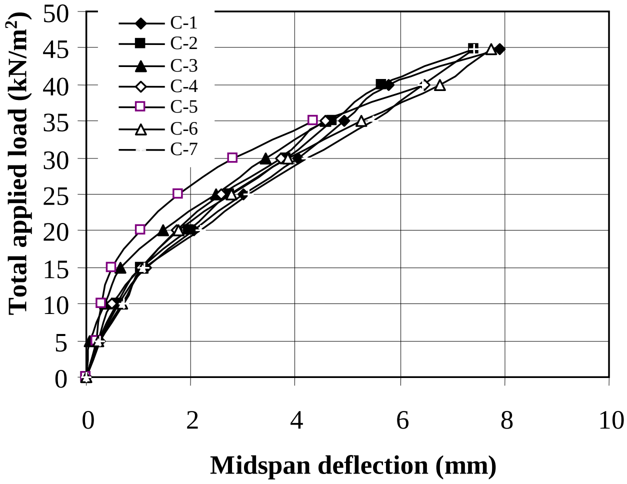

Figure (5-11) : Load versus deflection for slab in series C.

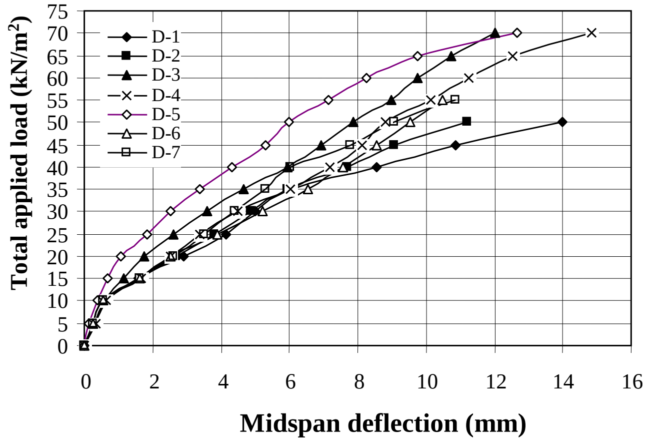

Figure (5-12) : Load versus deflection for slab in series D.

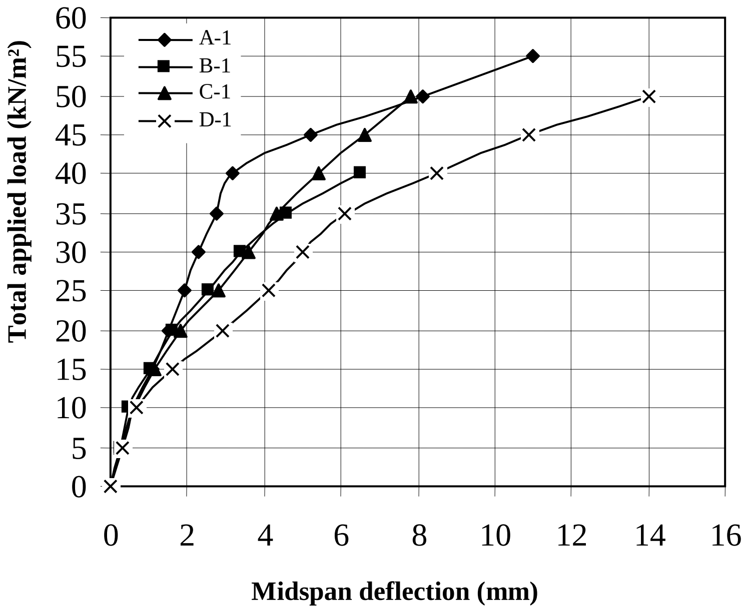

Figure (5-13): Load versus deflection for control slabs A-1,B-1,C-1,D-1.

Generally, the deflection of the slabs strengthened with CFRP was lower than the deflection of the corresponding control slab. The reduction in the midspan deflections for each slab specimen is given in table (5-2).

Table (5-2): Midspan deflection for each slabs.

Specimen	Max.midspan deflection (mm)	Reduction in the midspan deflection (%)	Specimen	Max.midspan deflection (mm)	Reduction in the midspan deflection (%)
A-1	11	N.A	B-8	6.19	5
A-2	8.5	22.7	C-1	7.8	N.A
A-3	10	9	C-2	7.41	5
A-4	11.69	-6.27	C-3	6.94	11
A-5	10.51	4.45	C-4	6.47	17
A-6	9.5	13.6	C-5	6.47	17
A-7	9	18.18	C-6	7.79	0.15
A-8	10.52	4.4	C-7	7.41	5
B-1	6.53	N.A	D-1	14	N.A
B-2	6.21	5	D-2	11.2	20

B-3	5.81	11	D-3	12.04	14
B-4	5.43	17	D-4	14.84	-6
B-5	5.42	17	D-5	12.67	9.5
B-6	6.52	0.15	D-6	10.5	25
B-7	6.41	5	D-7	10.85	22.5

From figure (5-9) and (5-10) show no large difference between repaired specimens (A-8,B-8) and the corresponding strengthening specimen (A-5,B-2) in load deflection curve.

5.4 Ductility Ratios

The ductility of a slab can be defined as its ability to sustain inelastic deformation without loss in its load carrying capacity prior to failure. Following this definition, ductility can be expressed in terms of deformation. Ductility can be evaluated as the ratio of ultimate deformation to deformation at yield. The deformation can be strains, deflections, or curvatures. The Ductility ratio and reduction in ductility ratio is shown in table (5-3).

Table (5-3): Ductility ratio and reduction in ductility ratio for the tested slabs.

specimen	Deflection (mm)		Ductility ratio	Redaction in ductility ratios %
	yielding	ultimate		
A-1	3.2	11	3.4	N.A
A-2	4.4	8.5	1.93	43
A-3	6.66	10	1.5	56
A-4	6.87	11.69	1.7	50
A-5	8.08	10.51	1.3	62
A-6	4.75	9.5	2.00	41
A-7	4.73	9	1.9	44
A-8	8.4	10.52	1.29	62
D-1	6.08	14	2.3	N.A
D-2	5.96	11.2	1.9	17

D-3	7.87	12.04	1.5	35
D-4	8.72	14.84	1.7	26
D-5	9.7	12.67	1.3	43
D-6	6.56	10.5	1.6	30
D-7	6.03	10.85	1.8	22

In specimens serieses (B and C) failed in shear before reaching yield of flexural reinforcement due to cut in concrete and steel in location of opening. The overall and clear message of the data given in table (5-3) is that the premature and brittle nature of debonding failure may reduce the level of safety of the strengthened RC slab by decreasing its ductility.

5.5 Concrete Strains

The distribution of concrete strains along two axes (x,z) in tension face of the tested slab specimens was measured using sixteen demec discs. The presence of CFRP laminates at the bottom tension zone surface reduced the concrete strains, and this reduction was reflected to strains in the bottom tension steel bar reinforcement (i.e., reducing the tension steel bar strains), and that means increasing the tension strength and some tensile stresses were carried by CFRP laminates. Figures (5-14), (5-15), (5-16), (5-17) show the concrete strain in X-direction and the corresponding distance for each slab specimen.

80

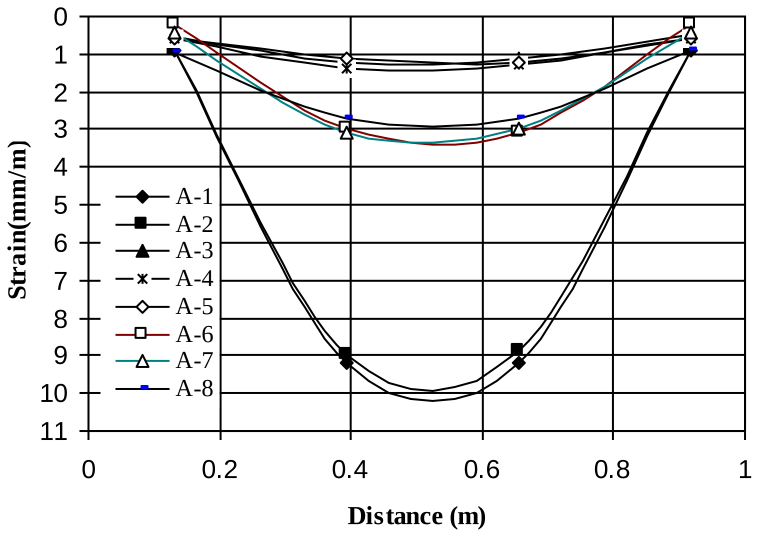

Figure (5-14) : Distance versus strain in X-direction for slabs in series (A) at load 50 kN/m^2.

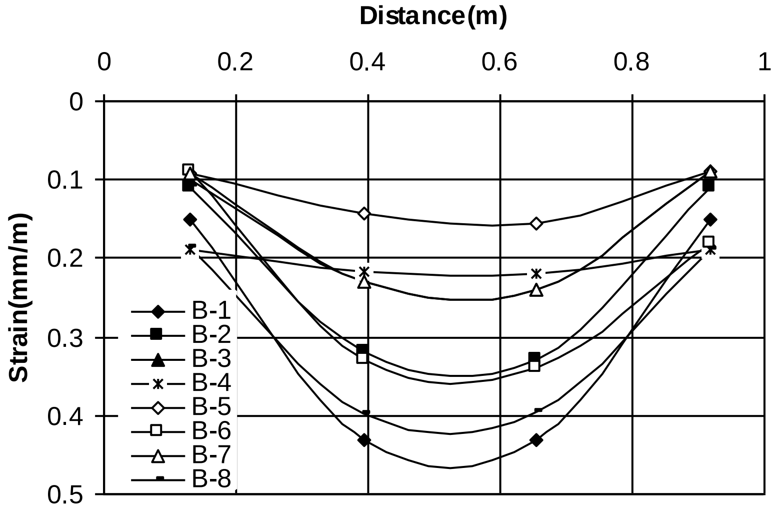

Figure (5-15) : Distance versus strain in X-direction for slabs in series (B) at load 20 kN/m^2.

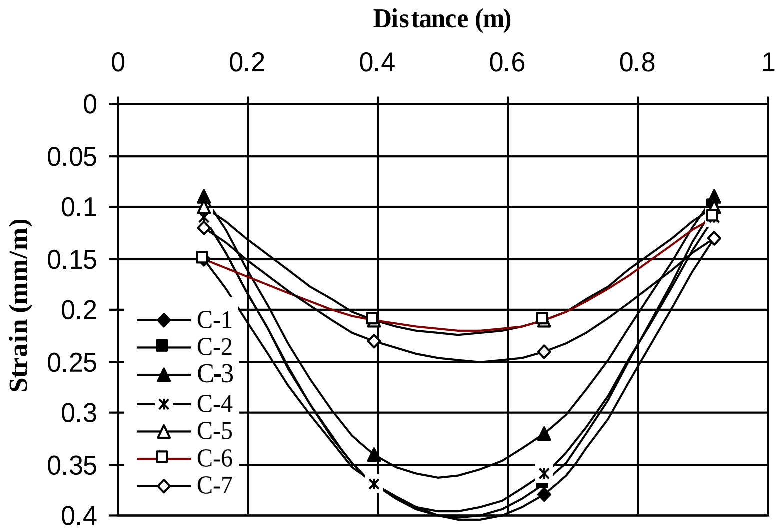

Figure (5-16) : Distance versus strain in X-direction for slabs in series (C) at load 25 kN/m^2.

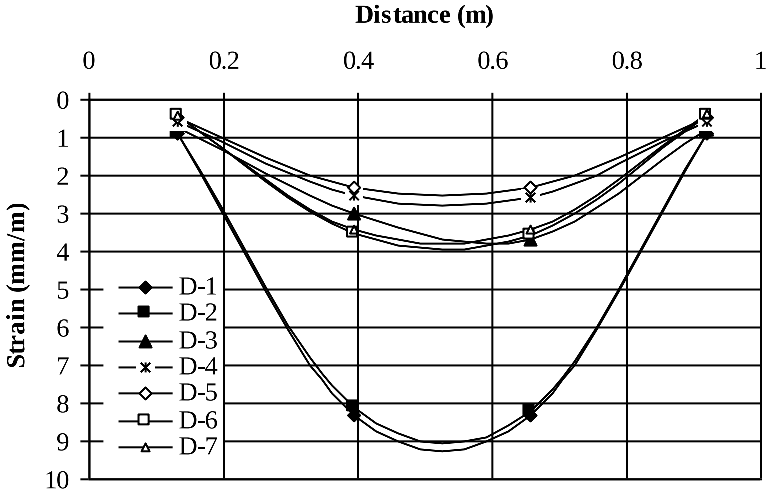

Figure (5-17) : Distance versus strain in X-direction for slabs in series (D) at load 40 kN/m^2.

5.6 Ultimate load and Failure modes

All the unstrengthened and strengthened RC slab specimens were tested up to failure. The recorded ultimate loads and failure modes for these slab specimens are presented in Table (5-4).

Table (5-4): Ultimate load capacity and failure mode for tested slabs.

Specimen	Ultimate load (kN/m^2)	Increase in ultimate load , %	Failure mode	Specimen	Ultimate load (kN/m^2)	Increase in ultimate load , %	Failure mode
A-1	**55**	**N.A**	**Typical flexural failure**	**B-8**	**38.5**	**-3.75**	**Shear**
A-2	**55.5**	**0.94**	**debonding**	**C-1**	**46**	**N.A**	**Shear**
A-3	**76**	**38**	**debonding**	**C-2**	**45**	**-2.5**	**Shear**
A-4	**75**	**36**	**debonding**	**C-3**	**35.5**	**-23**	**Shear**

A-5	**78**	**42**	**debonding**	**C-4**	**37**	**-19.5**	**Shear**
A-6	**58**	**5.5**	**debonding**	**C-5**	**35**	**-24**	**Shear**
A-7	**59**	**6.5**	**debonding**	**C-6**	**43.5**	**-4.5**	**Shear**
A-8	**77**	**40**	**debonding**	**C-7**	**43**	**-6.5**	**Shear**
B-1	**40**	**N.A**	**Shear**	**D-1**	**49**	**N.A**	**Typical flexural failure**
B-2	**39**	**-2.5**	**Shear**	**D-2**	**49.5**	**1**	**debonding**
B-3	**31**	**-23**	**Shear**	**D-3**	**67**	**36**	**debonding**
B-4	**32**	**-20**	**Shear**	**D-4**	**66**	**35**	**debonding**
B-5	**30**	**-25**	**Shear**	**D-5**	**69**	**41**	**debonding**
B-6	**38**	**-5**	**Shear**	**D-6**	**51**	**4**	**debonding**
B-7	**37**	**-7.5**	**Shear**	**D-7**	**52**	**6.8**	**debonding**

For the slab specimen A-1, which unstrengthened with CFRP sheet and without opening, the ultimate load capacity for this slab is calculated by yield line theory and found it equal to 58 kN/m^2 and by method -3 found it equal to 67kN/m^2 (see Appendix B), while in experimental result it equal to 55kN/m^2. The increasing in the ultimate load of A-2 is only 0.94%. Only stiffness increases in this specimen. This is because the fiber directions are parallel to the yield lines of the slab. The transverse strength of laminate is quite lower than that in the longitudinal direction. Once the concrete cracks, the CFRP can not take over the tensile force, the ultimate load of A-4 is higher than that of the reinforced concrete slab by 36%. Two cross lines are along the direction of the maximum bending stress and the advantages of CFRP strips can be raised. The stiffness of type A-6 is almost the same with that of A-2. The increasing in ultimate load is 5.5%, a little higher than that of A-2. The drawback of this strengthening scheme is dismissing the place where the maximum bending moments take place. The increase in ultimate load capacity of slab specimen A-3 is more than others in the same group results from that it's CFRP distribution is a combination of that in A-2 and A-4 specimens. Also, A-5 is combination of that in A-4 and A-6, while the increase in ultimate load capacity of slab specimen A-7 from that it's CFRP distribution is a combination of that in A-2 and A-6 specimens. A-8 is a repaired specimen, the ultimate load capacity for this specimen is approximately similar to the ultimate load capacity of specimen A-5. While the slab specimen D-1, which unstrengthened in CFRP and with opening in region of intersection of middle strip and middle strip, showed a decrease of 11 % in ultimate load capacity when compared with the control slab A-1. While the slab specimen D-2,D-3,D-4,D-5,D-6,D-7 which strengthened by CFRP sheet and with opening in region of intersection of middle strip and middle strip, the increase in ultimate load capacity was about 1,36,35,41,4,6.8 percent when compared with the corresponding control slab specimen D-1, from result of series slab specimen (D). The strengthening scheme adopted here could return the slab to its original strength prior to the hole having been cut.

In general, the stiffness and strength of the slabs increase when CFRP sheet are adhered to the tensile plane of the slab. However, the slab specimen B-2,B-3,B-4,B-5,B-6,B-7,B-8 which strengthened by CFRP sheet and with opening in region of intersection of column strips, the decrease in ultimate load capacity were about 2.5,23,20,25,5,7.5,3.75 percent when compared with the corresponding control slab specimen B-1. Also the slab specimen C-2,C-3,C-4,C-5,C-6,C-7 which strengthened by CFRP sheet and with opening in region of intersection of column strips and mid strip, the decrease in ultimate load capacity were about 2.5,23,19.5,24,5,4.5,6.5 percent when compared with the corresponding control slab specimen C-1. These slabs with an opening near to the support line all experienced shear failure in the concrete near the support, with no positive contribution from the CFRP. All these slabs failed in shear suddenly. Clearly, the strengthening scheme adopted here could not return the slab to its original strength prior to the hole having been cut. In fact, the ‘strengthening’ seems to have precipitated premature failure at a load well below the unstrengthened specimen B-1 and C-1. It seems to have been particularly weakened by the presence of the CFRP. In all these slabs specimen the presence of the bottom-surface surroundings in the opening laminates would extend the elastic range of the section and transfer the behavior of this section from ductile behavior to brittle behavior resulting in reduction in available shear contribution from the concrete (due to the cutout), premature shear failure occurred, (**Casadei et al., 2006**). When the opening in region of intersection of middle strip and middle strip (i.e. in specimen D-1) a reduction in ultimate load capacity is 11%, while in region of intersection column strips and column strips (i.e. in specimen B-1) a reduction in ultimate load capacity is 27% with shear failure of this specimen, while the opening in region of intersection of middle strip and column strip (i.e. in specimen C-1) a reduction in ultimate load capacity 25% with shear failure of this specimen. This result insures the ACI-code limit, when the opening in region of intersection of column strip and column strip is danger than when in region of intersection of column and middle strips. Finally, when the opening is in region of intersection of middle strip and middle strip is the best case. The ACI-code recommendation emphasized through the dimensions of the opening when in region of intersection column strip and column strip.

5.7 CFRP strains

The use of externally FRP to strengthen and rehabilitate exiting concrete structures is a relatively new technique. Until recently, there is a lack of design code and guidelines for their use **(Al-Mahaidi, 2003)**. The design specification of ACI Committee 440 recommended using a limitation on the strain of FRP sheets using a bond dependent coefficient in order to prevent debonding of FRP sheets. Section 9.5 of ACI 440.2R-02 discusses fatigue stress limits in the CFRP. To mitigate debonding under static loading conditions, ACI 440.2R-02 limits the strain in the FRP to $k_m \varepsilon_{fu}$, where ε_{fu} is the rupture strain of the FRP and,

$$k_m = \frac{1}{60\varepsilon_{fu}}\left(1-\frac{nE_f t_f}{360000}\right) \le 0.9 \qquad \text{for } n\,E_f\,t_f \le 180000\ \text{N/mm} \;\ldots\ldots\ldots(5\text{-}1a)$$

$$k_m = \frac{1}{60\varepsilon_{fu}}\left(\frac{90000}{nE_f t_f}\right) \leq 0.9 \qquad \text{for } n\,E_f\,t_f \geq 180000 \text{ N/mm} \quad \text{.........(5-1b)}$$

where n is the number of layers of FRP and E_f and t_f are the modulus and thickness of a single layer of FRP. This limitation was derived based on visual observation and experience, but the theoretical justification is unclear **(Al-Mahaidi, 2003)**. These strain limits depend only on the stiffness properties of the FRP plates and do not take into account the concrete-FRP interface properties, width of the FRP plate or the plate curtailment location, all of which should be expected to affect debonding **(Achintha et al., 2006)**. For the particular CFRP external strengthening used, the limiting effective strain is calculated in accordance with the ACI Committee 440 (2002) as ε_{fu} = 0.0152, the Max. CFRP strain for all specimen were showed in table (5-5). Comparison of this limit with the experimental results indicated that this calculated strain limit is nonconservative for all strengthened slabs presented in this study which failed through debonding at a CFRP strain level below 0.0055.

Table (5-5) : Max. CFRP strain.

specimen	Max.* CFRP strain	specimen	Max.* CFRP strain	specimen	Max.* CFRP strain
A-2	0.0019	B-4	0.000098	C-6	0.00016
A-3	0.00040	B-5	0.000098	C-7	0.00011
A-4	0.00043	B-6	0.000012	D-2	0.002
A-5	0.00048	B-7	0.000019	D-3	0.0041
A-6	0.00021	B-8	0.00003	D-4	0.0039
A-7	0.00023	C-2	0.00013	D-5	0.0055
A-8	0.00053	C-3	0.00015	D-6	0.0031

B-2	0.000025	C-4	0.00019	D-7	0.0032
B-3	0.000031	C-5	0.00014		

* measurement at load before the load of failure by 5 kN/m^2.

When comparing between strain in concrete and CFRP for the same level of load, the strain in concrete is larger than strain in CFRP and this indicates slip occurrence. This slip is one of the reasons of debonding in CFRP strip in slab specimen strengthening by CFRP.

CHAPTER SIX

Finite Element Modeling

6.1 Introduction

The finite element method has become a powerful tool for the numerical solution of a wide range of engineering problems. In this chapter the formulation of the finite element method used for analyzing the tested slabs is introduced. The use of **ANSYS-9** to create the finite element model is adopted. Out line of **ANSYS-9** program and all the necessary steps to create the calibrated model are explained in details and the steps taken to generate the analytical load-deflection response of the slabs are discussed.

6.2 ANSYS Computer Program

ANSYS (ANalysis SYStem) (version 9) is a powerful and impressive engineering tool that may be used to solve a variety of problems. ANSYS is a comprehensive general-purpose finite element computer program that contains over 100,000 lines of codes with about 165 different elements conducted in the program. ANSYS is capable of performing static (linear and nonlinear problems), dynamic, heat transfer, and fluid flow and electromagnetism analyses. It has been a leading finite element analyses program for well over 20 years. The current version of ANSYS has a completely new look, with multiple windows incorporating Graphical User Interface (GUI), Pull-down menus, dialog boxes, and a tool bar.

The main objective of the program is to analyze reinforced concrete members strengthened with CFRP under general three-dimensional states of loading up to failure.

In the present study, the program has been preceded using a personal computer. The program has been implemented on Pentium IV, 1700MHz IBM compatible computer with 256 megabyte RAM.

The adopted program is suitable for analyzing reinforced concrete slabs strengthened with CFRP under general states of loading.

6.3 Nonlinear Finite Element Analysis for Structures

Most phenomena in solid mechanics are nonlinear. However, in many applications it is convenient and practical to use linear formulation for problems to obtain engineering solutions. On the other hand, some problems definitely require nonlinear analysis if realistic results are to be obtained such as post-yielding and large deflection behavior of structures. Depending on the sources of nonlinearities, the nonlinear problems can be divided into three categories. In brief, these categories are:

a- Problems involving material nonlinearity.

b- Problems involving geometric nonlinearity.

c- Problems involving both materials and geometric nonlinearity.

The present study deals with material nonlinearity in analyzing the tested slabs. This is because for RC members, similar to this work, geometric nonlinearity effects are insignificant **(Maurizio et al., 2002).**

6.4 Nonlinear Solution Techniques

In general applying the finite element method for any structural problem leads to a set of algebraic equations of the following form:

$[K]\{u\}=\{f\}$……………………(6.1)

where: { u } is the unknown nodal displacement vector.

(vector of unknown DOF).

{ f } is the nodal applied force vector.

$[K]$ is the stiffness matrix.

and $[K] = (\int [B]^T [D][B] dV)$ …………..(6.2)

where: $[B]$ Strain-nodal displacement matrix based on the element shape functions.

$[D]$ Stress-strain matrix.

The solution for these equations for linear elastic structural problems can be obtained directly. In nonlinear problems, a direct solution is no longer possible since the stiffness matrix $[K]$ depends on the displacement level ($[K]$ = [$K(u)$]), and therefore it can not be exactly calculated before the determination of the unknown nodal displacement $\{u\}$. For nonlinear solution the state of equilibrium of a structural system corresponding to the applied load must be found. These equilibrium equations can be derived by applying the equilibrium to the structural system. The equilibrium equations can be expressed as:

$\{r\}=\{p\}-\{f\}$ …………….(6.3)

where:{ r} out of balance force vector .

$\{p\}$ represents the vector of the nodal forces equivalent to the internal stress level and is given by:

$\{P\} = \int_V [B]^T \{\sigma\} dV$ …………….(6.4)

The equivalent internal forces also depend on the displacement level $\{p\}=\{p(u)\}$ and have to be approximated in successive steps until Eq (6.3) is satisfied.

The solution of nonlinear problems by the finite element method is usually attempted by one of the following three basic techniques :

1- Incremental techniques.

2-. Iterative techniques.

3- Incremental-iterative techniques.

In the incremental procedure, the load is applied in several small increments and the structure is assumed to respond linearly within each increment with its stiffness recomputed based on the structural geometry and member end action at the end of the previous load increment. This is a simple procedure which requires no iterations but errors are likely to accumulate after several increments unless very fine increments are used. Figure (6.1a).

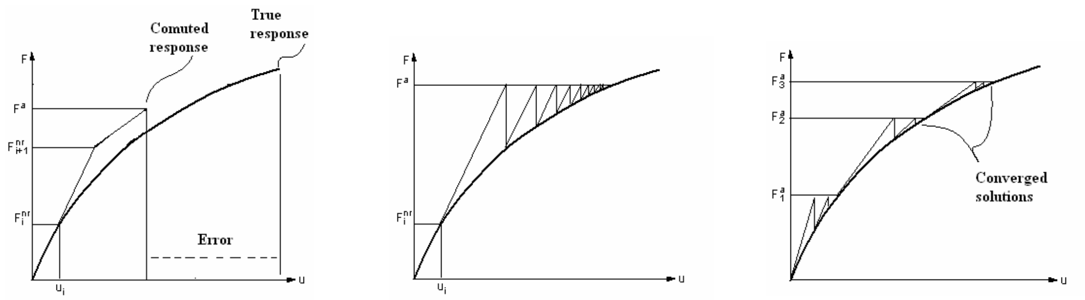

(a) (b) (c)

Figure (6.1)**:** Basic technique for solving nonlinear equation

(a) Incremental **(b)** Iterative **(c)** Incremental-Iterative.

In the iterative procedure, the total load is applied in one increment at the first iteration, the out of balance forces are computed and used in the next iteration to obtain progressively improved solution. The iterative process is continued until the final converged solution would be in equilibrium such that the internal load vector would equal the applied load vector or within some tolerance. This process can be written as:

$\left[K_i^T\right]\left\{\Delta U_i\right\} = \left\{F^a\right\} - \left\{F^{nr}\right\}$…………….(6.5)

$\left\{U_{i+1}\right\} = \left\{U_i\right\} + \left\{\Delta U_i\right\}$………………...(6.6)

where: $\left[K_i^T\right]$= stiffness matrix.

i = subscript representing the current equilibrium iteration.

$\left\{F^{nr}\right\}$=internal load vector.

This procedure fails to produce information about the intermediate stage of loading. For structural analysis including path-dependent nonlinearities (such as plasticity), the solution process requires that some intermediate increments be in equilibrium in order to correctly follow the load path. This can be achieved by using the combined incremental-iterative method.

The combined incremental-iterative procedure is a combination of the incremental and iterative methods performed in order to obtain converged solution corresponding to the stage of loading under consideration. Figure (6.1c).

The incremental-iterative solution procedure is used in this study with Full Newton-Raphson procedure. The stiffness matrix is formed at every iteration. The advantage of this procedure is that it may give more accurate results. The disadvantage of this procedure is that a large amount of computational effort may be required to form and decompose the stiffness matrix as shown in figure (6.2).

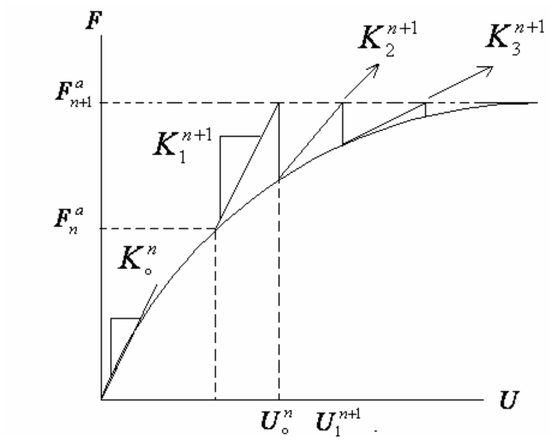

Figure (6.2**):** Incremental-iterative procedure with full Newton-Raphson procedure. **(Maurizio et al., 2002).**

6.4.1 Convergence Criteria

For every incremental load the iteration continues until convergence is achieved. The convergence criterion for the nonlinear analysis of structural problems can be classified as:

1- Force criterion

2- Displacement criterion

3- Stress criterion

The displacement criterion has been used in this study. In the displacement criterion, the incremental displacements at iteration and the total displacement are determined. The solution is considered to be converged when the norm of the incremental displacements is within a given tolerance of the norm of the total displacement; infinite norm* $\|\{R\}\|_\infty = \max|R_i|$ is used and takes the form:

$$\|\{\Delta U_i\}\| = (\max|\Delta U_i|) \leq T_n\ (\max|\Delta U_i|) \ \ldots\ldots\ldots\ldots\ldots(6.7)$$

where U may be equal u, v, w For forces criteria the norm of the residual forces at the end of each iteration are checked against the norm of the current applied forces as:

** Infinite norm: is simply the maximum value in the vector (maximum residual or maximum DOF increment)*

$\|\{R\}\| = (Max|R|) \leq T_n(\max R_i)$ ……….(6.8)

where $\{R\}$ is the residual vector:

$\{R\} = \{F^a\} - \{F^{na}\}$ …………..........(6.9)

In this study the tolerance Tn is taken equal to 0.05 near the ultimate load for loads control.

6.4.2 Analysis Termination Criterion

In the physical test under load control, collapse of a structure takes place when no further loading can be sustained. This is usually indicated in the numerical test by successively increasing iterative displacements and a continuous growth in the dissipated energy. Hence, the convergence of the iterative process cannot be achieved. A maximum number of iterations for each increment are specified to stop the nonlinear solution if the limited convergence has not been achieved for this study. It has been observed that a minimum number about 15 iterations is generally sufficient to predict the solution divergence or failure (**Anthony, 2004**). This maximum number of iterations depends on the type of the problem, extent of nonlinearities and on the specified tolerance. In the present study a maximum number of iterations equal to 100 are adopted for load control problems.

6.5 Finite Element Representation of Reinforced Concrete Slab with External CFRP Flexural Reinforcement

In the field of solid mechanics, the finite element method is usually used to find approximate solutions for structures having complicated shapes and /or loading arrangement.

The element types for this model are shown in Table (6.1).The **SOLID65** element was used to model the concrete. This element has eight nodes with three degrees of freedom at each node translation in the nodal x, y and z directions. This element is capable of plastic deformation, cracking in three orthogonal directions and crushing. Link 8 was used to represent the flexural reinforcement while Shell41 represents the CFRP strips.

Table (6.1): Element types for working model.

Material type	ANSYS element
Concrete	SOLID 65
Flexural Reinforcement	LINK 8
CFRP strips	SHELL 41

6.5.1 Concrete Brick Element

The 8-node isoperimetric linear element (SOLID65) in ANSYS 9 program is shown in figure (6.3) and used in this study. Each of the eight corner nodes has three degrees of freedom u, v, and w in the X, Y and Z directions respectively.

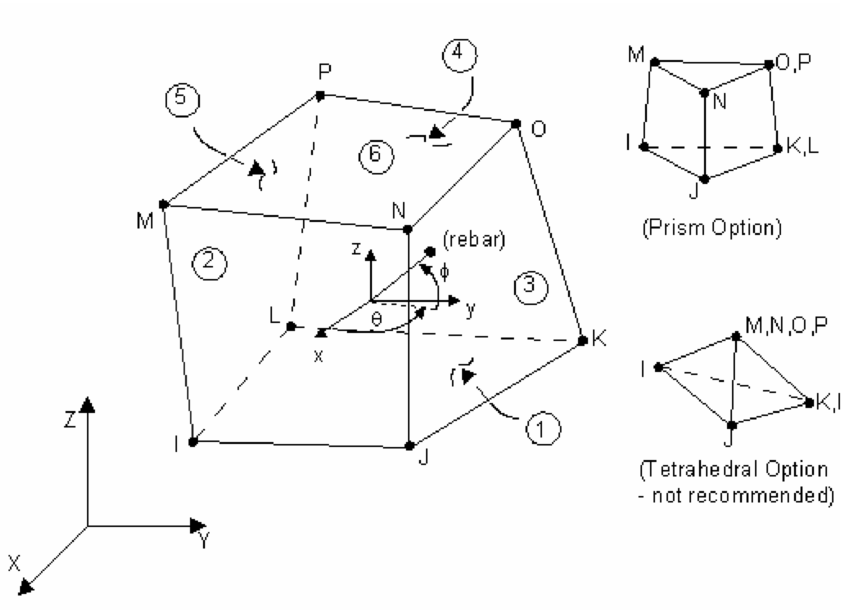

Figure (6.3): Brick element with 8 nodes (SOLID65 in ANSYS 9).

Solid 65 Input Data

The element is defined by eight nodes and the isotropic material properties. The element has one solid material and up to three rebar materials. MAT. command is used to input the concrete material properties while link8 is used to represent the main reinforcement so, the volume ratio which is defined as the rebar volume divided by the total element volume is equal to zero. Additional concrete material data such as the shear transfer coefficients, tensile strength, and compressive strength are described in table (6-2).

Table (6-2):SOLID 65 concrete material data.

Constant	Meaning
1	Shear transfer coefficients for an open crack .
2	Shear transfer coefficients for a closed crack.
3	Uniaxial tensile cracking stress.
4	Uniaxial crushing stress (positive).
5	Biaxial crushing stress (positive).
6	Ambient hydrostatic stress state for use with constants 7 and 8.
7	Biaxial crushing stress (positive) under the ambient hydrostatic stress state (constant 6).
8	Uniaxial crushing stress (positive) under the ambient hydrostatic stress state (constant 6).
9	Stiffness multiplier for cracked tensile condition, used if KEYOPT (7) = 1 (defaults to 0.6).

Typical shear transfer coefficient ranges from 0.0 to 1.0, with 0.0 representing a smooth crack (complete loss of shear transfer) and 1.0 representing a rough crack (no loss of shear transfer). These specifications may be made for both the closed and open crack.

6.5.2 Link 8 Element

A link 8 element was used to model steel reinforcement. This is a 3D spar element and it has two nodes with three degrees of freedom; translations in the nodal x, y and z directions. This element is also capable of plastic deformation. This element is shown in figure(6.4).

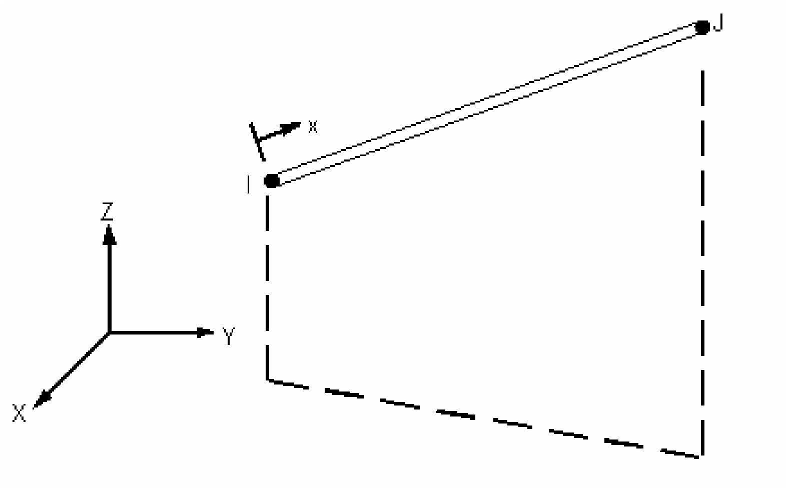

Figure (6.4)**:** Link 8 element.

Link 8 Input Data

The element is defined by two nodes, the cross-sectional area, an initial strain, and the material properties.

Real Constant

AREA - Cross-sectional area
ISTRN – Initial strain

Material Properties

EX, ALPX (or CTEX or THSX), DENS, DAMP

6.5.3 SHELL41 Element (Membrane shell)

A shell 41 element was used to model CFRP strips. SHELL 41 is a 3-D element having membrane (in-plane) stiffness but no bending (out-of-plane) stiffness. It is intended for shell structures where bending of the elements is of secondary importance. The element has three degrees of freedom at each node: translations in the nodal x, y, and z directions. The element can have variable thickness, stress stiffening and large deflection.

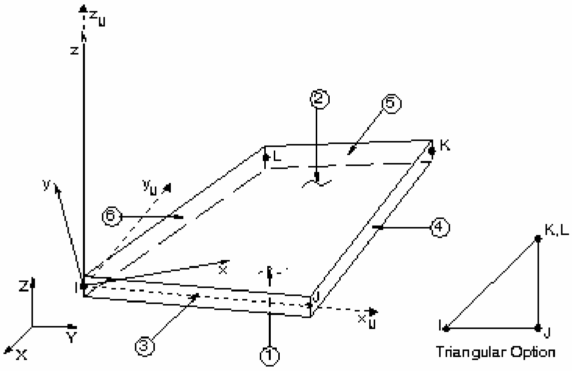

Figure (6.5): SHELL 41 geometry.

SHELL 41 Input Data

The element is defined by four nodes, four thicknesses, a material direction angle and the orthotropic material properties. The element may have variable thickness. The thickness is assumed to vary smoothly over the area of the element. In present study the element has a constant thickness, only TK(I) need be input. Even if the thickness is constant, all four thickness values must be input.

Table (6.3): SHELL41 real constants.

No.	Name	Description
1	TK(I)	Shell thickness at node I
2	TK(J)	Shell thickness at node J (defaults to TK(I))
3	TK(K)	Shell thickness at node K(defaults to TK(I))
4	TK(L)	Shell thickness at node L (defaults to TK(I))
5	THET A	Element x-axis rotation
6	EFS	Elastic foundation stiffness

6.5.4 Real Constant

The real constants for this model are shown in appendix C . It is noted that individual elements contain different real constants.

Real constant Set 1 is used for the Solid 65 element. It requires real constants for rebars assuming a smeared model. Values can be entered for Material Number, Volume Ratio, and Orientation Angles. The material number refers to the type of material for the reinforcement. The volume ratio refers to the ratio of steel to concrete in the element. The orientation angles refer to the orientation of the reinforcement in the smeared model. ANSYS 9 allows the user to enter three rebar materials in the concrete. Each material corresponding to x, y and z directions in the element, figure(6.3). The reinforcement has uniaxial stiffness and the directional orientation is defined by the user. In the present study the slab is modeled using discrete reinforcement. Therefore, a value of zero was entered for all real constants which turned the smeared reinforcement capability of the Solid65 element off.

Real constant Set 2 are defined for the Link 8 element. Values for cross-sectional area and initial strain were entered. Cross-sectional area in set 2 refers to the area of main reinforcement bar Ø 4 mm, Set 3 are defined for the shell 41. Values for shell thickness, Element X axis rotation theta, Elastic foundation stiffness and Added mass/unit area were entered. Shell thickness in set 3 refers to the thickness of CFRP sheet.

The reinforcement in the discrete model figure (6.6a) uses bar or beam elements that are connected to concrete mesh nodes. Therefore, the concrete and the reinforcement mesh share the same nodes and concrete occupies the same regions occupied by the reinforcement. A drawback to this model is that the concrete mesh is restricted by the location of the reinforcement and the volume of the mild-steel reinforcement is not deducted from the concrete volume.

The smeared model figure (6.6b) assumes that reinforcement is uniformly spread throughout the concrete element in a defined region of the finite element mesh. This approach is used for large-scale models where the reinforcement does not significantly contribute to the overall response of the structure **(Anthony, 2004).** Figure (6.7) shows the details of the merging element of the main reinforcement.

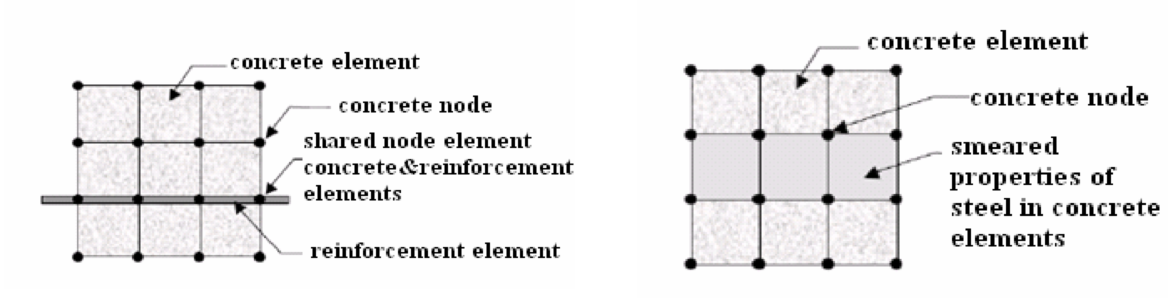

(a) discrete **(b)** smeared

Figure (6.6)**:** Models for reinforcement in reinforced concrete member.

Figure (6.7)**:** Details of the steel reinforcement for slab specimen B-1.

6.5.5 Material Properties

Parameters needed to define the material models can be found in appendix C. As seen in these tables there are multiple parts of the material model for each element. Material number 1 refers to the Solid 65 element. The Solid 65 element requires linear isotropic and multilinear isotropic material properties to properly model concrete as shown in figure (6.8). EX is the modulus of elasticity of the concrete (*Ec***)** and PRXY is the Poisson's ratio (γ). The modulus of elasticity was calculated by equation of (ACI-code 2005).

$$\mathrm{E}c = 4730\sqrt{f'_c} \quad \ldots\ldots\ldots\ldots\ldots(6.10)$$

The **ANSYS** program requires the uniaxial stress-strain relationship for concrete in compression in figure(6-8). Numerical expressions, equations (6.11) and (6.12), were used along with equation (6.13) (**Gere et al., 1997**) to construct the uniaxial compressive stress-strain curve for concrete in this study.

$$f = \frac{E_c \varepsilon}{1 + \left(\frac{\varepsilon}{\varepsilon_o}\right)^2} \quad \ldots\ldots\ldots\ldots\ldots\ldots\ldots\ldots(6.11)$$

$$\varepsilon_o = \frac{2f'c}{E_c} \ldots\ldots\ldots\ldots\ldots\ldots\ldots\ldots\ldots\ldots(6.12)$$

$$E_c = \frac{f}{\varepsilon} \ldots\ldots\ldots\ldots\ldots\ldots\ldots\ldots\ldots\ldots\ldots(6.13)$$

Where:

f = Stress at any strain ϵ.

ϵ = Strain at stress f.

ϵ_o = Strain at the ultimate compressive strength f'c**.**

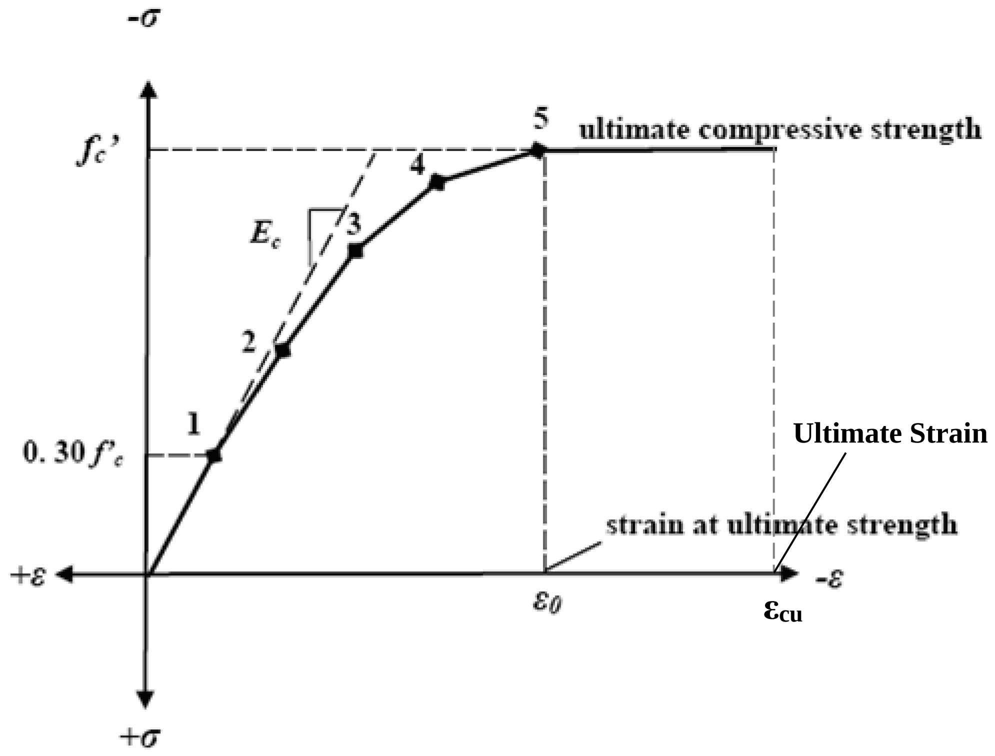

Figure (6-8): Simplified compressive uniaxial stress-strain curve for concrete **(Kachlakev et al., 2001)**.

The simplified stress-strain curve for each slab model is constructed from six points connected by straight lines. The curve starts at zero stress and strain. Point No. 1, at 0.30*f'*c, is calculated for the stress-strain relationship of the concrete in the linear range (Equation (6-13)). Point Nos. 2, 3, and 4 are obtained from Equation (6-11), in which ε_o is calculated from equation (6-12). Point No. 5 is at ε_o and *f'c.* In this study, an assumption was made of perfectly plastic behavior after Point No. 5 **(Kachlakev et al., 2001)** . Poisson's ratio was assumed to be 0.15. The compressive uniaxial stress was f_c' =27.05 MPa.

Material model in **ANSYS 9** requires that different constants be defined. These constants are as listed in appendix C.
A number of comparative analytical studies have been attempted by **(Hemmaty, 1998),** and **(Kachlakev et al.,2001)** to evaluate the influence of shear transfer coefficient βt. They used finite element models for reinforced concrete beams and bridge decks with βt values within the range

0.05-0.25. Convergence problems occurred when the shear transfer coefficient for the open crack dropped below 0.2. No deviation of the response occurs with the change of the coefficient. For all slabs without shear reinforcement the (ShrCf-Op) shear transfer coefficient for the open cracks used was 0.05 and (ShrCf-Cl) the shear transfer coefficient for the closed cracks was 0.4, because there was not any shear reinforcement to restrict the cracking growth if it was formed and the closed cracks were not capable to perform as close cracks for a long time of loading. The value of the uniaxial tensile strength (f_t) is as obtained from the experimental cylinder splitting test according to the ASTM standard method. The biaxial crushing stress refers to the ultimate biaxial compressive strength f'_{cb} and the ambient hydrostatic stress state denoted as σ_h table (5.2). This stress is defined as:

$$\sigma_h = \frac{1}{3}(\sigma_{xp} + \sigma_{yp} + \sigma_{zp}) \ldots\ldots\ldots\ldots\ldots\ldots\ldots (6.14)$$

where σ *xp*, σ *yp* and σ *zp* are the principal stress values in the principal directions. The biaxial crushing stress under the ambient hydrostatic stress state refers to the ultimate compressive strength for a state of biaxial compression superimposed on the hydrostatic stress state f_1. The uniaxial crushing stress under the hydrostatic stress state refers to the ultimate compressive strength for a state of uniaxial compression superimposed on the hydrostatic stress state f_2. The failure surface can be defined with a minimum of two constants f_t and f_c'. The remainders of the variables in the concrete model are left to default based on these equations **(Willam et al., 1975)**:

$$f'_{cb} = 1.2 f'_c \ldots\ldots\ldots\ldots\ldots (6.15)$$

$$f_1 = 1.45 f'_c \ldots\ldots\ldots\ldots\ldots (6.16)$$

$$f_2 = 1.725 f'_c \ldots\ldots\ldots\ldots (6.17)$$

These stress states are only valid for stress state satisfying the condition

$$|\sigma_h| \le \sqrt{3} f_c' \quad \text{.............(6.18)}$$

Material model number 2 refers to the link 8 element. The link 8 element is being used for all the steel reinforcement and it is assumed to be bilinear isotropic. The bilinear model requires the yield stress f_y as well as the hardening modulus of the steel to be defined. The yield stress was 525MPa, for the main reinforcement and its hardening modulus was 10GPa (a horizontal part of the stress-strain curve). **(Kachlakev et al., 2001)**.

Material number 3 refers to the Shell 41 element which represents the CFRP strips. The CFRP is assumed to be orthotropic material, where the properties of the FRP composites are the same in any direction perpendicular to the fibers. EX is the modulus of elasticity of the CFRP (E_{CFRP}) and PRXY is the Poisson's ratio (γ). The modulus of elasticity was taken to be 238GPa from chapter four and the Poisson's ratio was assumed to be equal to zero.

Note -For the repair slabs :-

Because the slabs were removed from the loading frame and transmitted to another place, the continuous process of loading steps for calculating the slab stiffness matrix which depends on the materials information at the higher loading stage (nonlinear materials behavior) in the first cycle of loading by ANSYS must be restarted by vanishing all the deformations. In this situation the modulus of elasticity of the concrete *Ec* must be assumed and using less values of its initial curve values. It is assumed that *Ec* started from just after the elastic limit as illustrated in appendix C **(Santhakumar, 2004)**.

6.5.6 Meshing

To obtain good results from the Solid65 element, the use of a rectangular mesh is recommended. Therefore, the mesh was set up such that rectangular elements were created, as shown in figure (6-9).

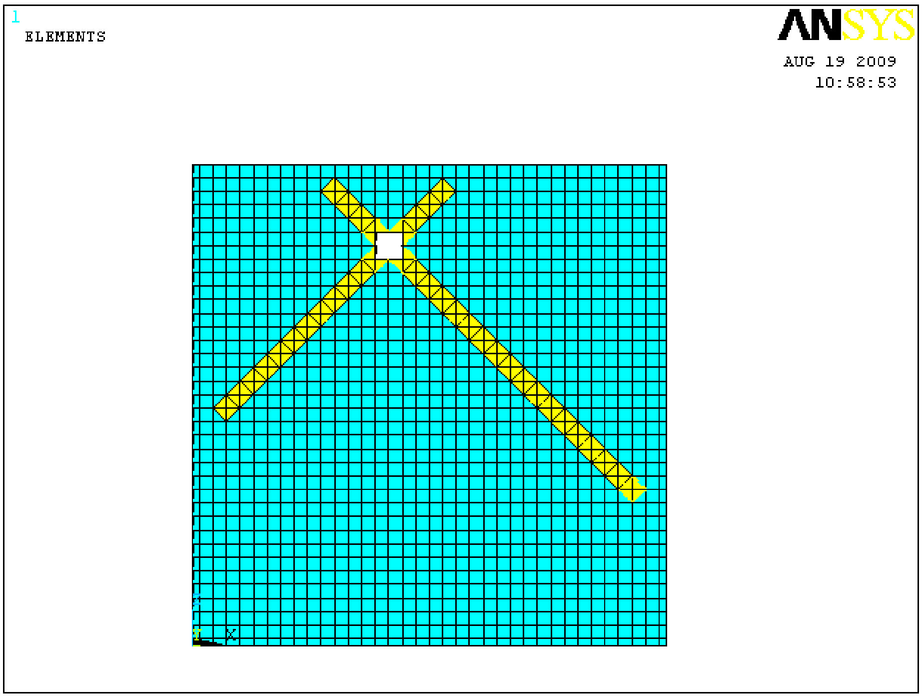

Figure (6-9) **:** Mesh of the concrete and CFRP strips for the slab C-2.

To determine the number of elements needed to model the slab a finite element analysis of a simply supported homogeneous concrete slab was carried out. The result was compared with an elastic analysis and maximum deflection under the load of 5 kN/m^2 with different designs of the mesh. Size of elements in x-z plane varied from 30*30 mm to 60*60 mm and number of elements through slab height varied from 3 to 6. Only three-dimensional linear solid elements were being examined both for reduced and full integration.

As a references the development of levy's equation described by **(Timoshenko et al., 1959)** is used. According to this approximation of theory of plates maximum deflection is to be calculated with following equation, derivation of this equation found in appendix D.

............(6.19) $w_{Max} = 0.00406\dfrac{qa^4}{D}$

Where : q is magnitude of uniformly distributed load.
a is size of square plate.
D is flexural rigidity of plate.

Flexural rigidity of plate D is defined as ;

$$D = \frac{Eh^3}{12(1-\gamma^2)} \quad \ldots\ldots\ldots\ldots(6.20)$$

Where : E is Young modulus.

h is height of plate.

v is poisson's ratio.

Data needed to calculate maximum deflection is listed in table (6-4)

Table (6-4): Slab properties.

q (kN/m^2)	5.0
a(m)	0.95
h(m)	0.03
E(GPa)	24.6
v(-)	0.15

Using data from table (6-4) in equations (6-19) and (6-20), the maximum deflection of slab (A-1) amounts to :

$w_{Max} = 0.29mm$

Table (6-5) contains values of deflection for different mesh designs and their errors towards value obtained from theory of plates. Errors Δ are calculated according to the following equation :

$$\Delta = \frac{w_{Max,FEM} - w_{Max}}{w_{Max}} \ldots\ldots\ldots\ldots\ldots\ldots\ldots(6.21)$$

Table (6-5): Slab deflection for different mesh designs.

integration	x-z size of elements (mm)	Number of elements on height	Total Number of nodes	Total Number of elements	Deflection (mm)	Error%
Reduced	60*60	6	2457	1944	0.15	-0.48
Reduced	30*30	6	9072	7350	0.28	-0.03
Reduced	30*30	3	5184	3675	0.065	-0.77
Reduced	30*30	4	6480	4900	0.22	-0.24
Reduced	60*60	3	16807	13824	0.043	-0.85

Comparison with the analytic solution of different mesh arrangements indicates that the biggest influence on accuracy is the number of elements through slab height. Using 6 elements gives good correspondence with the theory. Fully integrated elements give poor results even with very fine meshes due to shear locking. In the further FE analysis, meshes with 6 elements through height and element size 30*30 mm will be used. Though the difference in time, related directly to total number of elements, is significant. The mesh of the slab C-2 with a small hole is shown in figure (6-9).

No mesh of the reinforcement is needed because individual elements were created in the modeling through the nodes created by the mesh of the concrete (Solid65). Same thing for the CFRP strips. Figure (6-10) shows the applied load and boundary conditions of model slab A-8.

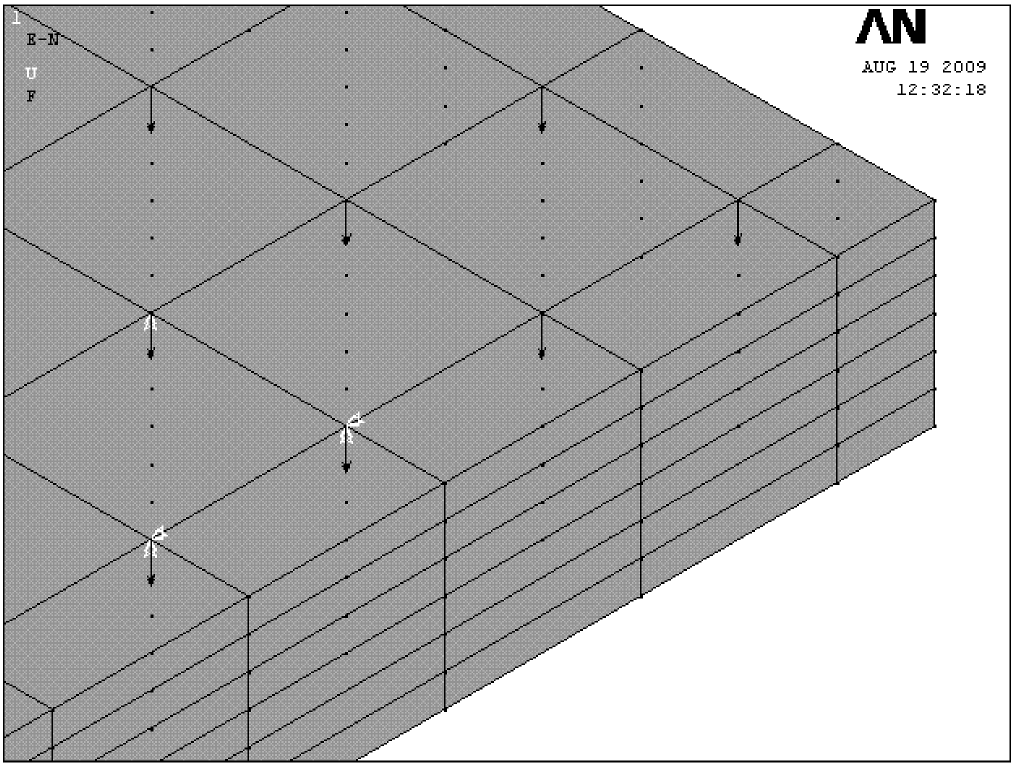

Figure (6-10): The applied load and boundary conditions of model specimen A-8.

6.5.7 Analysis Type

The model for this analysis is a simple slab under uniform distributed load. For this model the static analysis type is utilized. The restart command is utilized to restart analysis after the initial run or load step has been completed. The Sol'n Controls command dictates the use of a linear or non-linear solution for the finite element model. Typical commands utilized in a nonlinear static analysis are shown in appendix C. In the particular case considered in this thesis the analysis is based on static small displacements. The time at the end of the load step refers to the ending load per load step. The sub-steps are set to indicate load increments used for this analysis. The commands used to control the solver and output are shown in appendix C. Also, the commands used for the nonlinear algorithm and convergence criteria are given in appendix C. The values for the convergence criteria are set to default except for the tolerances. The tolerances for displacement are set as in appendix C. Also, it shows the commands used for the advanced nonlinear settings. The program behavior upon no convergence for analysis was set such that the program will terminate but not abolish.

6.5.8 Analysis Process for the Finite Element Model

The Newton-Raphson method of analysis was used to compute the nonlinear response. The application of the loads up to failure was done incrementally as required by the Newton-Raphson procedure. The time at the end of each load step corresponds to the applied loading. The convergence criterion used for the analysis was displacement, when the slab began cracking, convergence for the nonlinear analysis was impossible with the default values, so, the tolerance value of 0.01 was used during the nonlinear solution for convergence. A small criterion must be used to capture correct response. This criterion was used for the remainder of the analysis. As shown in appendix C, failure of the slab occurs when convergence fails.

CHAPTER SEVEN

VERIFICATION OF THE FINITE ELEMENT MODEL

7.1 Introduction

A series of examples are presented in this chapter to demonstrate the ability of the finite element model presented in previous chapter to describe the behavior of unstrengthened, strengthened and repaired RC slab with and without openings under monotonic load. The numerical results in this chapter are obtained with computer program **ANSYS** whose numerical implementation was discussed in the previous chapter. The goal of the comparison of the FE model and the tested slabs is to ensure that the elements, material properties, real constant and convergence criteria are adequate to model the response of the slabs.

7.2 Results of the Finite Element Model

To illustrate the validity of the nonlinear finite element model for the analysis of RC slab strengthened by CFRP sheet with and without openings, all tested slab specimens will be analyzed by using **ANSYS** computer program, as mentioned previously.

7.2.1 First Cracking Loads :-

Table (7.1) shows the numerical results that are related to the first cracking load. It can be observed that the first cracking load in strengthened slabs increases with the increasing the CFRP amount when compared with the corresponding unstrengthened control slabs.

Table (7.1): Numerical first cracking loads for the tested slab.

Specimen	First cracking Load (kN/m^2)		Difference ratio ,%	Specimen	First cracking Load (kN/m^2)		Difference ratio ,%
	Experimental	Numerical			Experimental	Numerical	
A-1	12	12	0	B-8	8	8	0
A-2	12	12	0	C-1	9	10	-11
A-3	15	16	-6	C-2	9	10	-11
A-4	15	16	-6	C-3	8	9	-12
A-5	18	17	5	C-4	8	9	-12
A-6	13	12	7	C-5	8	7	12
A-7	15	14	6	C-6	9	10	-11
A-8	12	10	16	C-7	9	9	0
B-1	8	9	-12	D-1	10	11	-10
B-2	8	9	-12	D-2	10	11	-10
B-3	7	8	-14	D-3	11	12	-9
B-4	7	6	14	D-4	12	13	-8
B-5	7	6	14	D-5	15	16	-6
B-6	8	9	-12	D-6	12	13	8
B-7	8	9	-12	D-7	13	14	7

The first cracking load obtained from the numerical results showed good agreement with experimental data recorded with difference ranging from 0 to 14 percent, except repaired slab A-8 the difference ratio of it equal 16 percent. This may be due to decreasing the theoretical concrete strength properties (modulus of elasticity).

7.2.2 Cracking Patterns :-

The cracking behavior of same slab specimen is discussed in the following to compare between ANSYS and experimental results :

In control slab A-1 the appearance of flexural cracks was first at 12 kN/m^2 in ANSYS analysis and experimental test within the mid span. At 20 kN/m^2, new flexural cracks formed and developed diagonally from the mid span of the specimen, as shown in figure (7-1).

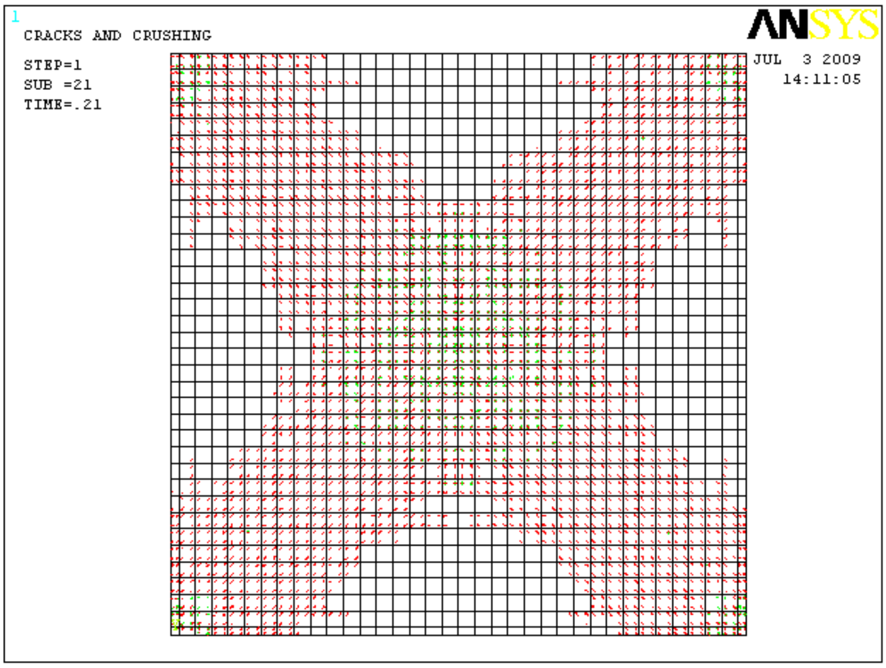

Figure (7-1) : Flexural crack of slab A-1 failure load.

The shear crack appeared at a load of 30 kN/m^2 along the support side of slab model A-6, as shown in figure (7-2).

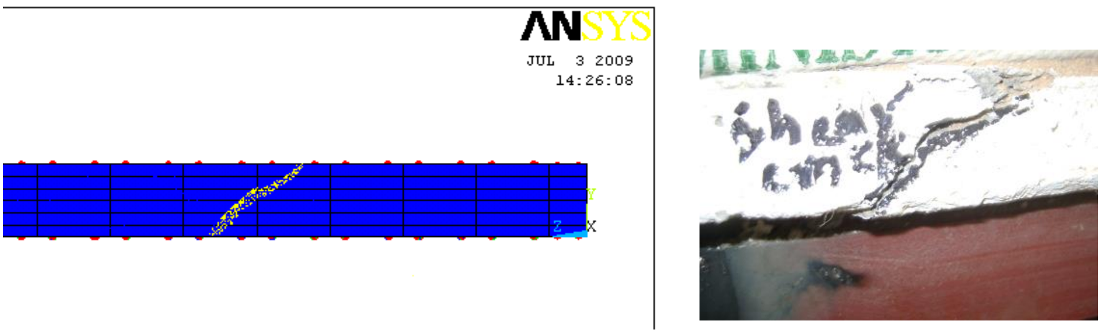

Figure (7-2) : Shear crack of slab A-6.

In compression of slab A-4 face, the cracks appeared at the corner of specimen due to holding down force as shown in figure (7-3).

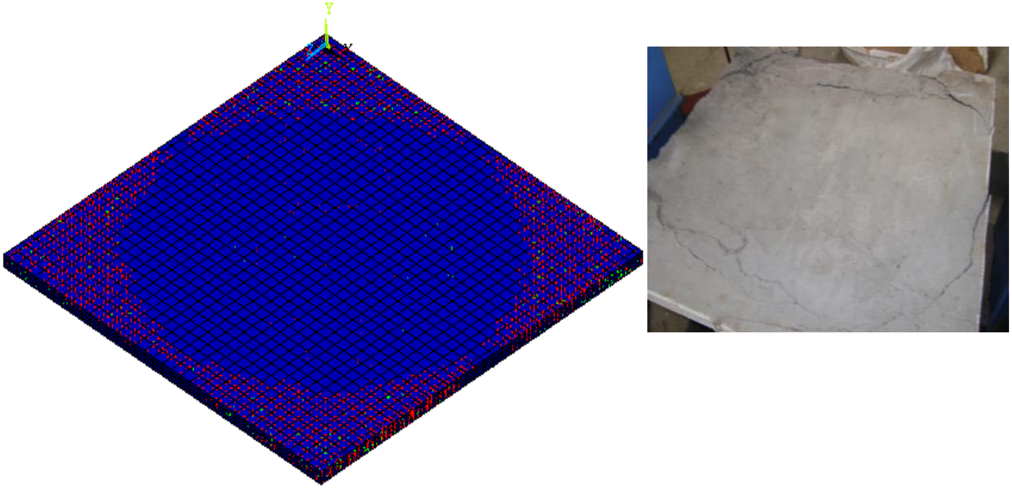

Figure (7-3) : Cracks at the corner of slab A-4.

In slab models of series (B,C) the shear cracks at the corner of opening wide speared diagonally at top face, in bottom face cracks developed radially around the opening as shown in figure (7-4).

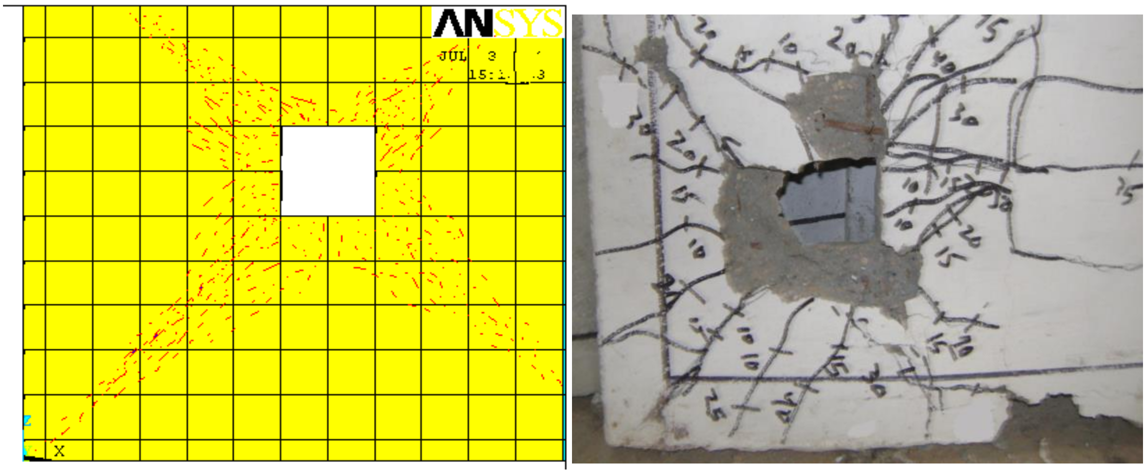

Figure (7-4): Cracking pattern around the opening in bottom face of slab (B-1).

7.2.3 Load Deflection Curves:-

A comparison between experimental and numerical load versus mid span deflection curves are shown in figures (7.5) to (7.8).

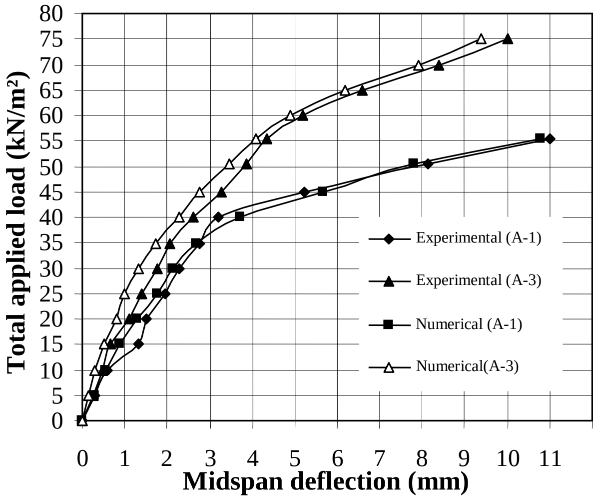

Figure (7.5): Load versus midspan deflection for slab (A-1)&(A-3).

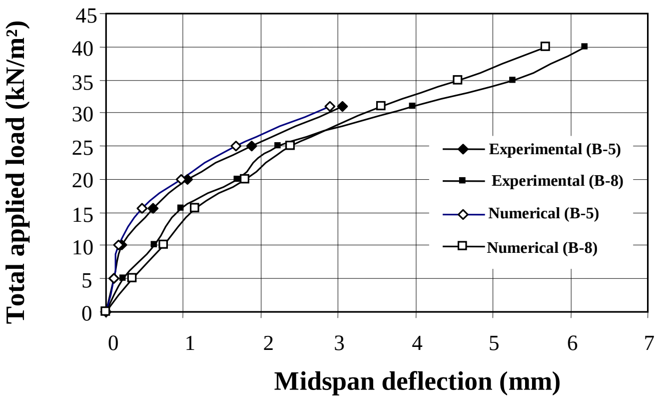

Figure (7.6): Load versus midspan deflection for slab (B-5)&(B-8).

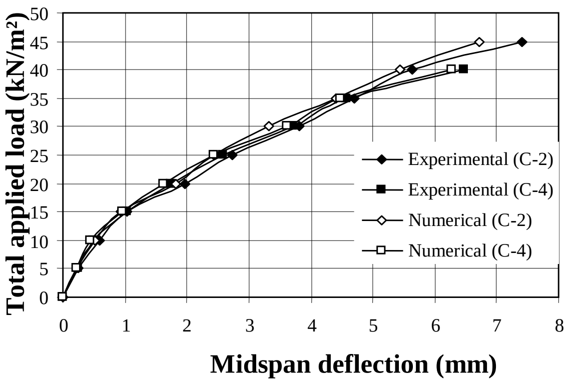

Figure (7.7): Load versus midspan deflection for slab (C-2)&(C-4).

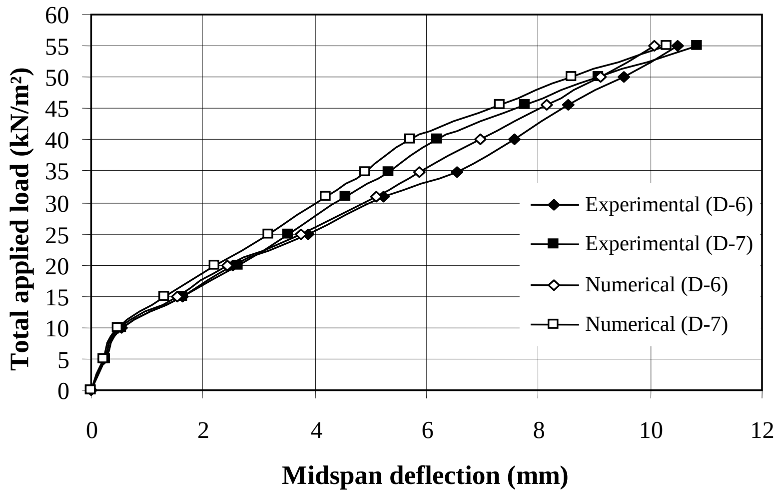

Figure (7.8): Load versus midspan deflection for slab (D-6)&(D-7).

The finite element results for the control slab specimen A-1 and strengthening slab A-3, figure (7.5), show stiffer response compared with the experimentally recorded curve for the pre-cracking and post-cracking as well as for the ultimate stage. Figures (7.6) and (7.7) show a comparison between the load versus midspan deflection curves for experimental and numerical results for the strengthened slab specimens B-5, C-2, C-4 and repaired slab B-8, respectively. Again, slightly stiffer behaviors are obtained in the numerical results when compared with that obtained from experiments. An experimental and numerical load versus midspan deflection comparisons are made in figure (7.8) for the strengthening slab D-6 and D-7. In spite of the fact that numerical curve in figure (7.8) show a slightly stiffer behavior in the pre-cracking and post-cracking stages.

7.2.4 Concrete Strain Distribution :-

The distribution of concrete strains at along of two axes (x,z) in tension face of the tested slab specimens was measured using demec discs. The concrete strain distribution for each slab. The same numerical result can be seen in figure (7-9) to figure (7-12). In addition to that, the presence of CFRP laminates at the bottom tension zone surface reduced the concrete strains, and this reduction was reflected to strains in the bottom tension steel bar reinforcement (i.e., reducing the tension steel bar strains), and that means increasing the tension strength and some tensile stresses were carried by CFRP laminates.

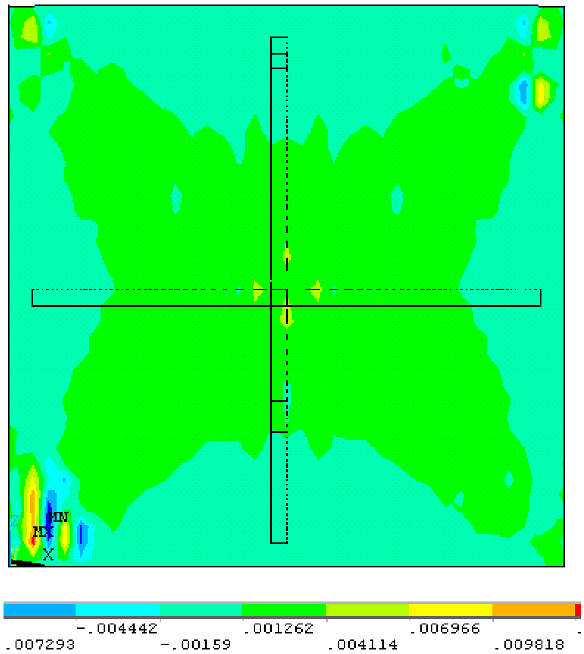

Figure (7-9) : Concrete strain distribution in X-direction of slab A-4 at load 50 kN/m^2.

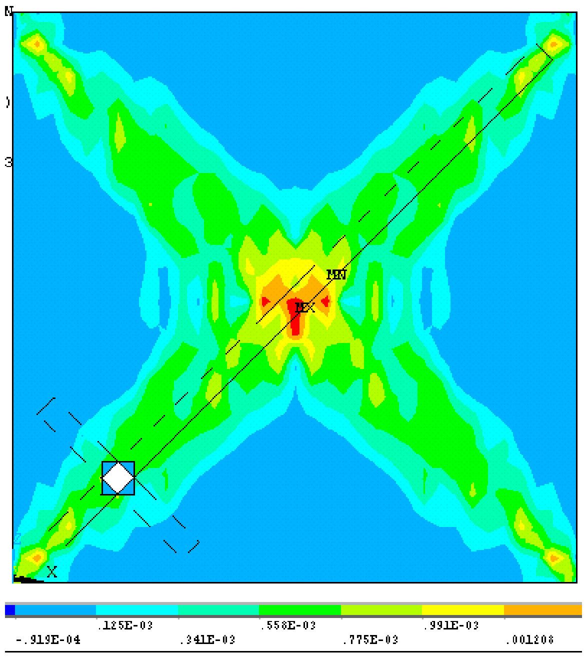

Figure (7-10) : Concrete strain distribution in X-direction of slab B-2 at load 20 kN/m^2.

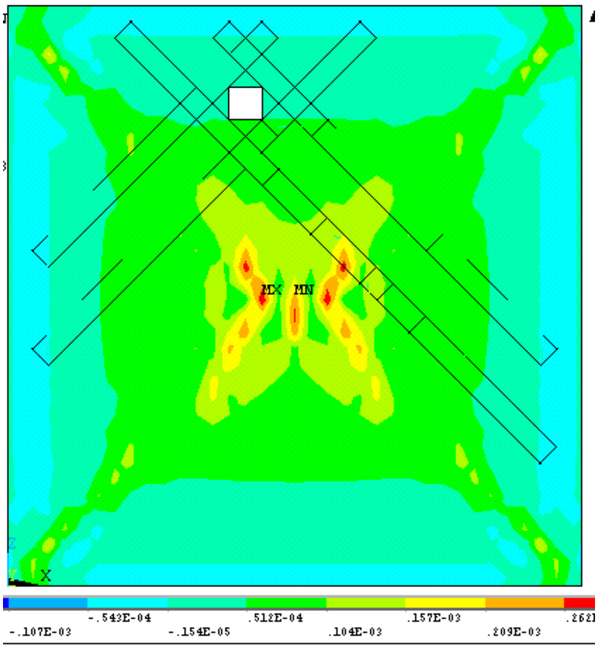

Figure (7-11) : Concrete strain distribution in X-direction of slab C-6 at load 25 kN/m^2.

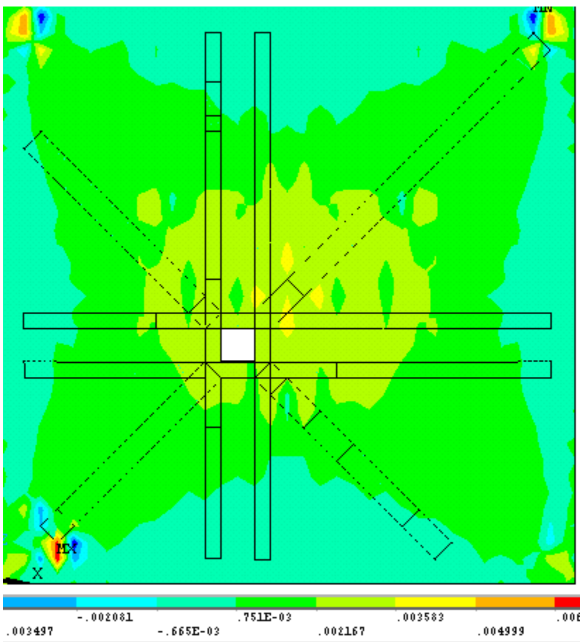

Figure (7-12) : Concrete strain distribution in X-direction of slab D-3 at load 40 kN/m^2.

7.2.5 Ultimate Load :-

Table (7-2) shows the failure load and its mid span deflection for each slab. This can be made by changing the tolerance till finding this value of load. The failure of the modeled slab was indicated by the state that the slab no longer can support additional load as indicated by the convergence failure of **ANSYS** program in failing to find a solution. The failure load predicted is very close to the failure load measured during experimental testing.

Table (7-2) : The experimental and ANSYS deflection values of the slabs at the experimental failure load.

Specimen	Failure load (kN/m^2)		Mid span deflection (mm)		Difference ratio , %	Specimen	Failure load (kN/m^2)		Mid span deflection (mm)		Difference ratio , %
	Experimental	ANSYS	Experimental	ANSYS			Experimental	ANSYS	Experimental	ANSYS	
A-1	55	55	11	10.78	2	B-8	38.5	39	6.19	5.69	8
A-2	55.5	56	8.5	8.24	3	C-1	46	46	7.80	7.64	2
A-3	76	76	10	9.4	6	C-2	45	45	7.41	6.82	8
A-4	75	75	11.69	10.75	8	C-3	35.5	36	5.56	5.28	5
A-5	78	78	10.51	11.03	-5	C-4	37	37	6.47	6.27	3
A-6	58	58	9.5	9.88	-4	C-5	35	35	4.36	4.19	4
A-7	59	59	9	9.27	-3	C-6	43.5	44	7.79	7.17	8
A-8	77	77	10.91	12.65	-16	C-7	43	43	7.41	7.56	-2
B-1	40	40	6.53	6.33	3	D-1	49	49	14	13.72	2
B-2	39	39	6.21	5.96	4	D-2	49.5	50	11.2	10.53	6
B-3	31	31	4.00	3.76	6	D-3	67	67	12.04	11.44	5
B-4	32	32	5.43	5.86	-8	D-4	66	66	14.84	14.09	5
B-5	30	30	3.05	2.89	5	D-5	69	69	12.67	12.29	3
B-6	38	38	6.52	6.25	4	D-6	51	51	10.5	10.08	4
B-7	37	37	6.41	6.21	3	D-7	52	52	10.85	10.3	5

CHAPTER EIGHT

CONCLUSIONS AND RECOMMENDATIONS

8.1 Introduction

In this chapter, the conclusions drawn from the experimental and numerical results are described. The limitations of the present work and suggestions for future work are also presented.

8.2 Conclusions

Based on the results obtained from the experimental work and finite element analysis by **ANSYS** program for the externally strengthened R.C. two-way slabs with and without openings by CFRP sheets, the following conclusions can be drawn:

1. For the tested slabs without opening or with opening in the middle strips zone and subjected to monotonic transverse loading up to failure, the ultimate flexural loads may increased up to 42 percent when externally strengthened by CFRP sheets. The best strengthening of R.C. slabs with opening in the middle strips zone is that using CFRP sheets parallel to opening sides (as in specimen D-4).

2. The experimental and numerical results of strengthened slabs with opening in the column strips showed a decrease in ultimate load capacity ranging from 2.5 to 25 percent as compared to the control slabs. That because the suddenly shear failure in these specimens. It was observed that the presence of CFRP sheet on the tension face will transfer behavior of the structure from ductile to brittle.

3. The structural ductility of the CFRP strengthened R.C. slabs is low when compared with the corresponding control specimen. The reduction in ductility ratio was about 17 to 62 percent based on deflection.
4. The design equation suggested by ACI Committee 440 (2002) is evaluated based on the comparison made along with the present experimental results. Generally, it is found that this equation is inadequate with present investigation and needs further refinement.
5. The finite element model used in the present study is able to simulate the strengthened reinforced concrete slabs with CFRP sheet. The cracking loads, crack patterns, strain in CFRP sheets, strain in concrete and ultimate loads predicted are very close to that measured during the experimental testing with difference about (2 %-8%) based on deflection.
6. The presence of CFRP sheets on the tension face restrained cracking propagation resulted in an increase in load carrying capacities prior to and beyond the first cracking. The cracking loads of slabs without opening or with opening in the middle strips zone may increased up to 50 percent.
7. The presence of CFRP laminates at the bottom tension zone surface reduced the tensile concrete strains, and this reduction is reflected to strains in the bottom tension steel bar reinforcement (i.e., reducing the tension steel bar strains), and that means increasing the tension strength and some tensile stresses would be carried by CFRP sheets.
8. No evidence of debonding of the CFRP sheets was observed until yielding of the reinforcement. The formation of secondary cracks adjacent to existing flexural cracks is an indication of initiation of debonding of the CFRP sheets.
9. The debonding in slab specimens is very sudden and the only indication of incipient failure is few popping sounds as the debonding cracks propagated quickly to the end of the sheet. The clear message of the experimental results is that the premature and brittle nature of debonding

failure may reduce the level of safety of the strengthened R.C. slabs by decreasing its ductility.

8.3 Recommendations

The following subjects are recommended for future works :

1. Finite element analysis of flexural CFRP plate-concrete slabs with interface element (slip bond) between the concrete and CFRP plate.

2. Behavior of CFRP sheets-concrete slabs subjected to dynamic and impact loading and also to cyclic loading.

3. The extension of the present work to prestressed concrete is required to make the program applicable to wider range of CFRP plate-concrete structures.

4. Time dependent effects are urgently needed to be incorporated in the present study. These effects should include concrete shrinkage, creep and aging of concrete.

5. Analysis of CFRP sheets-concrete slabs subjected to bending and torsional loading.

6. Studying the effect of GFRP bars on behavior of R.C. two-way slab with and without openings.

7. Experimental and nonlinear finite element analysis of reinforced concrete beams and slabs.

8. Studying the effect of CFRP sheets as protection material on the fire resistance of the reinforced concrete slabs.

9. Studying the effect of support conditions on the behavior of reinforced concrete slabs after strengthening by CFRP sheets.